



TESE DE DOUTORADO

**DESIGN OF DATA VALIDATION SOLUTIONS USING HIGH DENSITY
2D COLORED CODES AND A (2,2) XOR-BASED COLOR
INTERFERENCE VISUAL CRYPTOGRAPHY SCHEME**

MAX EDUARDO VIZCARRA MELGAR

Brasília, Março de 2018

UNIVERSIDADE DE BRASÍLIA

FACULDADE DE TECNOLOGIA

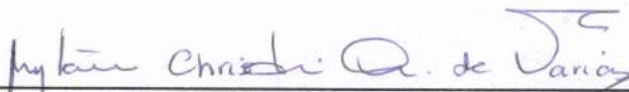
UNIVERSIDADE DE BRASÍLIA
FACULDADE DE TECNOLOGIA
DEPARTAMENTO DE ENGENHARIA ELÉTRICA

DESIGN OF DATA VALIDATION SOLUTIONS USING HIGH
DENSITY 2D COLORED CODES AND A (2,2) XOR-BASED
COLOR INTERFERENCE VISUAL CRYPTOGRAPHY SCHEME

MAX EDUARDO VIZCARRA MELGAR

TESE DE DOUTORADO SUBMETIDA AO DEPARTAMENTO DE ENGENHARIA
ELÉTRICA DA FACULDADE DE TECNOLOGIA DA UNIVERSIDADE DE BRASÍLIA,
COMO PARTE DOS REQUISITOS NECESSÁRIOS PARA A OBTENÇÃO DO GRAU
DE DOUTOR.

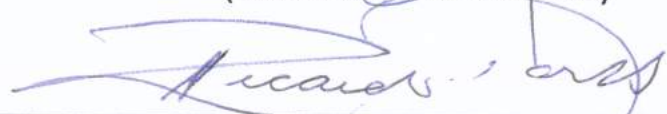
APROVADA POR:



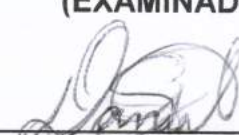
MYLENE CHRISTINE QUEIROZ DE FARIAS, Dra., ENE/UNB
(ORIENTADORA)



FRANCISCO ASSIS DE OLIVEIRA NASCIMENTO, Dr., ENE/UNB
(EXAMINADOR INTERNO)



RICARDO DAHAB, Dr., UNICAMP
(EXAMINADOR EXTERNO)



DANIEL GUERREIRO E SILVA, Dr., ENE/UNB
(EXAMINADOR INTERNO)

Brasília, 21 de março de 2018.

FICHA CATALOGRÁFICA

VIZCARRA, MAX

DESIGN OF DATA VALIDATION SOLUTIONS USING HIGH DENSITY 2D COLORED CODES AND A (2,2) XOR-BASED COLOR INTERFERENCE VISUAL CRYPTOGRAPHY SCHEME [Distrito Federal] 2018.

xvi, 68 p., 210 x 297 mm (ENE/FT/UnB, Doutor, Engenharia Elétrica, 2018).

Tese de Doutorado - Universidade de Brasília, Faculdade de Tecnologia.

Departamento de Engenharia Elétrica

1. HD2DCC

2. Color 2D Barcode

3. Visual Cryptography

4. Visual Secret Sharing

I. ENE/FT/UnB

II. Título (série)

REFERÊNCIA BIBLIOGRÁFICA

VIZCARRA, M. (2018). *DESIGN OF DATA VALIDATION SOLUTIONS USING HIGH DENSITY 2D COLORED CODES AND A (2,2) XOR-BASED COLOR INTERFERENCE VISUAL CRYPTOGRAPHY SCHEME*. Tese de Doutorado em Engenharia de Sistemas Eletrônicos e de Automação, Publicação PGEA.TD-127/2018, Departamento de Engenharia Elétrica, Universidade de Brasília, Brasília, DF, 68 p.

CESSÃO DE DIREITOS

AUTOR: MAX EDUARDO VIZCARRA MELGAR

TÍTULO: DESIGN OF DATA VALIDATION SOLUTIONS USING HIGH DENSITY 2D COLORED CODES AND A (2,2) XOR-BASED COLOR INTERFERENCE VISUAL CRYPTOGRAPHY SCHEME.

GRAU: Doutor em Engenharia de Sistemas Eletrônicos e Automação ANO: 2018

É concedida à Universidade de Brasília permissão para reproduzir cópias desta Tese de Doutorado e para emprestar ou vender tais cópias somente para propósitos acadêmicos e científicos. Os autores reservam outros direitos de publicação e nenhuma parte dessa Tese de Doutorado pode ser reproduzida sem autorização por escrito dos autores.



MAX EDUARDO VIZCARRA MELGAR

Depto. de Engenharia Elétrica (ENE) - FT

Universidade de Brasília (UnB)

Campus Darcy Ribeiro

CEP 70919-970 - Brasília - DF - Brasil

Acknowledgments

I am deeply grateful to my doctoral advisor, Prof. Ph.D. Mylène C. Q. Farias, for her academic support, patience, and dedication during the last 5 years. I extend my sincere gratitude to Prof. Ph.D. Alexandre Zaghetto, who has given me valuable support during my Master's degree period. I am also very grateful to the examiners of this Thesis: Prof. Ph.D. Francisco Assis de Oliveira Nascimento, Prof. Ph.D. Daniel Guerreiro e Silva, and Prof. Ph.D. Ricardo Dahab for their contributions, valuable comments and suggestions.

Special thanks to my wife, attorney Luiza de Castro Vizcarra, for her help on collecting experimental data of my research in the Laboratory of Ambient Control and Energetic Efficiency (LACAM), and for her important motivation to finish this work.

I am also very grateful to the unconditional love and support of my parents, MSc. Aida Melgar Santander and Ph.D. Max W. Vizcarra Maldonado, who raised me and taught me to study and work hard. Thanks to my sister, Dr. Julissa Vizcarra Melgar, for taking care of our parents in Lima and giving me important advice over the past few years. I would also wish to express my gratitude to my aunt, Prof. Ph.D. Luz Melgar Santander, for her academic and professional guidance over all my life.

This thesis has been written during my stay at the University of Brasilia. I would like to thank the Department of Electrical Engineering for providing excellent working conditions and Coordenação de Aperfeiçoamento de Pessoal de Nível Superior (CAPES), for its financial support.

RESUMO

A validação de dados nos sistemas de informação utiliza majoritariamente algoritmos criptográficos em sistemas que, geralmente, não utilizam materiais não eletrônicos como parte da infraestrutura do criptossistema. Nesse trabalho, foram desenvolvidos dois sistemas de armazenamento e recuperação de dados através da proposta de uma nova tecnologia de códigos de barra colorido bidimensional e de um novo esquema de criptografia visual.

Os códigos de barras bidimensionais têm sido amplamente estudados, mas ainda continuam sem contar com um padrão que consiga transmitir alta quantidade de informação em pequenos espaços impressos. As aplicações desse modelo de transmissão tem como motivação a necessidade de armazenar (e recuperar) uma alta quantidade de informação em pequenas áreas impressas, como por exemplo, para utilização de dados criptográficos que sejam processados sem conexão e armazenados em pequenos espaços impressos, como os de caixas de remédios ou caixas de cigarros. O código de barras colorido 2D proposto nesse trabalho é chamado de High Density 2 Dimensional Code (HD2DC) e possui 8 diferentes tamanhos. O HD2DC permite a utilização de 5 ou 8 cores em cada tamanho e conta com o algoritmo de correção de erro Reed-Solomon com 3 diferentes níveis (10%, 20% e 30%). O HD2DC foi desenvolvido com o objetivo de ser um padrão de código de barras colorido 2D para operações de transmissão de grande quantidade de informações em pequenas ou médias áreas de impressão.

Criptografia visual é uma técnica que cifra uma imagem secreta em duas ou mais imagens chave. A decodificação de qualquer esquema de criptografia visual depende do sistema visual humano e a maioria das propostas existentes consideram para a decodificação a utilização da sobreposição de duas ou mais lâminas físicas com $n \times n$ ($n \geq 2$) pixels expandidos. O esquema de criptografia visual proposto nesse trabalho considera a utilização de duas imagens. A primeira é uma lâmina física feita por uma impressão colorida em Policloreto de Polivinila (PVC) transparente de 3 milímetros, enquanto que a segunda é uma imagem colorida apresentada na tela do visor de um smartphone. Ambas as imagens não geram expansão de pixels. A obtenção das melhores cores utilizadas nesse criptossistema foi realizada através de estudos físicos do comportamento da interferência de cor entre a tela do smartphone e a cor utilizada na impressão do PVC transparente. Essa nova proposta possui um alto nível de usabilidade para validação de dados em transações eletrônicas e conta com um custo muito baixo de implementação.

Um sistema robusto de validação de dados é criado quando é combinada a criptografia visual proposta com o HD2DC. O HD2DC tem a capacidade de armazenar uma das imagens chave, no caso a que deve ser mostrada no visor do celular, essa arquitetura de codificação aumenta a percepção de segurança e explora a usabilidade do celular por meio da utilização da câmera e da tela como ferramentas para mostrar a imagem cifrada da criptografia visual.

Palavras-Chave: HD2DCC, Códigos de barra 2D Coloridos, Criptografia Visual, Compartilhamento Visual Secreto.

ABSTRACT

Digital data validation generally requires that algorithms are ran into on cryptographic systems that, usually, do not use non-electronic devices as part of their information security infrastructure. This work presents two information storage and retrieval systems: a new colored two-dimensional barcode technology and a novel visual cryptography scheme.

Two-dimensional barcodes have been a topic of research for several decades, but there is still no standard that stores and retrieves high amounts of data. Recently, new requirements have been imposed on applications that use 2D barcodes as a communication channel, such as the capability of storing information into a small printed area. This particular requirement is specially important for 2D barcodes that store cryptographic primitives to be processed off-line. This is the case of barcodes in products like cigarettes and medicines, which are used for data validation and product verification. The proposed 2D colored barcode is called High Density Two-Dimensional Code (HD2DC) and is currently one of the 2D barcodes with the highest data density. HD2DC can be generated in 8 different sizes, with 5 or 8 colors. To increase robustness, the system uses a Reed-Solomon error correction algorithm with 3 different levels: Low, Medium and High, which provide approximately 10%, 20% and 30% error correction, respectively.

Visual cryptography (VC) is a technique that encodes the content of a secret image into two or more images, which are called shares. These shares are printed on transparencies and superimposed (requiring a good alignment) to reveal (visually) the original secret image, i.e. without requiring any computation. Current visual cryptography schemes use at least 2 shares (transparencies) as keys. With respect to the secret image size, most of these schemes produce a $n \times n$ ($n \geq 2$) size expansion of the shares and the decoded image. The proposed Visual Cryptography scheme, on the other hand, uses two shares and does not require a size expansion. The first share is a colored film printed on a Polyvinyl Chloride (PVC) surface of 3 millimeters, while the second share is a colored image displayed on a smartphone or tablet. In this work, we performed a physical evaluation of the color interference properties of these two shares (the printed PVC transparency and the image displayed on the mobile device) to find the most adequate color space to be used in the proposed cryptosystem.

We also propose a strong validation system combining our Xor-Based Visual Cryptography scheme with HD2DC. HD2DC has the capability of storing the share that is shown on the mobile device display. This encoding architecture enhances security perception and explores the mobile device usability, using its screen to display a Visual Cryptography share.

Keywords: HD2DCC, Color 2D barcode, Visual cryptography. Visual secret sharing

CONTENTS

1	INTRODUCTION	1
1.1	PROBLEM STATEMENT	1
1.2	PROPOSED APPROACH	2
1.3	DOCUMENT OUTLINE	3
2	BACKGROUND	5
2.1	TWO-DIMENSIONAL BARCODES	5
2.1.1	QR CODE	5
2.1.2	HCCB, HCC2D AND PER CHANNEL DATA ENCODING	6
2.1.3	CQR CODE-5 AND 9	7
2.2	VISUAL CRYPTOGRAPHY	9
2.2.1	BLACK AND WHITE VISUAL CRYPTOGRAPHY	9
2.2.2	COLOR VISUAL CRYPTOGRAPHY	11
2.2.3	XOR-BASED VISUAL CRYPTOGRAPHY	14
2.2.4	DISCUSSION ON CURRENTLY AVAILABLE 2D BARCODES AND VC SCHEMES	15
3	A TWO-DIMENSIONAL COLORED BARCODE: HD2DC	17
3.1	HD2DC - ENCODING PROCESS	17
3.1.1	STRUCTURE: FUNCTION PATTERNS	17
3.1.2	STRUCTURE: ENCODING REGION	18
3.2	HD2DC - DECODING PROCESS	20
3.2.1	VERSION ESTIMATIVE	21
3.2.2	ALIGNMENT: PROJECTIVE TRANSFORMATION	22
3.2.3	COLOR SEGMENTATION	23
3.2.4	INFORMATION RETRIEVAL	25
3.3	HD2DC DECODING RESULTS: PRINT-SCAN CHANNEL	25
3.3.1	DATA DENSITY	26
3.4	HD2DC DECODING RESULTS: COMPRESSION ROBUSTNESS	28
3.4.1	HD2DC COMPRESSION ALGORITHMS	29
4	A (2,2) XOR-BASED VISUAL CRYPTOGRAPHY SCHEME USING COLOR INTER- FERENCE	37
4.1	PROPOSED VISUAL CRYPTOGRAPHY SHARES STRUCTURE	37
4.2	PROPOSED VISUAL CRYPTOGRAPHY ANALYSIS	39
4.3	PROPOSED VISUAL CRYPTOGRAPHY RESULTS: COLOR SELECTION AND SHARES GENERATION	41
4.4	PROPOSED VISUAL CRYPTOGRAPHY RESULTS: DECRYPTED IMAGE	44

4.5	ANIMATED VISUAL CRYPTOGRAPHY DECRYPTION	46
4.6	DATA VALIDATION SYSTEM: PROPOSED VC SCHEME AND HD2DC.....	47
5	CONCLUSIONS.....	51
5.1	COMPUTER-IMPLEMENTED INVENTIONS AND PATENTS	52
5.2	PUBLICATIONS	53
	BIBLIOGRAPHY	54
6	APPENDIX	58
6.1	COMPUTER-IMPLEMENTED INVENTIONS	58
6.2	ONGOING PATENTS REQUEST.....	58
6.3	HD2DC COMPRESSION RESULTS	58

Figure List

2.1	Examples of 2D barcodes: (a) regular QR Code [1], (b) Microsoft HCCB [2], (c) HCC2D prototype for 4-colors HCC2D [3] and (d) HCC2D prototype for 8-colors HCC2D [3,4].	6
2.2	Examples of CQR Codes (a) CQR Code-5 [1] and (b) CQR Code-9 [5]. CQR Code characteristic: (c) CQR Code structure [5] and (d) CQR Code positioning in the encoding region [5].	7
2.3	Block diagram of a communication system that considers print-scan storage and transmission stages [1].	8
2.4	Traditional VC shares: Three possible complementary pixel expansions.....	10
2.5	Examples of traditional VC scheme: (a) secret image, (b) share 1, (c) share 2 and (d) share 1 and share 2 superimposed to recover (visually) the secret image.	10
2.6	Example of EVC: (a) Share 1, (b) Share 2 and (c) decoded secret image [6]......	11
2.7	Halftoning decomposition on C, M and Y colors [7].	11
2.8	Color composition for superposed shares on method 1 [7]......	12
2.9	Color composition for superposed shares on method 2 [7]......	13
2.10	Two sharing transparencies and the stacked effect for method 2 [7].	13
2.11	Third method of Color VC: (a) color composition, (b) share 1, (c) share 2 and (d) decoded image [7].	14
2.12	Hardware implementation of colour XOR-Based VC scheme [8]......	15
2.13	Optical arrangement of polarizers and retarder films [9]......	15
3.1	Examples of HD2DC of: (a) Version 1, 5 colors, Low error correction capacity and 120 stored bytes, (b) Version 1, 8 colors, High error correction capacity and 90 stored bytes, (c) Version 8, 5 colors, High error correction capacity and 966 stored bytes, and (d) Version 8, 8 colors, Low error correction capacity and 2,906 stored bytes.....	18
3.2	HD2DC structure bits composition.....	19
3.3	HD2DC structure.	19
3.4	HD2DC modules: (a) BCH(63,18) distribution, and (b) HD2DC filling direction. ..	20
3.5	Color space constellation for used encoding and decoding processes: (a) RGB Cube and (b) HSV with normalized boundaries between HD2DC selected colors... ..	23
3.6	HD2DC Version 5, 8-colors, and High error correction level: (a) image snapshot captured at a distance of 7 cm from the camera (Samsung Galaxy J5) and (b) rotated and processed version of (a).	24
3.7	Flowchart of HD2DC decoding process.	27
3.8	HD2DC Version 1 decoding results due to capture distance (7 cm to 20 cm) on Samsung Galaxy S5 and J5.	28

3.9	HD2DC Version 2 decoding results due to capture distance (7 cm to 20 cm) on Samsung Galaxy S5 and J5.	28
3.10	HD2DC Version 3 decoding results due to capture distance (7 cm to 20 cm) on Samsung Galaxy S5 and J5.	29
3.11	HD2DC Version 4 decoding results due to capture distance (7 cm to 20 cm) on Samsung Galaxy S5 and J5.	29
3.12	HD2DC Version 5 decoding results due to capture distance (7 cm to 20 cm) on Samsung Galaxy S5 and J5.	30
3.13	HD2DC Version 6 decoding results due to capture distance (7 cm to 20 cm) on Samsung Galaxy S5 and J5.	30
3.14	HD2DC Version 7 decoding results due to capture distance (7 cm to 20 cm) on Samsung Galaxy S5 and J5.	31
3.15	HD2DC Version 8 decoding results due to capture distance (7 cm to 20 cm) on Samsung Galaxy S5 and J5.	31
3.16	HD2DC Version 6 and 8-color, captured and correctly decoded with 5.69% corrupted symbols at a distance of 13cm with the Samsung Galaxy S5 camera.	32
3.17	Enlarged 5-colors HD2DC of Version 4, compressed with: (a) JPEG@0.4908 bpp and 17.03% corrupted symbols, (b) JPEG2000@0.4720 bpp and 2.92% corrupted symbols, finally (c) H.264/AVC@0.4727 bpp and 0.97% corrupted symbols.	32
3.18	Enlarged 8-colors HD2DC of Version 1, compressed with: (a) JPEG@0.4151 bpp and 27.93% corrupted symbols, (b) JPEG2000@0.4002 bpp and 1.80% corrupted symbols, finally (c) H.264/AVC@0.3929 bpp and 0% corrupted symbols.	33
3.19	Enlarged 8-colors HD2DC of Version 8, compressed with: (a) JPEG@0.4654 bpp and 25.92% corrupted symbols, (b) JPEG2000@0.1106 bpp and 29.50% corrupted symbols, finally (c) H.264/AVC@0.5725 bpp and 1.82% corrupted symbols.	33
3.20	Percentage of corrupted symbols of HD2DC Version 1 versus compression bitrate (0-1.2 bpp).....	34
3.21	Percentage of corrupted symbols of HD2DC Version 2 versus compression bitrate (0-1.2 bpp).....	34
3.22	Percentage of corrupted symbols of HD2DC Version 3 versus compression bitrate (0-2 bpp).....	34
3.23	Percentage of corrupted symbols of HD2DC Version 4 versus compression bitrate (0-1.9 bpp).....	35
3.24	Percentage of corrupted symbols of HD2DC Version 5 versus compression bitrate (0-2 bpp).....	35
3.25	Percentage of corrupted symbols of HD2DC Version 6 versus compression bitrate (0-2 bpp).....	35
3.26	Percentage of corrupted symbols of HD2DC Version 7 versus compression bitrate (0-2.8 bpp).....	36
3.27	Percentage of corrupted symbols of HD2DC Version 8 versus compression bitrate (0-2.5 bpp).....	36

4.1	Color in PVC transparency: (a) Non-printed PVC transparency index refraction and (b) Color wavelengths of warm and cool colors.	38
4.2	Proposed VC scheme with single pixel structure.	40
4.3	Luminance detection: (a) Lumens measurement of a blue printed PVC transparency superimposed on the Samsung Galaxy S5 screen with blue color and (b) Schematic representation.	42
4.4	Measured luminance values for combinations of Shares 1 and 2, with cool and warm colors. Measurements were performed considering the first structure of Table 4.3 (lines 2-5) and using a Samsung Galaxy S7 Edge (Share 2) and a set of color printed PVC transparencies (Share 1).	45
4.5	(a) Secret image (S), (b) Share 1 (F_1), and (c) Share 2 (F_2).	45
4.6	Proposed VC scheme shares: (a) Share 1 with 60×60 pixels, (b) Share 1 with 136×136 pixels, (c) Share 2 of soccer player image with 60×60 pixels, and (d) Share 2 of Lena image with 136×136 pixels.	46
4.7	Proposed VC scheme decoded images: (a) Soccer player with 60×60 pixels, (b) Lena with 60×60 pixels, (c) Dog paw symbol captured in a dark environment with 60×60 pixels, (d) Tilted snapshot of (c), (e) Soccer player with 136×136 pixels, (f) Lena with 136×136 pixels, (g) Dog paw symbol with 136×136 pixels, and (h) Tilted snapshot of (g).	47
4.8	Proposed animated VC scheme images of 200×200 pixels: (a) Share 1, (b) Share 2, (c) first wrong decoded secret image, (d) second wrong decoded secret image, (e) third wrong decoded secret image, and (f) correctly decoded secret image.	48
4.9	HD2DC and proposed VC Scheme Cryptosystem.	49
4.10	Proposed VC scheme and HD2DC Cryptosystem: (a) Share 1 with 136×136 pixels, (b) Share 2 with 136×136 pixels, (c) HD2DC carrying the 1024-RSA encrypted Share 2, and (d) Decoded secret image.	50
6.1	HD2DC Computer-Implemented Invention certificate.	59
6.2	COLOR VC SYSTEM Computer-Implemented Invention certificate.	60
6.3	Código de Barras de Alta Densidade patent request support document.	61
6.4	Lâmina de Criptografia Visual patent request support document.	62

Table List

3.1	HD2DC-5 color information structure.....	21
3.2	HD2DC-8 color information structure.....	22
3.3	Sizes and information bits density of HD2DC printed at 600 dpi.	26
3.4	Density performance of 2D-Barcodes.	28
4.1	Proposed VC scheme decoding architecture.	40
4.2	Undesired color combinations of Share 1 and 2.....	43
4.3	Proposed VC color blocks with color interference.	44
6.1	HD2DC-5 color JPEG Results: Corrupted Symbols (%) versus Compression Bitrate (bpp).....	63
6.2	HD2DC-8 color JPEG Results: Corrupted Symbols (%) versus Compression Bitrate (bpp).....	64
6.3	HD2DC-5 color JPEG2K Results: Corrupted Symbols (%) versus Compression Bitrate (bpp).	65
6.4	HD2DC-8 color JPEG2K Results: Corrupted Symbols (%) versus Compression Bitrate (bpp).	66
6.5	HD2DC-5 color H.264/AVC Results: Corrupted Symbols (%) versus Compression Bitrate (bpp).	67
6.6	HD2DC-8 color H.264/AVC Results: Corrupted Symbols (%) versus Compression Bitrate (bpp).	68

Acronyms

2D	Two-Dimensional
BCH	Bose-Chaudhuri-Hocquenghem
CII	Computer-Implemented Invention
CMOS	Complementary Metal-Oxide Semiconductor
CQR Code	Colored Quick Response Code
EVC	Embedded Extended Visual Cryptography
GIF	Graphics Interchange Format
H.264/AVC	Advanced Video Coding
HCC2D	High Capacity Colored Two Dimensional Code
HCCB	High Capacity Color Barcode
HD2DC	High Density 2 Dimensional Code
HSV	Hue, Saturation and Value
ISO	International Organization for Standardization
IEC	International Electrotechnical Commission
JPEG	Joint photographic experts group
JPEG2000	Joint photographic experts group 2000
LDPC	Low-Density Parity-Check
MitM	Man in the Middle
PVC	Polyvinyl Chloride
QR Code	Quick Response Code
RF	Radio Frequency
RS	Reed-Solomon
RSA	Rivest-Shamir-Adleman
TAN	Transaction Authentication Number
VC	Visual Cryptography

1 INTRODUCTION

Nowadays, smartphones are the top-selling electronic devices by far in consumer electronics market. Based on Gartner's report, cellphones and tablets sales surpassed one billion units in 2014 [10]. Most smartphones have a camera that is capable, among other things, of decoding barcodes. Also, high-end smartphones have a high resolution display screen with current models providing up to 4K pixel resolution, which is capable of reproducing colored pixels with a high precision level.

According to Gartner IT Glossary, mobile payments are transactions accomplished within a mobile phone and payment instruments that include cash, bank account, or debit/credit card. Data is processed through Stored Value Accounts, such as transport card, gift card, Paypal or mobile wallet [11]. By 2018, more than 50 percent of electronic devices customers will use a tablet or a smartphone for all online activities, this includes e-commerce and Internet banking. In emerging economies, users are adopting smartphones as their exclusive devices while in developed economies, multi-device households are becoming the norm [12].

1.1 PROBLEM STATEMENT

In the first semester of 2016, there were R\$685 millions (approximately equivalent to US\$207 millions) in loss due to electronic frauds in Brazil. This represents an increase of around 36% when compared to the first semester of 2010 [13]. Also in 2016, according to the Brazilian Banking Federation (FEBRABAN), there was a record number of system invasions or electronic frauds in banking systems. Most invasions are consequences of Man-in-the-Middle (MitM) attacks, which are one of the most common attacks to information security systems [14–17]. Most cryptosystems generally focus on the algorithm networking functionality and, usually, do not take into account the way users interact with the digital system.

Most of current e-commerce applications rely on login and password authentications, which can be easily stolen in real-world scenarios. Generally, authentication and data validation are processed using algorithms, without the use of a physical (non-electronic) device, which reduces the security perception level at the user side. Cryptographic software (encryption algorithms, hash functions, etc) or hardware run their algorithms in a way such that users do not understand how the cryptographic primitives work. But, the notion of trust is strongly associated with the perception of security [18] and it is considered an important characteristic of the usability of the human-machine interfaces.

Some cryptosystems use physical-electronic devices as part of their solutions for transaction authentication. Examples of such devices include Transaction Authentication Number cards (TANs), secure tokens, and mobile communication devices. These technologies are robust enough

for authentication purposes in e-commerce applications, but they are vulnerable to attacks to their physical electronic structure. Unfortunately, statistics show that frauds in these devices, caused by attacks at the user side, grow every year [19].

Monochromatic and colored 2D barcodes can also be used in cryptosystems. Among barcodes, the Quick Response Code (QR Code) [20] is the most used one [21–24]. Two-dimensional barcodes generally carry short cryptographic primitives (in bits), which are decoded to access data in a server. To increase the amount of data stored in a QR Code, it is necessary to use larger versions of QR Code. Because of problems of image size and misalignments [25, 26], these QR Codes are not easily decoded by existing Android and iOS applications. Therefore, currently available 2D barcodes are not reliable for high density information retrieval.

As mentioned earlier, in cryptography, the perception of security is also associated to the notion of ‘trust’. Most people agree that e-commerce can only become a success if the general public trusts the virtual environment [19]. Therefore, the perception of security is important for the adoption of new systems. In systems that use physical tools as part of coding and decoding processes, the perception of security is high due to factors like experience, perception, intuition, and reasoning [19].

Another interesting method for data validation is Visual Cryptography, which is a technology that allows users to decode concealed images without the use of any computation or software. The user visually decodes the concealed image by superimposing two or more printed images called shares. Most Visual Cryptography schemes increase the image pixel size to allow visual decryption, this technique is known as pixel expansion. A pixel expansion is performed with at least $n \times n$ ($n \geq 2$) pixels, for each of the 2 or more shares. In other words, to create the shares, the encoding algorithms expand the representation of the secret (concealed) images in the shares and, consequently, of the decoded secret image. Pixel expansion restricts the usability of Visual Cryptography in real scenarios because of the large image sizes necessary to transmit information and the poor visual quality.

Using mobile screens, as one share, and printed transparencies, as a second (or third) share, makes it possible to merge digital-mobile communication tools and non-electronic devices for data validation. This approach increases the perception of security. It is worth pointing out that current Visual Cryptography schemes use two or more transparencies as shares and require a pixel expansion. Therefore, these methods generate images with low quality, which are far from ideal for mobile security applications.

1.2 PROPOSED APPROACH

Considering the preceding discussion, in this work we develop two data validation systems. The first is a new 2D-colored barcode standard called High Density Two Dimensional Code (HD2DC). This proposed 2D barcode can be used as main tool of an off-line information re-

trieval system, which uses a printed or screen-displayed 2D barcode. HD2DC is a standard with 8 versions. The first version has 30×30 modules and, for each version, the module size increases by 10×10 . Version 8 has 100×100 modules. Also, each version can be generated with 5 or 8 colors and three error correction levels: Low, Medium and High.

In its highest version, with the lowest error correction level, and a printed area of $2\text{cm} \times 2\text{cm}$, HD2DC is able to transmit 2,906 bytes. This maximum storage capacity is close to a QR Code version 40, which counts with 177×177 modules and carries 2,953 information Bytes [27]. The main difference between HD2DC and QR Code is that the QR Code requires a much larger printed area in order to be correctly decoded [25, 26], i.e. HD2DC requires only 31.92% the printed area required by a QR Code to store the same information. Additionally, HD2DC is robust to JPEG, JPEG2000, and H.264/AVC compressions. The HD2DC prototype was implemented in a Matlab programming environment. Up to our knowledge, the proposed 2D-barcode is currently the barcode with the highest data density (bytes/in²) in the literature.

The second system proposed in this work is a Visual Cryptography scheme that does not require a pixel expansion in the coding and decoding steps. The scheme uses a superposition of a colored printed-transparency (share 1) of Polyvinyl Chloride (PVC) on a mobile screen (share 2). An animated version of this Visual Cryptography approach was created, and uses $p > 1$ Shares 2 stored into a GIF image sequence, where only one of the p Shares 2 reveals the secret image when superimposed on Share 1. This approach improves the reusability of Share 1. The details of the proposed cryptosystem were chosen according to color spectrum theory, taking into account the measured luminance and color interference of the PVC printed material. Images that compose Shares 1 and 2 are created in a Matlab programming environment. The usage of physical devices, such as 2D barcodes and printed PVC transparencies, increases the user perception of security, which is a fundamental element on the notion of trust and usability of a cryptosystem. Up to our knowledge, the proposed VC scheme is the first real-time Xor-Based (without pixel expansion) VC scheme with only 2 shares.

In order to improve the security perception of the proposed VC scheme, an HD2DC can be used as storage tool for Share 1. A VC validation system is created using the HD2DC as storage and retrieval tool for Share 2, using the 1024-bit Rivest-Shamir-Adleman (RSA) data encryption algorithm. This system allows displaying Share 1 only to users that have access to the HD2DC, its decoding software, and the 1024-bit RSA private key. Since an HD2DC barcode is capable of encoding 2,906 bytes, a 140×140 image (Share 2) can be decoded scanning an HD2DC barcode. Next, Share 1 can be superimposed to Share 2 on the mobile screen to reveal the secret image.

1.3 DOCUMENT OUTLINE

The remainder of this document is organized as follows. Chapter 2 gives a brief introduction to 2D barcodes and Visual Cryptography. Chapter 3 presents the HD2DC structure, coding and

decoding steps, and shows robustness tests on the print-scan scenario and JPEG, JPEG2000 and H.264/AVC algorithms. Chapter 4 describes the proposed Visual Cryptography structure, detailing the generation of shares and the obtained results. The data validation system with HD2DC and the proposed VC scheme is also presented in Chapter 4. Finally, Chapter 5 shows our conclusions.

2 BACKGROUND

This Chapter briefly describes the most important characteristics of 2D barcodes and Visual Cryptography technologies present in literature.

2.1 TWO-DIMENSIONAL BARCODES

Barcodes are one of the most prevalent automatic identification and information storage technologies. Two-dimensional barcodes are widely used in several applications as optical machine-readable tool on channel transmission mediums. While barcodes store information in one direction (horizontal), two-dimensional barcodes store information in two directions (horizontal and vertical), providing a higher data capacity. When compared to other technologies like radio frequency (RF) tags or chips, two-dimensional barcodes are a cheaper solution for automated data transmission applications. However, 2D-barcode systems need to “see” the code, while RF-based systems do not.

2.1.1 QR Code

Among two-dimensional barcode techniques, the QR Code is one of the most popular standards. It was originally proposed in 1994 by the Japanese company Denso Wave Incorporated. In 2005, it was approved as the ISO/IEC 18004 standard [20]. QR Codes are frequently used in advertisements, business cards, storefront displays, t-shirts, letter stamps, movie posters, product labels, information security, etc [22, 26, 28]. Figure 2.1 (a) shows an example of a QR Code.

The basic component for storing information in a two-dimensional barcode is a module (square or triangle). In the QR Code standard, each module represents a single bit, with a black module storing a bit ‘1’ and a white module a bit ‘0’ in the encoding region. Most applications link the stored data to additional on-line server content, thus, the 2D barcode can be used as a tool to obtain a higher data storage capacity.

The QR Code standard has 40 versions. The first version has 21×21 modules. For each version the size of the modules increases by 4×4 , with version 40 having 171×171 modules. QR Codes also work with four Reed-Solomon error correction levels: L - 7%, M - 15%, Q - 25% and H - 30% [20]. The redundancy symbols of the error-correction algorithm allow the correction of wrong decoded modules on the image capture process.

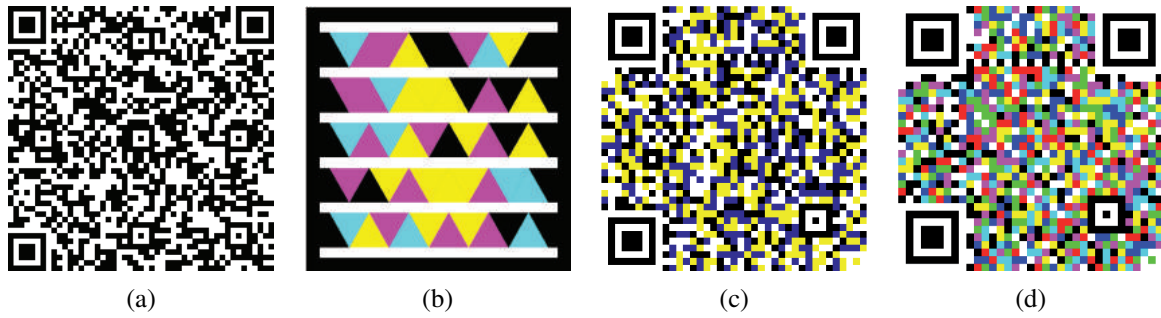


Figure 2.1: Examples of 2D barcodes: (a) regular QR Code [1], (b) Microsoft HCCB [2], (c) HCC2D prototype for 4-colors HCC2D [3] and (d) HCC2D prototype for 8-colors HCC2D [3, 4].

2.1.2 HCCB, HCC2D and Per Channel Data Encoding

Recently, two-dimensional barcodes that use colors for improving data storage have been proposed with the goal of increasing the amount of stored bits within the printed area [2, 3, 29, 30]. An example of a two-dimensional barcode with colors is the High Capacity Color Barcode (HCCB) created by Microsoft Corporation [2], shown in Figure 2.1 (b). This type of barcode uses rows of strings with triangular modules and with consecutive rows separated by white lines. In its two versions, HCCB uses four and eight different colors respectively. HCCB is a non-open source software and there is no easily available documentation describing its functionality and its robustness to image compression algorithms and to print-scan processes.

Another example of a two-dimensional barcode is the High Capacity Colored Two Dimensional Code (HCC2D) [3]. This two-dimensional barcode prototype is based on the QR Code standard, using a similar QR Code structure, error-correction algorithm, and data masking process. HCC2D can be created using 4 and 8 colors. Figures 2.1 (c) and (d) show examples of HCC2D for 4 and 8 colors, respectively [3]. HCC2D has a high information storage capacity per printed square inch, which is similar to HCCB and higher than regular QR Codes [3, 4]. Marco Querini and Giuseppe F. Italiano report performance decoding results considering module colors and data density for this 2D colored barcode [4]. In this article, the 2D barcode reaches a data density of $3,819.76 \text{ bytes}/\text{in}^2$ with 95% decodification success rate using K-means segmentation algorithm on the decoding process.

An alternative high capacity 2D barcode encoding and decoding system was proposed by Orhan Bulan and Gaurav Sharma [31]. Their scheme can be used by any monochrome 2D Barcode structure, by considering an orientation modulation with elliptical dot arrays over the 3 channel colors (cyan, magenta, and yellow). This method reaches a data density of $2,800 \text{ bytes}/\text{in}^2$. The authors also proposed a per-colorant channel interference cancellation [32] to improve the estimated decoded color of each module.

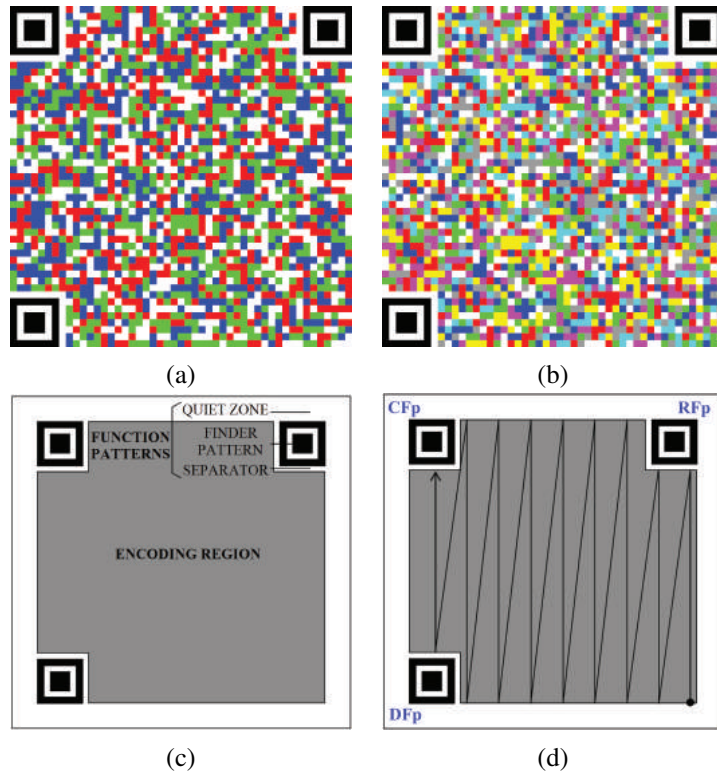


Figure 2.2: Examples of CQR Codes (a) CQR Code-5 [1] and (b) CQR Code-9 [5]. CQR Code characteristic: (c) CQR Code structure [5] and (d) CQR Code positioning in the encoding region [5].

2.1.3 CQR Code-5 and 9

Two 2D-colored barcodes were proposed in our previous work: CQR Code-5 [1] (initially called CQR Code) and CQR-9 [5]. Sample barcode images of these two schemes are shown in Figures 2.2 (a) and (b), respectively. They have the same structure (which is similar to the QR Code structure) and filling bits direction see Figure 2.2(d)). The CQR Code structure is made up of 49×49 modules, which are distributed over two discriminate regions: the function patterns' and the encoding region.

The function patterns have exactly the same aspect for all CQR Codes and are divided into: (a) quiet zone; (b) finder patterns; and (c) separators. Figure 2.2 (c) illustrates these elements. The quiet zone is the 4×4 module white area that surrounds the barcode on all four sides [1]. Separators are the 1×8 or 8×1 -module elements that separate encoding region and finder patterns. Finder patterns are the three identical symbols located at the upper-left, upper-right, and lower-left corners of the code and are used for correct image positioning at the decoder. The encoding region contains information and redundancy bits. The positioning of the modules in the encoding region is vertical bottom-up, from the most right to the most left column, as shown in Figure 2.2 (d).

CQR Code-5 stores 2 bits per module and uses 4 different information and redundancy modules (00 - red, 01 - green, 10 - blue and 11-white), while CQR Code-9 stores 3 bits per module and employs 8 different modules (000 - red, 001 - green, 010 - blue, 011 - cyan, 100 - magenta,

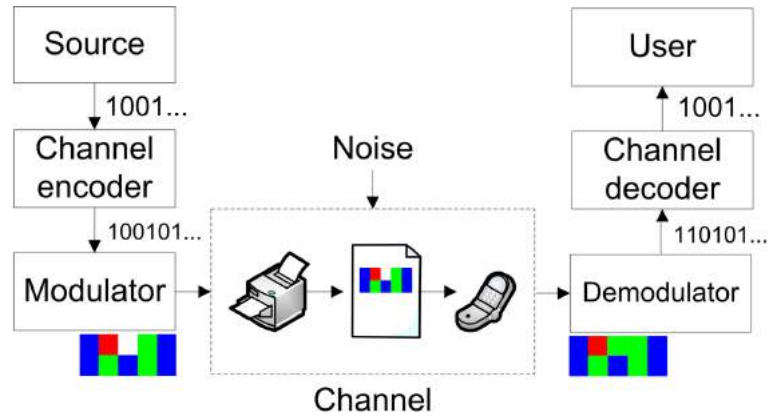


Figure 2.3: Block diagram of a communication system that considers print-scan storage and transmission stages [1].

101 - yellow, 110 - white and 111 - gray). In both cases, black modules are used only for rotation and alignment purposes. CQR Codes use the Berlekamp Reed-Solomon [33] error-correction code. This error correction algorithm has the following parameters: n (total amount of symbols), k (amount of information symbols), and t (error correction capacity in symbols).

CQR Code-5 is capable of encoding 1,024 bits of information bits plus 3,392 redundancy Berlekamp Reed-Solomon bits [33]. On the other hand, CQR Code-9 allows encoding up to 2,048 information bits in the same printed area, requiring 4,576 redundancy Berlekamp Reed-Solomon bits [33]. Each Berlekamp Reed-Solomon symbol for both CQR Codes has 16 bits, CQR Code-5 and CQR Code-9 employ the error correction configuration of RS(276, 64) and RS(414, 128), respectively, with the following primitive polynomial:

$$p(D) = D^{16} + D^{12} + D^3 + 1. \quad (2.1)$$

A Berlekamp Reed-Solomon decoder can correct up to t symbols that contain errors in n symbols, t is being determined by the following equation:

$$t = \frac{n - k}{2}. \quad (2.2)$$

The print-scan process may be modeled as a communication system, where the 2D barcode is generated to store and retrieve binary information. This communication model is illustrated in Figure 2.3. Therefore, information transmitted through a CQR Code structure may be susceptible to errors. For CQR Code-5, $t = 106$. Therefore, it is possible to completely recover the 64 information symbols, even if up to 38.41% of the n symbols are lost or degraded. CQR Code-9 can correct 143 symbols, i.e. it provides an error correction rate of 34.54%.

The impact of compression algorithms on the decoding process of the CQR Code-5 was described in a previous publication [34], where it was shown what are the maximum JPEG, JPEG2000, and H.264/AVC compression bitrates that can be used by the CQR Code-5. The compression rates are measured on Bits Per Pixel (bpp). It was verified that the CQR Code-5

is successfully decoded for compression rates higher than 0.3877 bpp, 0.1093 bpp, and 0.3808 bpp for JPEG, JPEG2000, and H.264/AVC, respectively. The algorithm that presented the best performance was H.264/AVC, followed by JPEG2000, and, finally, by JPEG [34].

For the smallest module size, CQR Code-9 can store and transmit 6,624 bits of information and redundancy data. In a printed area of $1.3\text{cm} \times 1.3\text{cm}$, this gives a rate of 3.086 KBytes information data per square inch. A printed version of CQR Codes was also tested on a real print-scan channel communication scenario. Performance tests of printed versions of CQR Codes-5 and 9, with size of $1.3\text{cm} \times 1.3\text{cm}$, using a printer Ricoh MP C2051 and regular office A4 paper with $75\text{g}/\text{m}^2$ density are detailed in previous work [1, 5]. Further details of the decoding process, such as decoding flowchart, image segmentation and experimental results, can be found in these previous publications [1, 5].

2.2 VISUAL CRYPTOGRAPHY

Visual cryptography (VC) techniques were originally proposed by Moni Naor and Adi Shamir [35]. In these techniques, a secret image is encoded in $n=2$ or more shares. Each share does not reveal details of the secret image. The first step of any VC algorithm is to choose a secret image and encode it into a number of images (known as shares). When these shares are printed onto transparencies, the secret image can be visually detected by stacked together (physically superimposed) k out of n ($k \leq n$) concealed shares. . This way, an average person is able to recover the secret image without any knowledge of cryptography and without performing any computation.

In a traditional VC system, the original secret image is retrieved by superimposing k share images and detecting a pattern, symbol, or message in the resulting image. Generally, a VC scheme has (k, n) as parameters that satisfy the following conditions: (1) we can recover the secret image with any k out of n share images; (2) with less than k share images, it is not possible to recover or get any information about the secret image.

2.2.1 Black and White Visual Cryptography

The first ever proposed VC scheme represents a black or white pixel by choosing a pair of 2×2 (expanded) pixels, which are used for representing a single pixel of the secret image. Figure 2.4 shows three possible chosen pixels. This method has the following parameters: $k=2$ and $n=2$, with a resulting pixel expansion of 2×2 for each original pixel [35]. Expanded pixels are generated according to two basic rules: (1) If the pixel of the original binary image is white, randomly pick the same pattern of four pixels for both shares. (2) If the pixel of the original image is black, a complementary pair of patterns is randomly chosen. Therefore, in this case a pixel expansion of 2×2 is necessary to generate the shares.

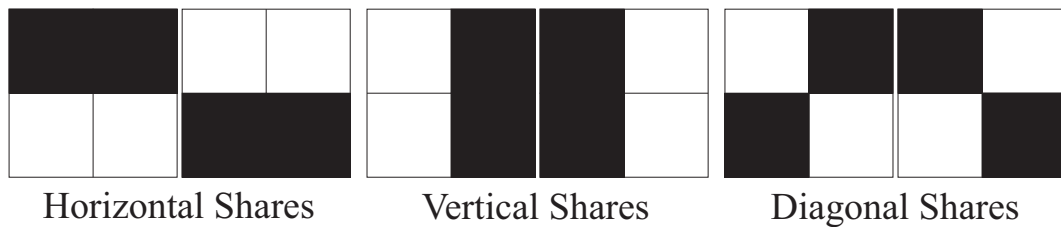


Figure 2.4: Traditional VC shares: Three possible complementary pixel expansions.

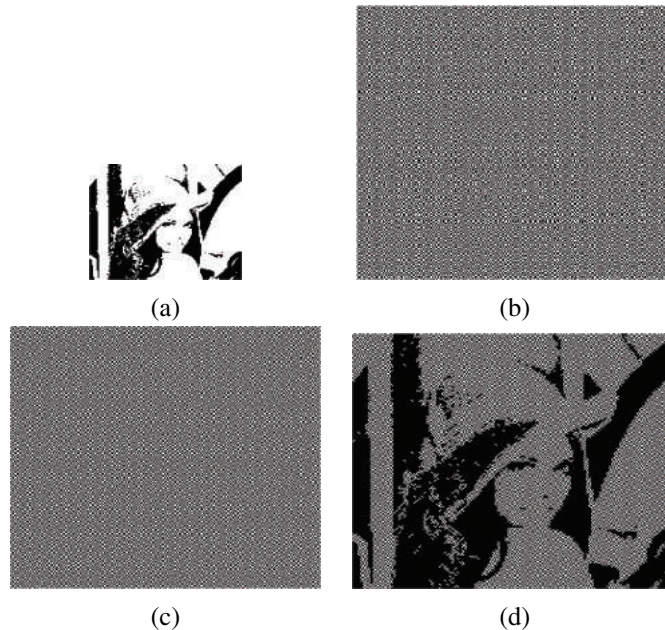


Figure 2.5: Examples of traditional VC scheme: (a) secret image, (b) share 1, (c) share 2 and (d) share 1 and share 2 superimposed to recover (visually) the secret image.

When the transparencies are overlapped and correctly aligned, the expanded pixels in the combined shares are represented by the Boolean OR of the columns and rows in the matrix. An example of an expected result of a traditional VC scheme is shown in Figure 2.5. In this illustration the secret image is shown in (a), while (b) and (c) show the shares, and (d) shows the decoded secret image. Here, the two shares and the decoded image have $2 \times 2 = 4$ times the size of the secret image. As this method uses pixel expansion of 2×2 pixels, its implementation is possible [35].

Embedded Extended Visual Cryptography (EVC) schemes allow the construction of n meaningful images on shares using gray color images, which are represented using digital Halftoning algorithm. The Halftoning algorithm simulates continuous tone color regions through the use of dots. In a Halftone VC, a secret binary pixel is encoded into an array of sub pixels, called a halftone cell [36]. As each pixel of the original image is enlarged on halftone cells and the two (or more) shares are created, the pixel expansion will be equal to the expansion caused by the halftone algorithm plus the expansion caused by the traditional VC. This high size demand results in low quality images, making this technique less adequate for practical applications. In

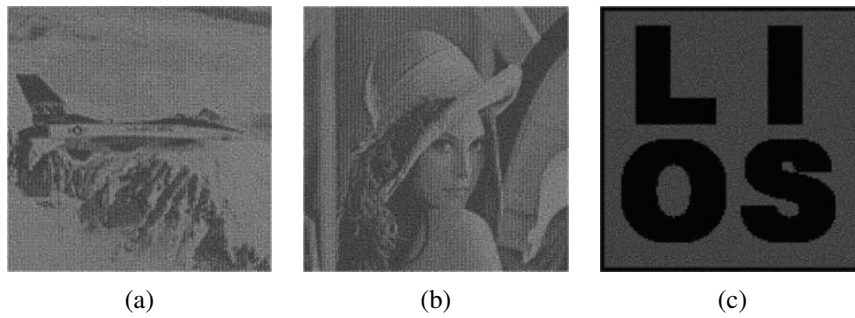


Figure 2.6: Example of EVC: (a) Share 1, (b) Share 2 and (c) decoded secret image [6].

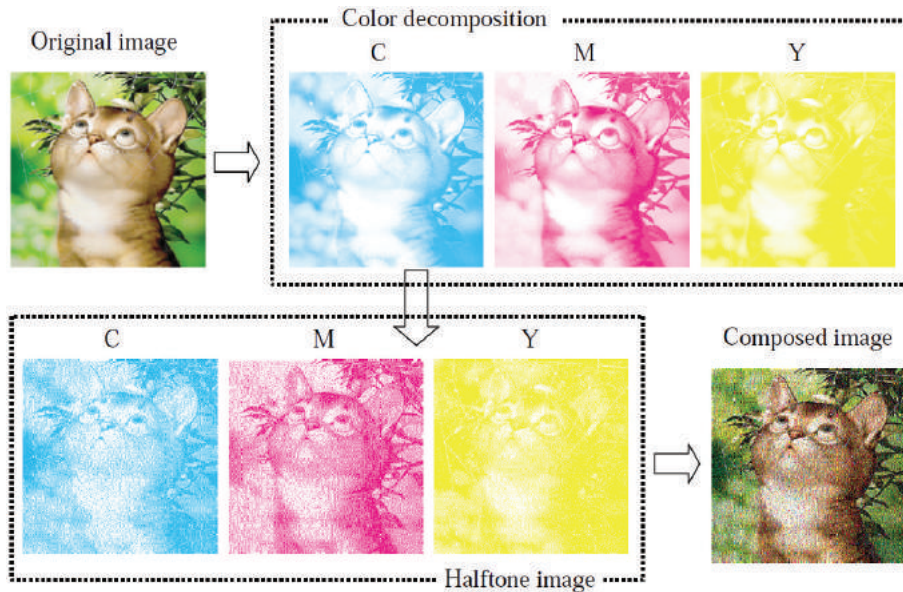


Figure 2.7: Halftoning decomposition on C, M and Y colors [7].

these schemes, shares are superimposed, causing the meaningful information to disappear and the secret to be recovered [6]. For this VC scheme, limitations include a large pixel expansion and a bad visual quality of both the shares and recovered secret image [37]. An example of EVC is illustrated in Figures 2.6 (a), (b) and (c).

2.2.2 Color Visual Cryptography

Color VC uses additive (red, green and blue) and subtractive (cyan, magenta and yellow) colors to describe pixels on shares. The desired colors are obtained by mixing different color components. The three most popular Color VC methods were proposed by Young-Chang Hou [7]. The first method takes as input a color secret image and creates three C (cyan), M (magenta), and Y (yellow) halftone images. Figure 2.7 shows the steps of this process. For each halftone, a pixel expansion of 1:4 is necessary. Every pixel in the shares includes two transparent (white) pixels and two color pixels (C, M or Y). This system also includes a black-and-white mask to generate unexpected colors on the stacked sharing images.

Mask	Revealed color (C,M,Y)	Share1(C)	Share2(M)	Share3(Y)	Stacked image	Revealed color quantity (C,M,Y)
	(0, 0, 0)					(1/2, 1/2, 1/2)
	(1, 0, 0)					(1, 1/2, 1/2)
	(0, 1, 0)					(1/2, 1, 1/2)
	(0, 0, 1)					(1/2, 1/2, 1)
	(1, 1, 0)					(1, 1, 1/2)
	(0, 1, 1)					(1/2, 1, 1)
	(1, 0, 1)					(1, 1/2, 1)
	(1, 1, 1)					(1, 1, 1)

Figure 2.8: Color composition for superposed shares on method 1 [7].

The encoding and decoding processes use the superposition of three shares (C, M and Y) and a fourth transparency with a black mask pattern. The color composition of the overlapped transparencies is illustrated in Figure 2.8. Due to the mask, the stacked image always has 2 black pixels (upper left and bottom right), while the remainder two pixels carry the resulting color produced by a combination of secondary colors (cyan, magenta and yellow). Therefore, this method produces a non-continuous-tone image that can only be perceived using transparencies. The color superimposition in this method gives the proportion of each color (C, M and Y) that is used in the unmasked pixels to produce 8 different colors (primary colors, secondary colors, white and black) in 2 of the 4 expanded pixels.

We can notice that this method has the same challenges of EVC. It uses 4 transparencies (3 shares and 1 mask) and, because of alignment and pixel expansion difficulties, it has not been shown working in practical applications. The second Color VC scheme proposes the use of tiny printed pixels in 2 shares. In this case, users should be able to decode the superimposed shares observing an average color super pixel, which equalizes the effect of the four stacked pixels (cyan, magenta, yellow and transparent) and results in a single color being perceived. The color composition process used in this method is shown in Figure 2.9.

The color composition of this second method of colored VC considers the proportion (perceived color) of each expanded pixel to determine the final (desired) color. Naturally, after stacking the sharing images, the color contrast is 25% of the original contrast. Therefore, the color saturation of the image generated by this second method is worse than the color saturation of an image by the first method [7]. Since this second method uses several pixels for a single pixel expansion, its usability in a practical application is low due to alignment issues and the large amount of data required. Figure 2.10 shows the 2 shares and the decoded image for this method. Notice that for a non-theoretical application, the decoded image has a low image quality.

Finally, a third method uses 2 shares for decryption, while transforming a secret color image into three halftone images (C, M, and Y) and generating six temporary shared images (C1, C2,

Revealed color (C,M,Y)	Share 1	Share 2	Stacked image	Method	Resultant result	Revealed color quantity (C,M,Y)
(0, 0, 0)				Share 1 and Share 2 with the same permutation		(1/4, 1/4, 1/4)
(1, 0, 0)				Swap the position of cyan and transparent		(1/2, 1/4, 1/4)
(0, 1, 0)				Swap the position of magenta and transparent		(1/4, 1/2, 1/4)
(0, 0, 1)				Swap the position of yellow and transparent		(1/4, 1/4, 1/2)
(1, 1, 0)				Swap the position of cyan and magenta		(1/2, 1/2, 1/4)
(0, 1, 1)				Swap the position of yellow and magenta		(1/4, 1/2, 1/2)
(1, 0, 1)				Swap the position of cyan and yellow		(1/2, 1/4, 1/2)
(1, 1, 1)				Swap two positions in pair		(1/2, 1/2, 1/2)

Figure 2.9: Color composition for superposed shares on method 2 [7].

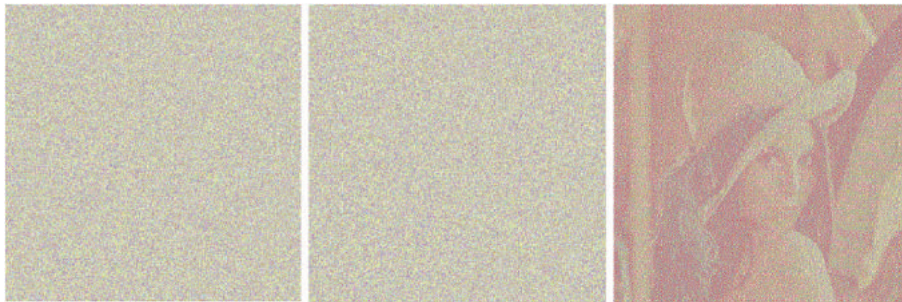


Figure 2.10: Two sharing transparencies and the stacked effect for method 2 [7].

M1, M2, Y1, and Y2). Each of the six shared images have two transparent pixels and two color pixels for every 2×2 expanded pixels. Then, the method combines C1, M1, and Y1 to form a colored halftone share 1 and combine C2, M2, and Y2 to form share 2 [7]. Figure 2.11 (a) shows an example of a color composition for a blue expanded pixel, while Figures 2.11 (b), (c) and (d) show examples of the decoding process.

For this third method, the resulting image has, after the Halftoning, a pixel expansion of 2×2 pixels. From these 4 pixels, 2 diagonal pixels (upper right and bottom left) are black due to the subtractive color combination (see combination of red and green pixels in Figure 2.11 (a)) and the remainder 2 pixels have the desired color (blue color in the example of Figure 2.11 (a)). The resulting expanded pixels always have 2 black pixels on the diagonal and 2 pixels representing the desired color. Therefore, this scheme shows a decoded image with 50% of dark pixels.

All 3 methods described require a large amount of expanded pixels (due to Halftoning and

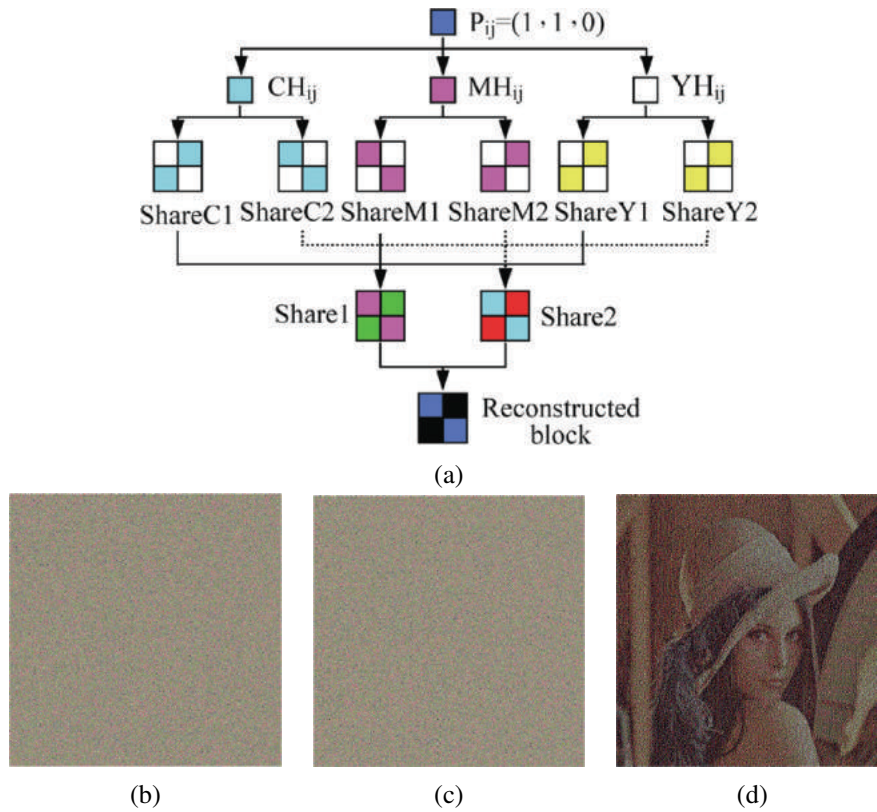


Figure 2.11: Third method of Color VC: (a) color composition, (b) share 1, (c) share 2 and (d) decoded image [7].

the pixel expansion). Unfortunately, the authors did not show results obtained using real printed transparencies. Since these VC schemes employ tiny printed pixels and 2 or more shares, its implementation might be impracticable. Also, none of these methods was proven to work using a digital screen as one of the shares.

2.2.3 Xor-Based Visual Cryptography

XOR-based VC schemes do not use pixel expansion, they are designed to improve the quality of the decoded image [38]. A real-time XOR-Based VC scheme was proposed by Tuyls *et al.* [8]. In their work, the colored secret image is revealed using a hardware implementation and the superimposition of four shares (2 polarization filters, 1 color filter, and 1 liquid crystal), as shown in Figure 2.12. Although the solution provides good contrast properties, the decrypted image has a limited spatial resolution and the method requires 4 shares, which leads to alignment problems. It is worth pointing out that F. Liu *et al.* [39] proposed VC and EVC schemes that use Tuyls' model and did not require a pixel expansion.

Recently, a color VC scheme with no pixel expansion was proposed by Shiori *et al.* [9], which is based on the interference color (different from color interference) theory. In this method, the color passes through a laboratory prepared mineral layer (thin-section mineral) composed of crossed polarizers layers of high-order and retarder films, which changes the phase of the incident light. The retarder films exhibit an interference color property when they are placed between two

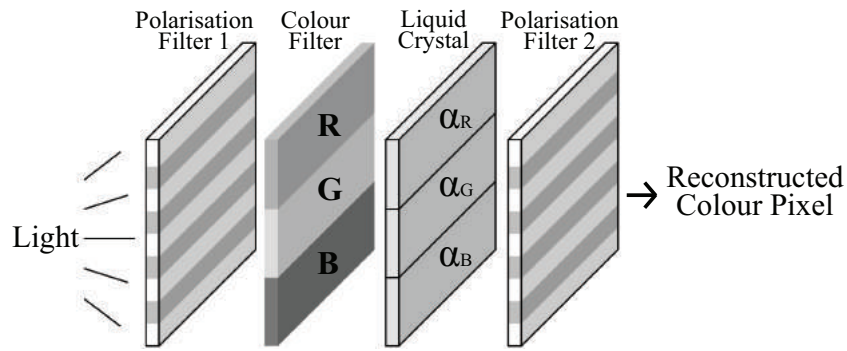


Figure 2.12: Hardware implementation of colour XOR-Based VC scheme [8].

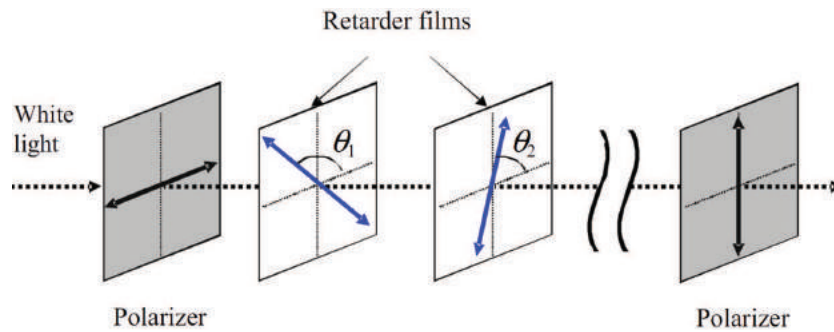


Figure 2.13: Optical arrangement of polarizers and retarder films [9].

polarizer films. The authors implement two versions of this VC scheme. Figure 2.13 shows the first version of the method, which uses 2 polarized films and 2 retarded films. The second one employs 2 polarized films and 3 retarded films as shares.

Notice that the angle between the transmission axis of the polarizers and retarder films can be varied to display a high-chroma image. Although these methods do not require a pixel expansion, they use at least 4 shares, which can produce alignment difficulties. Also, polarizers and retarder films are currently expensive, which reduces the range of practical applications.

2.2.4 Discussion on currently available 2D barcodes and VC schemes

We believe that a high information density 2D-barcode is necessary for applications that need to carry high information quantity in small available area, such as medicine and cigarette carton box. A tracking and validation system could be implemented using cryptographic data on a small area printed 2-D barcode. The next Chapter shows the proposed 2D-barcode, which is the denser 2D-barcode in literature.

There are no VC schemes with only 2 shares and without pixel expansion in literature. We believe that such VC scheme could improve spatial resolution and alignment issues. Chapter 4 shows the proposed VC scheme, which is the first work with only 2 shares and with no pixel

expansion.

3 A TWO-DIMENSIONAL COLORED BARCODE: HD2DC

In this Chapter we describe the specification of our proposed 2D-barcode: the High Density Two Dimensional Code (HD2DC).

3.1 HD2DC - ENCODING PROCESS

The proposed HD2DC has 8 versions. Version 1 corresponds to 30×30 modules, version 2 corresponds to 40×40 modules, and so on. Each version represents an increase of 10×10 modules, with version 8 corresponding to 100×100 modules. For each version, two set of colors can be used: HD2DC-5 uses 5 colors (black, white, red, green and blue), while HD2DC-8 uses 8 colors (black, white, red, green, blue, cyan, magenta and yellow). Also, each selected version and color can have three error correction levels: Low (L - 10%), M - Medium (20%) and High (H - 30%). Based on the amount of versions, colors, and error-correction levels, a HD2DC can be generated in 48 different formats. Figure 3.1 shows examples of HD2DCs with 5 and 8 colors, for their smaller and bigger versions. Figure 3.1 shows the HD2DC structure, All HD2DC versions have the same structure, which is divided into Function patterns and Encoding region areas.

3.1.1 Structure: Function Patterns

Function patterns are used to detect the HD2DC barcode location in a barcode image (even in a rotated or tilted capture). Detection is the first step in the decoding process of the HD2DC. As shown in Figure 3.3, Function patterns have exactly the same structure for all HD2DCs versions and are divided into the following areas:

- Quiet zone: Region that is free of any markings and located in the surrounding borders of the HD2DC barcode.
- Finder patterns: Four identical components of the finder pattern in HD2DC, which are located at the four corners (upper right, upper left, bottom right and bottom left) of the HD2DC barcode. Each finder pattern is composed by three superimposed concentric squares, they have as structure 7×7 black modules, 5×5 white modules, and 3×3 black modules. For 5-colors HD2DC, this is the only area where black modules are employed.
- Separators: One or two separators are constructed with white modules. Three Finder Patterns (upper right, upper left and bottom left) use one-module wide separators, while one Finder Pattern (bottom right) employs two-module wide separator. Separators are placed between each Finder pattern and the Encoding Region.

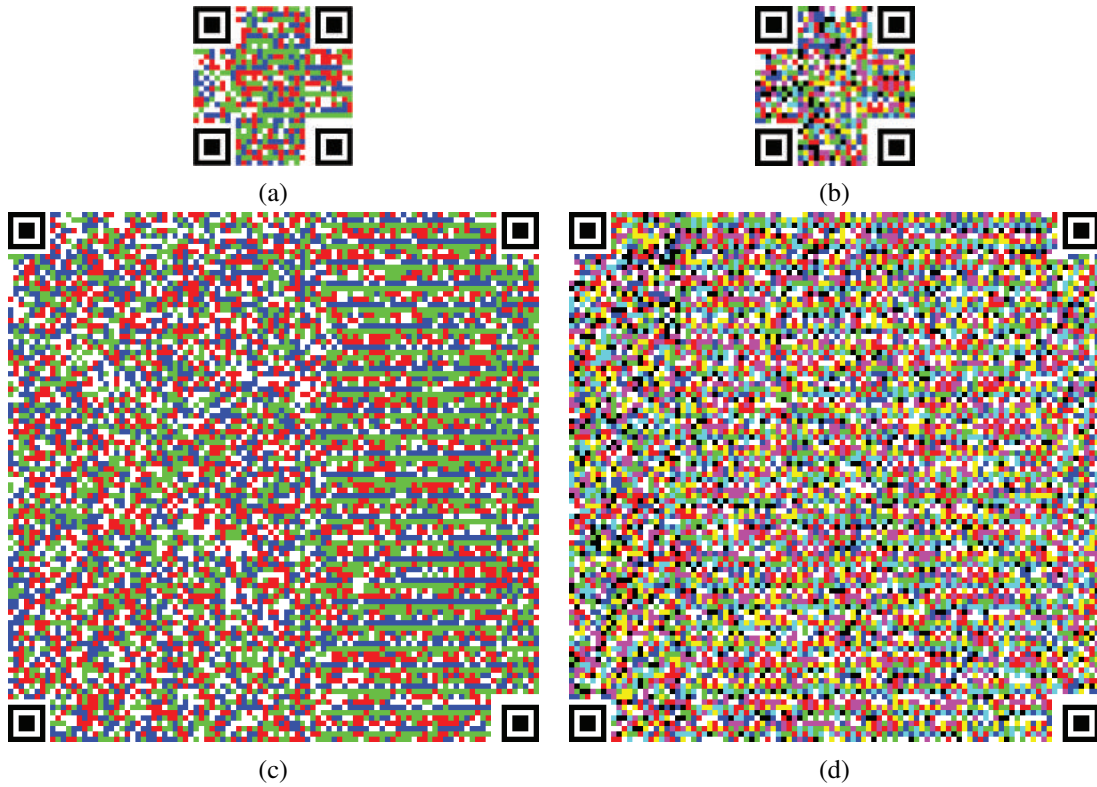


Figure 3.1: Examples of HD2DC of: (a) Version 1, 5 colors, Low error correction capacity and 120 stored bytes, (b) Version 1, 8 colors, High error correction capacity and 90 stored bytes, (c) Version 8, 5 colors, High error correction capacity and 966 stored bytes, and (d) Version 8, 8 colors, Low error correction capacity and 2,906 stored bytes.

3.1.2 Structure: Encoding Region

The Encoding region is divided in two areas that contain data for information retrieval. The Encoding region is illustrated in the dark and light gray area of Figure 3.3, divided in:

- **Decoding Symbols:** These symbols are distributed in 32 modules. Each symbol contains 2 bits, that can be mapped to red ('00' bits), green ('01' bits), blue ('10' bits), and white ('11') module colors. These 32 modules are shown in the light gray area of Figure 3.3. From the 64 available bits, 63 bits are reserved to Bose-Chaudhuri-Hocquenghem (BCH) [40] bits, more specifically, BCH (63,18), and the last bit is considered as a remainder bit and set with value '0'.

In this BCH scheme, $n = 63$ (redundant and information bits) and $k = 18$ (information bits). The k information bits carry the HD2DC structure information as follows: 12 bits specify the number of Bytes (from 1 to 2,906 possible Bytes), 1 bit is reserved for the Encoding Region color (HD2DC-5 or HD2DC-8), 3 bits specify the version information (from version 1 to version 8), and 2 bits are reserved for the error correction capacity of Information and Parity Symbols (Low, Medium or High). Figure 3.4 (a) and Figure 3.2 show an enlarged structure image of the HD2DC and the BCH(63,18) information bits, respectively.

- **Information and Parity Symbols:** This area is filled with Berlekamp Reed-Solomon [33]

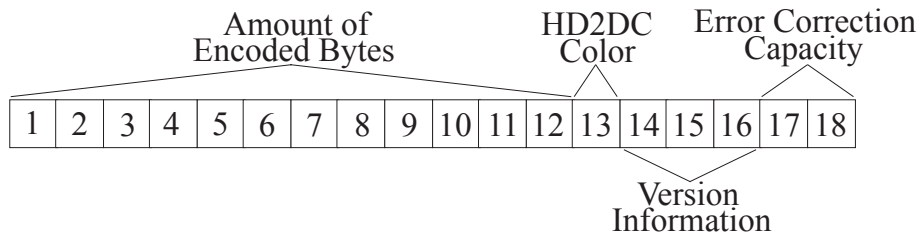


Figure 3.2: HD2DC structure bits composition.

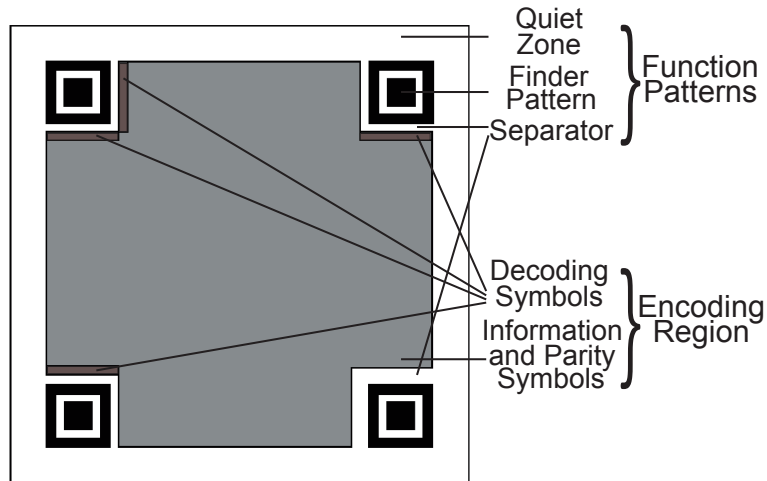


Figure 3.3: HD2DC structure.

information and parity symbols. This error-correction algorithm is employed due to its decodification robustness. It is also widely used by other 2D-barcodes, such as CQR Code, QR Code, HCCB, etc. The resulting bits of all information and redundancy symbols are placed in the dark gray modules of the encoding region, following the vertical bottom-up direction, from the most right to the most left column, as illustrated in Figure 3.4 (b).

The error correction primitive polynomial (shown in Equation 2.1) is the same used by CQR Codes. The quantity of bits per symbols in HD2DC is also the same ($s = 16$). As HD2DC has several versions and error correction levels, it has different n , k , and t Reed-Solomon parameters. There is a total of 48 possible HD2DC architectures (24 for each HD2DC color). Tables 3.1 and 3.2 show the HD2DC construction architectures for 5 and 8 colors respectively.

When 5 colors are used, each module of the Encoding Region contains the following colors: red '00', green '01', blue '10' and white '11'. For 8 color options, colors are red '000', green '001', cyan '011', magenta '100', yellow '101', white '110' and black '111'. The amount of encoded bytes is showed in the first 12 bits of the Decoding Symbols structure (see Figure 3.2). When the maximum amount of stored bytes in a HD2DC is not reached, the remaining bits are filled with uniform pseudo-random values.

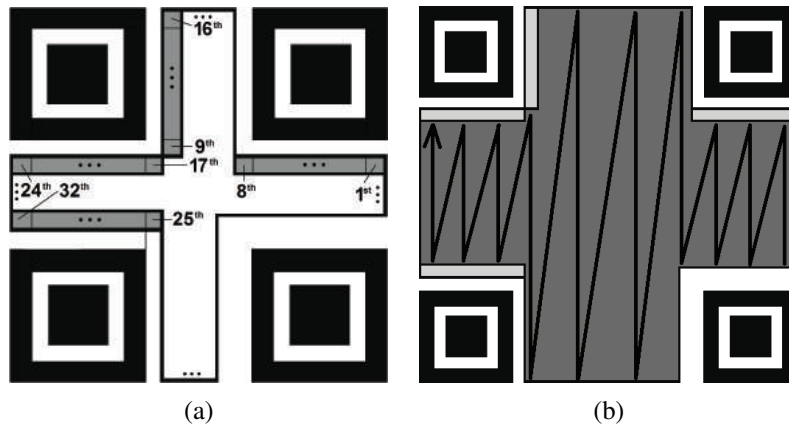


Figure 3.4: HD2DC modules: (a) BCH(63,18) distribution, and (b) HD2DC filling direction.

To generate the Berlekamp Reed-Solomon symbols (with $s=16$ bits per symbol), k symbols are generated (from the data information bytes) as input and n symbols are created as output of this error correction algorithm. The n symbols are mapped into $n \times s$ bits located into the Information and Parity Symbols area, according to the filling direction shown in Figures 3.3 and 3.4 (b). Naturally, the 8-colors structure reaches a higher data capacity than the 5-color structure, since it stores 3 bits per module.

The encoding region color constellation used in HD2DC-5 (red, green, blue and white), and HD2DC-8 (red, green, blue, cyan, magenta, yellow, white and black) was chosen because of their maximum equidistance in the Red, Green, Blue (RGB), and Hue, Saturation, Value (HSV) color spaces, as seen in Figures 3.5 (a) and (b). These colors make it easier to find the color threshold on the decoding step [41]. The bottom right Finder pattern and its two module wide separators are new features introduced in the HD2DC code. This extra white space in the bottom-right Finder Patterns allows to a differentiation of this Finder Pattern and, therefore, of the orientation of the barcode. More specifically, differently from previous 2D barcodes, HD2DC does not have alignment patterns nor timing patterns.

3.2 HD2DC - DECODING PROCESS

To decode a HD2DC, we first capture the barcode image using a digital camera. The HD2DC image can be captured in any rotation angle, the decoding algorithm locates the four Finder patterns that are used to rotate the HD2DC image to the ideal position. With this purpose, the image is first converted to gray scale. Then, thresholds th_1 , th_2 and th_3 are determined for each R, G and B plane using the Otsu's segmentation algorithm [42]. Using the Canny edge detection algorithm [43], the center of the four Finder Patterns are estimated with the calculation of the ratio of black and white modules in the Function Patterns. Results show that this edge detection process is an improvement in comparison to the technique used by the CQR Code, which uses a different Finder Pattern detection process.

Version	Encoding Region Modules	n	k	t	Error Correction %	Information Bytes	Remainder Bits/Modules
1	595	74	60	7	9.46%	120	6/3
1	595	74	46	14	18.92%	92	6/3
1	595	74	30	22	29.73%	60	6/3
2	1,295	161	129	16	9.94%	258	14/7
2	1,295	161	97	32	19.88%	194	14/7
2	1,295	161	65	48	29.81%	130	14/7
3	2,195	274	220	27	9.85%	440	6/3
3	2,195	274	166	54	19.71%	332	6/3
3	2,195	274	110	82	29.93%	220	6/3
4	3,295	411	329	41	9.98%	658	14/7
4	3,295	411	247	82	19.95%	494	14/7
4	3,295	411	165	123	29.93%	330	14/7
5	4,595	574	460	57	9.93%	920	6/3
5	4,595	574	346	114	19.86%	692	6/3
5	4,595	574	230	172	29.97%	460	6/3
6	6,095	761	607	77	10.12%	1,214	14/7
6	6,095	761	455	153	20.11%	910	14/7
6	6,095	761	303	229	30.09%	606	14/7
7	7,795	974	778	98	10.06%	1,556	6/3
7	7,795	974	584	195	20.02%	1,168	6/3
7	7,795	974	388	293	30.08%	776	6/3
8	9,695	1,211	967	122	10.07%	1,934	14/7
8	9,695	1,211	725	243	20.07%	1,450	14/7
8	9,695	1,211	483	364	30.06%	966	14/7

Table 3.1: HD2DC-5 color information structure.

3.2.1 Version Estimative

To estimate the size version of the HD2DC barcode, we use Euclidean geometry to compute the mean size (in pixels) of the modules around the four Finder Patterns of the barcode, S_{FP} . Next, for each version ($1 \geq i \geq 8$), we calculate the mean module size (in pixels), S_M , computed as:

$$S_M(i) = \frac{0.25 \times (D_{AB} + D_{BC} + D_{CD} + D_{DA})}{13 + 10 \times i}, \quad (3.1)$$

where D_{XY} corresponds to the distance (in pixels) between the consecutive center of Finder Patterns X and Y , with the 4 Finder Patterns being A , B , C , and D . Finally, the version is estimated using the following equation:

$$\text{Version} = \begin{cases} 1, & \text{if } \frac{S_M(1)+S_M(2)}{2} < S_{FP}; \\ 2, & \text{if } \frac{S_M(2)+S_M(3)}{2} < S_{FP} \leq \frac{S_M(1)+S_M(2)}{2}; \\ 3, & \text{if } \frac{S_M(3)+S_M(4)}{2} < S_{FP} \leq \frac{S_M(2)+S_M(3)}{2}; \\ 4, & \text{if } \frac{S_M(4)+S_M(5)}{2} < S_{FP} \leq \frac{S_M(3)+S_M(4)}{2}; \\ 5, & \text{if } \frac{S_M(5)+S_M(6)}{2} < S_{FP} \leq \frac{S_M(4)+S_M(5)}{2}; \\ 6, & \text{if } \frac{S_M(6)+S_M(7)}{2} < S_{FP} \leq \frac{S_M(5)+S_M(6)}{2}; \\ 7, & \text{if } \frac{S_M(7)+S_M(8)}{2} < S_{FP} \leq \frac{S_M(6)+S_M(7)}{2}; \\ 8, & \text{if } S_{FP} \leq \frac{S_M(7)+S_M(8)}{2}. \end{cases} \quad (3.2)$$

Version	Encoding Region Modules	n	k	t	Error Correction %	Information Bytes	Remainder Bits/Modules
1	595	111	89	11	9.91%	178	9/3
1	595	111	67	22	19.82%	134	9/3
1	595	111	45	33	29.73%	90	9/3
2	1,295	242	194	24	9.92%	338	13/4.33
2	1,295	242	146	48	19.83%	292	13/4.33
2	1,295	242	98	72	29.75%	196	13/4.33
3	2,195	411	329	41	9.98%	658	9/3
3	2,195	411	247	82	19.95%	494	9/3
3	2,195	411	165	123	29.93%	330	9/3
4	3,295	617	495	61	9.89%	990	13/4.33
4	3,295	617	371	123	19.94%	742	13/4.33
4	3,295	617	247	185	29.98%	494	13/4.33
5	4,595	861	689	86	9.99%	1,378	9/3
5	4,595	861	517	172	19.98%	1,034	9/3
5	4,595	861	345	258	29.97%	690	9/3
6	6,095	1,142	912	115	10.07%	1,824	13/4.33
6	6,095	1,142	684	229	20.05%	1,368	13/4.33
6	6,095	1,142	456	343	30.04%	912	13/4.33
7	7,795	1,461	1,167	147	10.06%	2,334	9/3
7	7,795	1,461	875	293	20.05%	1,750	9/3
7	7,795	1,461	583	439	30.05%	1,166	9/3
8	9,695	1,817	1,453	182	10.02%	2,906	13/4.33
8	9,695	1,817	1,089	364	20.03%	2,178	13/4.33
8	9,695	1,817	725	546	30.05%	1,450	13/4.33

Table 3.2: HD2DC-8 color information structure.

3.2.2 Alignment: Projective Transformation

Once the version is known, we need to correct the HD2DC final position. The perspective distortion [44], which is generated on image acquisition, is corrected applying a projective transformation on the four Finder Pattern centers ($n = 4$ matching points). A planar projective transformation is a linear transformation of 3 homogeneous vectors, which is represented by a non-singular 3×3 matrix, as shown in the following equation:

$$\begin{pmatrix} x'_1 \\ x'_2 \\ x'_3 \end{pmatrix} = \begin{bmatrix} h_{11} & h_{12} & h_{13} \\ h_{21} & h_{22} & h_{23} \\ h_{31} & h_{32} & h_{33} \end{bmatrix} \begin{pmatrix} x_1 \\ x_2 \\ x_3 \end{pmatrix}. \quad (3.3)$$

Equation 3.3 can be represented as $x' = Hx$. Its inhomogeneous form is given by:

$$x' = \frac{x'_1}{x'_3} = \frac{h_{11}x + h_{12}y + h_{13}}{h_{31}x + h_{32}y + h_{33}}, \quad (3.4)$$

and

$$y' = \frac{x'_2}{x'_3} = \frac{h_{21}x + h_{22}y + h_{23}}{h_{31}x + h_{32}y + h_{33}}. \quad (3.5)$$

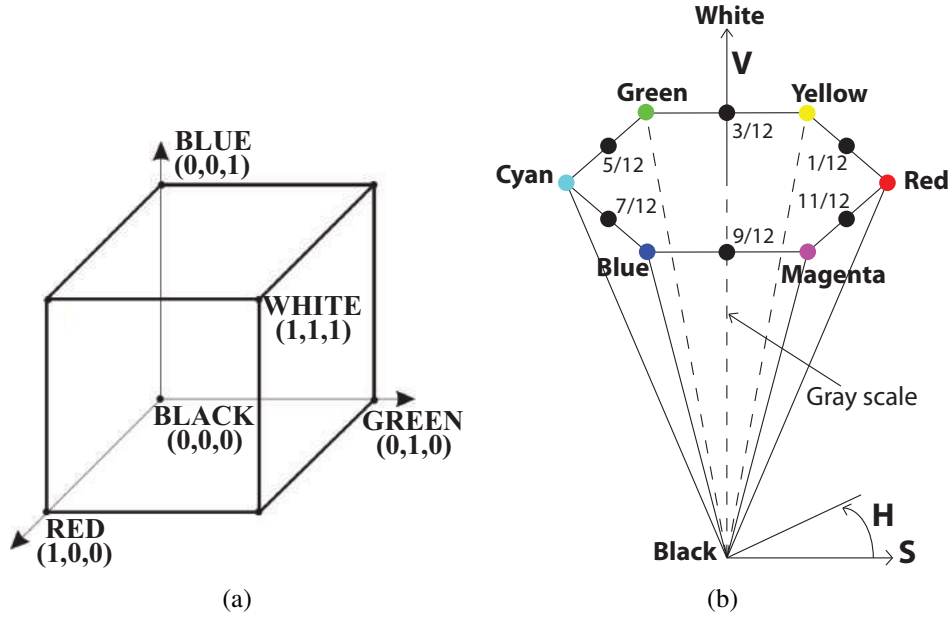


Figure 3.5: Color space constellation for used encoding and decoding processes: (a) RGB Cube and (b) HSV with normalized boundaries between HD2DC selected colors.

Each Finder pattern point generates two linear equations to the elements of H [44], which are given by the following equations:

$$x'(h_{31}x + h_{32}y + h_{33}) = h_{11}x + h_{12}y + h_{13}, \quad (3.6)$$

and

$$y'(h_{31}x + h_{32}y + h_{33}) = h_{21}x + h_{22}y + h_{23}. \quad (3.7)$$

Eight linear equations are created using the four Finder patterns points as inputs to Equations 3.6 and 3.7, what is sufficient to find the transformation matrix H and perform the projective transformation. In summary, the projective transformation matrix is found and applied on HD2DC to handle image changes caused by a tilt on the image plane. Figure 3.6 (a) illustrates an example of a printed version 3 HD2DC-8 barcode, while Figure 3.6 (b) illustrates its projective transformation followed by the final rotation.

After performing the Projective Transformation, the correct rotation of the four Finder patterns is computed and we can recover the Finder Pattern that has the two-modules wide separator (see Figure 3.3) located on the bottom right corner. In other words, the HD2DC image is rotated to correct the image position. Thanks to the projective transformation, we can determine the size of every module (in pixels) and the data contained in HD2DC barcode can be retrieved.

3.2.3 Color Segmentation

The next step consists on segmenting the colors of the captured barcode image. Color segmentation is performed in the HSV color space (Figure 3.5(b)). The captured image is first represented



Figure 3.6: HD2DC Version 5, 8-colors, and High error correction level: (a) image snapshot captured at a distance of 7 cm from the camera (Samsung Galaxy J5) and (b) rotated and processed version of (a).

in the HSV color space:

$$I(i, j, c) = [H(i, j), S(i, j), V(i, j)]. \quad (3.8)$$

where i and j are the spatial coordinates of the image and c corresponds to the color channel. A maximum and minimum value of the intensity component (V) is calculated for the entire image:

$$\text{MaxI} = \max (V(i, j)) \quad (3.9)$$

and

$$\text{MinI} = \min (V(i, j)). \quad (3.10)$$

Then, a 5-colors pixel segmentation is performed to retrieve the Decoding Symbols and the HD2DC parameters (HD2DC of 5 or 8 colors, HD2DC module size and error correction level), using the following equation:

$$\text{HD2DC}_5(i, j) = \begin{cases} \text{White,} & \text{if } V(i, j) > \frac{3 \times \text{MaxI} + \text{MinI}}{4}; \\ \text{Red,} & \text{if } -60^\circ < H(i, j) \leq 60^\circ; \\ \text{Green,} & \text{if } 60^\circ < H(i, j) \leq 180^\circ; \\ \text{Blue,} & \text{if } 180^\circ < H(i, j) \leq 300^\circ. \end{cases} \quad (3.11)$$

If the HD2DC barcode has 5-colors, there is no need to perform a second segmentation. On the other hand, if this is a barcode with 8 colors, an additional 8-colors segmentation is performed for

each pixel, as given by:

$$\text{HD2DC}_8(i, j) = \begin{cases} \text{White,} & \text{if } V(i, j) > \frac{3 \times \text{MaxI} + \text{MinI}}{4}; \\ \text{Black,} & \text{if } V(i, j) > \frac{3 \times \text{MinI} + \text{MaxI}}{4}; \\ \text{Red,} & \text{if } -30^\circ < H(i, j) \leq 30^\circ; \\ \text{Yellow,} & \text{if } 30^\circ < H(i, j) \leq 90^\circ; \\ \text{Green,} & \text{if } 90^\circ < H(i, j) \leq 150^\circ; \\ \text{Cyan,} & \text{if } 150^\circ < H(i, j) \leq 210^\circ; \\ \text{Blue,} & \text{if } 210^\circ < H(i, j) \leq 270^\circ; \\ \text{Magenta,} & \text{if } 270^\circ < H(i, j) \leq 330^\circ. \end{cases} \quad (3.12)$$

3.2.4 Information Retrieval

After the colors of each module are determined, the inverse of the filling process is performed to prepare for bit retrieval. Then, bits are extracted from the Encoding Region, forming a Berlekamp Reed-Solomon sequence of symbols [33] (each with $s = 16$ bits), which were created according to the parameters $\text{RS}(n, k)$ obtained from the HD2DC structure and the information in Tables 3.1 and 3.2. The Berlekamp Reed-Solomon decoding algorithm is applied and (possible) errors are corrected. If the decoded sequence of symbols has more than t errors, it will not be possible to recover all the information.

Table 3.3 shows the information data density for each version of the HD2DC barcode. Table 3.4 [3, 4] shows a comparison of information bits density between HD2DC and other 2D Colored barcodes. Notice that HD2DC is currently the 2D colored barcode with the highest data density. For a better understanding, Figure 3.7 shows a flowchart describing HD2DC decoding steps.

3.3 HD2DC DECODING RESULTS: PRINT-SCAN CHANNEL

To test the proposed scheme as a print-scan channel, we print HD2DC images at the smallest size and capture them using the mobile phones Samsung Galaxy S5 and Samsung Galaxy J5, with a 16 and 8 Megapixels built-in cameras, respectively. The image database built for our tests is composed of 14 snapshots of 3 different HD2DC barcodes, considering each color option and each HD2DC version. In total, we have 672 test images for each mobile phone. The printed 600 dpi barcode images have a module size of $0.2\text{mm} \times 0.2\text{mm}$, which is the smallest size that can be correctly decoded (see Table 3.3). A laser printer Xerox Color 560 was used to print the HD2DC barcode images at 600 dpi on a regular office A4 paper with 120 g/m^2 density. In our tests, all HD2DC were printed with error correction level H.

For a set of barcode images, we measured the percentage of corrupted symbols versus the dis-

Table 3.3: Sizes and information bits density of HD2DC printed at 600 dpi.

Version	HD2DC Color	HD2DC Area (in ²)	Information bytes (L)	Data Density (bytes/in ²)
1	5	0.0558	120	2,150.53
2	5	0.0992	258	2,600.80
3	5	0.1550	440	2,838.70
4	5	0.2232	658	2,948.02
5	5	0.3038	920	3,028.30
6	5	0.3968	1,214	3,059.47
7	5	0.5022	1,556	3,098.36
8	5	0.6200	1,934	3,119.35
1	8	0.0558	178	3,189.96
2	8	0.0992	338	3,407.25
3	8	0.1550	658	4,245.16
4	8	0.2232	990	4,435.48
5	8	0.3038	1,378	4,535.87
6	8	0.3968	1,824	4,596.77
7	8	0.5022	2,334	4,647.55
8	8	0.6200	2,906	4,687.09

tance (in centimeters) for each captured image. Average decoding results are shown in Figures 3.8 to 3.15. In these graphs, snapshots resulting in a percentage of corrupted symbols above the magenta dotted line (H error correction level limit) were not decoded, while percentages between cyan and magenta dotted lines corresponded to barcodes with errors that can only be decoded by a HD2DC with H error correction level. Between the yellow and cyan lines in these graphs, we can only decode HD2DC barcodes with an M error correction level. Finally, percentages of corrupted symbols under the yellow dotted line need only an L error correction level to be decoded. As seen in Table 3.3, decoded HD2DC barcodes with L error correction level obtain the highest information data density.

As illustrated in Figures 3.8 to 3.15, all printed HD2DC versions (1 to 8) were correctly decoded. Depending on the chosen version, both the Samsung Galaxy S5 and J5 were able to correctly decode barcodes with distances ranging from 7cm to 12cm. Results also show that the quality of the camera Complementary Metal-Oxide Semiconductor (CMOS) sensor affects the percentage of corrupted symbols. For all HD2DC versions, Samsung Galaxy S5 camera presented a better performance than the Samsung Galaxy J5 camera, for both HD2DC-5 and HD2DC-8 color versions. Figure 3.16 illustrates an example of a printed version 3 HD2DC-8 barcode. In this figure, besides the JPEG compression, Halftoning artifacts are present (more visible on cyan modules), what impacts the symbol error rate.

3.3.1 Data Density

Table 3.3 shows the information data density for each HD2DC version and color setup. Table 3.4 [3, 4] shows a comparison of information bits density between HD2DC and other 2D

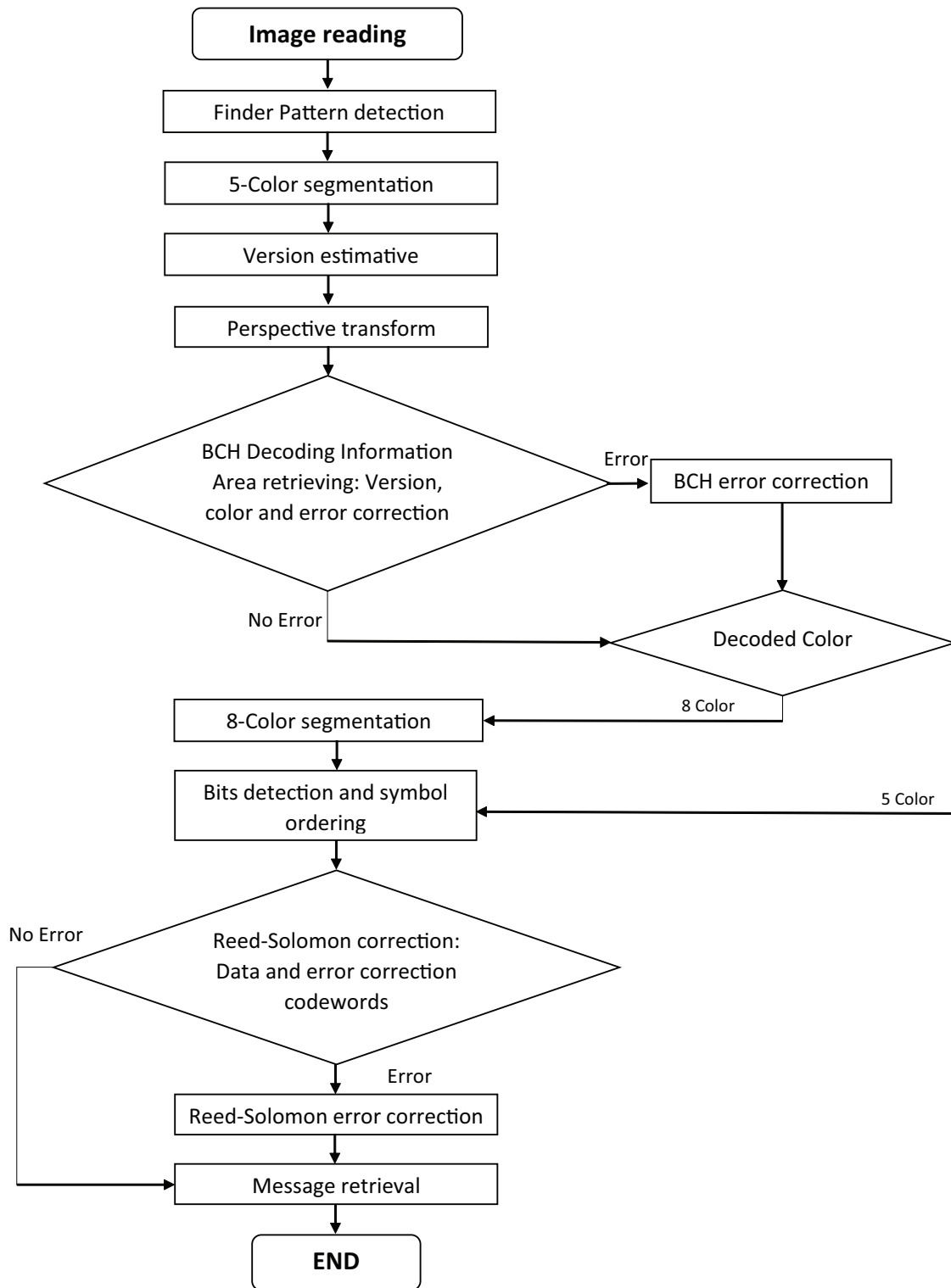


Figure 3.7: Flowchart of HD2DC decoding process.

Colored barcodes. This comparison shows that HD2DC is currently the 2D colored barcode with the highest data density on bytes per square inch, which is the main contribution of this 2D colored barcode.

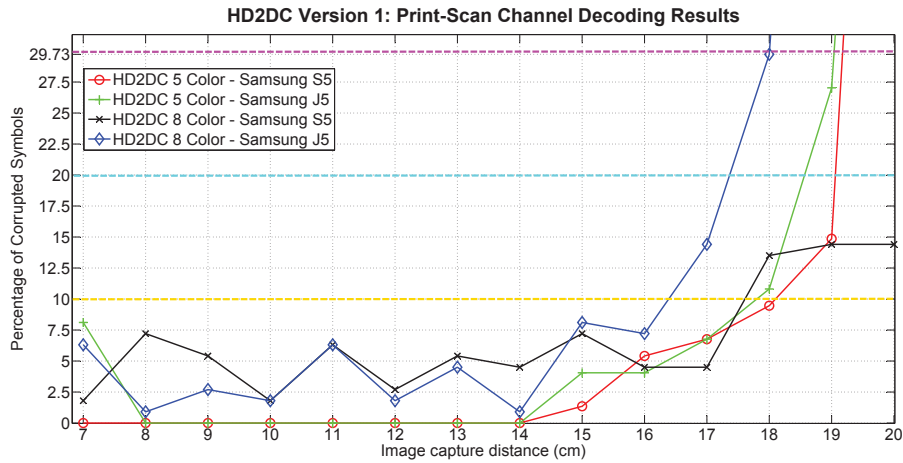


Figure 3.8: HD2DC Version 1 decoding results due to capture distance (7 cm to 20 cm) on Samsung Galaxy S5 and J5.

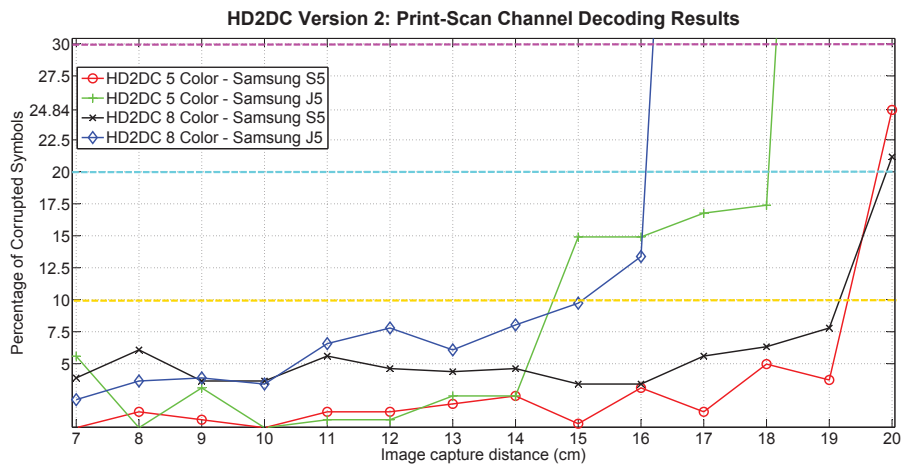


Figure 3.9: HD2DC Version 2 decoding results due to capture distance (7 cm to 20 cm) on Samsung Galaxy S5 and J5.

Table 3.4: Density performance of 2D-Barcodes.

2D Colored Barcode	Data Density (bytes/in ²)
HD2DC	4,687.09
HCC2D (second proposal) [4]	4,104.71
HiQ [45]	3,617.6
PCDE [31]	3,333.00
PCCC [32]	2,109.37
HCC2D (first proposal) [3]	1,881.00
QR Code [3]	627.00

3.4 HD2DC DECODING RESULTS: COMPRESSION ROBUSTNESS

Given that the data storage and transmission of a HD2DC will probably include a compression stage, it is necessary to evaluate the effect of lossy compression on the accuracy of HD2DC decoding. In this section, we evaluate the effects that common compression degradations have on

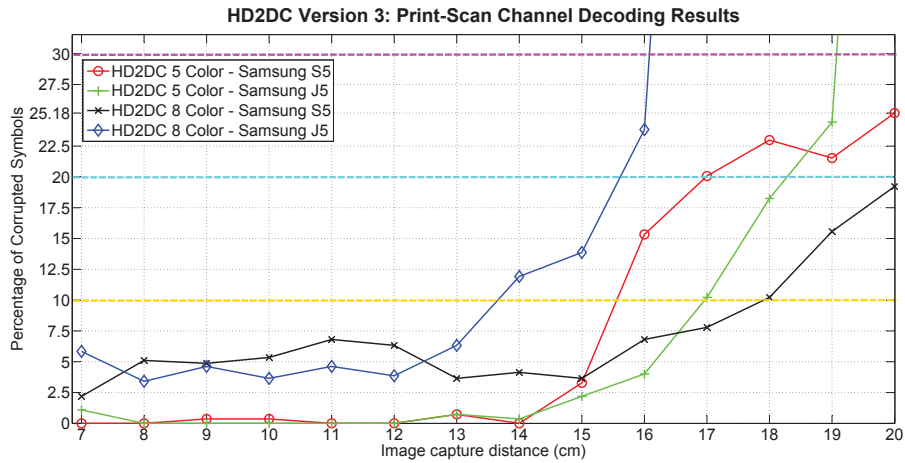


Figure 3.10: HD2DC Version 3 decoding results due to capture distance (7 cm to 20 cm) on Samsung Galaxy S5 and J5.

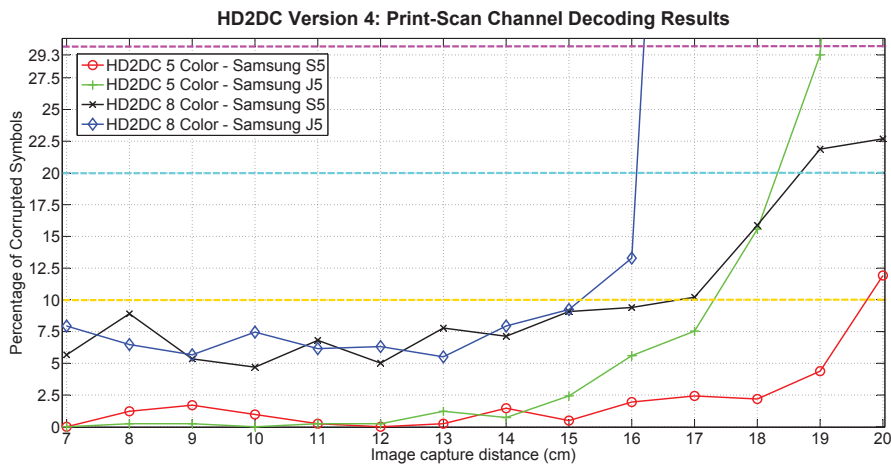


Figure 3.11: HD2DC Version 4 decoding results due to capture distance (7 cm to 20 cm) on Samsung Galaxy S5 and J5.

the decoding process.

3.4.1 HD2DC compression algorithms

Three popular compression algorithms are used in this work: JPEG [27], JPEG2000 [46, 47], and H.264/AVC [48–50]. All three standards are lossy algorithms that, depending on the bitrate, may introduce errors in the decoding of the HD2DC barcode. JPEG was chosen as one of the algorithms because it is still the most popular image compression standard. JPEG2000 was also chosen because it reaches high compression rates. We also used the video compression standard H.264/AVC, which although is a video compression algorithm, has been experimentally used for image compression with good results [51, 52].

Our tests were performed with input images on bitmap format (RGB), encoded with 24 bit/pixel. The original HD2DC images have 1 module per pixel, including regular four modules of

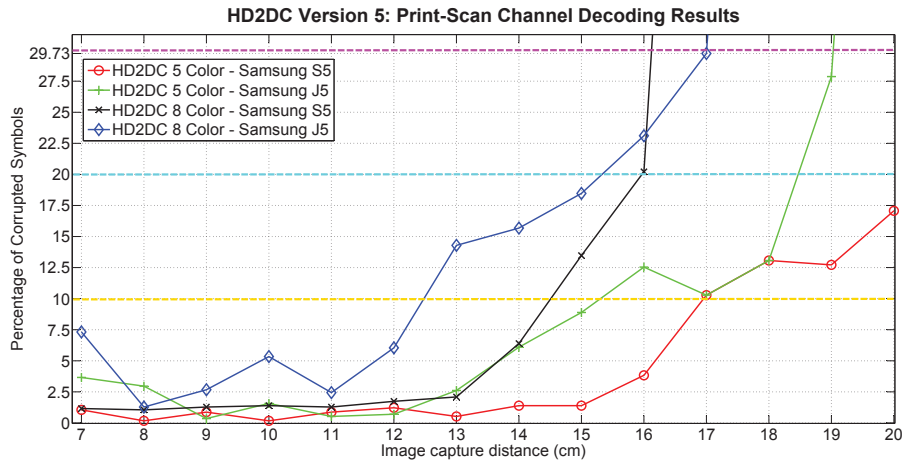


Figure 3.12: HD2DC Version 5 decoding results due to capture distance (7 cm to 20 cm) on Samsung Galaxy S5 and J5.

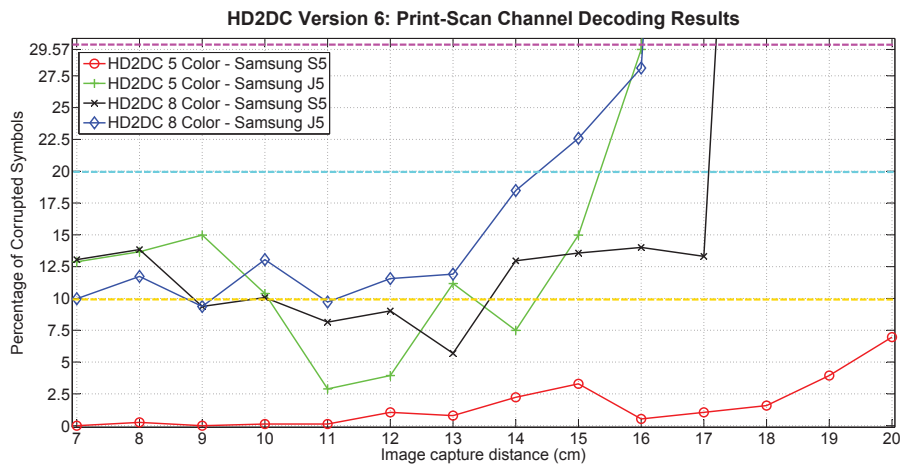


Figure 3.13: HD2DC Version 6 decoding results due to capture distance (7 cm to 20 cm) on Samsung Galaxy S5 and J5.

quiet zone on each side. These images was resized, using the nearest neighbor algorithm, making them ten times larger. After the initial image expansion, each module size is 10×10 pixels. Figures 3.1 (b) and (c) show some of the 240 HD2DC barcode images used in our tests. For a better analysis of the error rate due to compression, we used HD2DCs with a high error correction level.

To evaluate the effect of compression on the decoding of HD2DC barcodes, an analysis of the compression bitrate values (bits per pixel - bpp) versus the percentage of the total number of corrupted symbols was performed for all three compression algorithms. For a better visualization of the compression impact on HD2DC barcodes, figures in this chapter show only an enlarged area around the upper left Finder pattern. Figures 3.17(a), (b), and (c) depict examples of the HD2DC-5 in Figure 3.1 (c), compressed with similar bitrates using JPEG, JPEG2000, and H.264/AVC, respectively. Figures 3.18(a), (b), and (c) show the impact of compression with JPEG, JPEG2000 and H.264/AVC on HD2DC-8. The compression bitrates used in this example are around 0.41 bpp: 0.4156 bpp for JPEG, 0.4155 bpp for JPEG2000, and 0.4142 bpp for H.264/AVC.

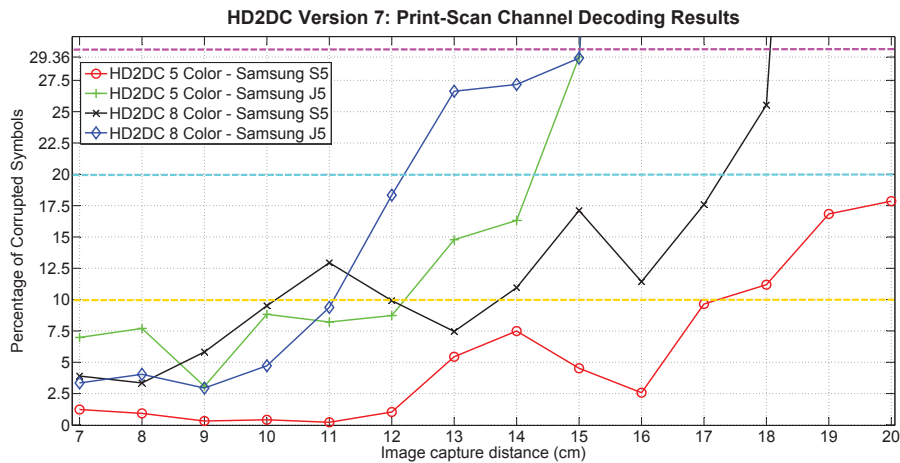


Figure 3.14: HD2DC Version 7 decoding results due to capture distance (7 cm to 20 cm) on Samsung Galaxy S5 and J5.

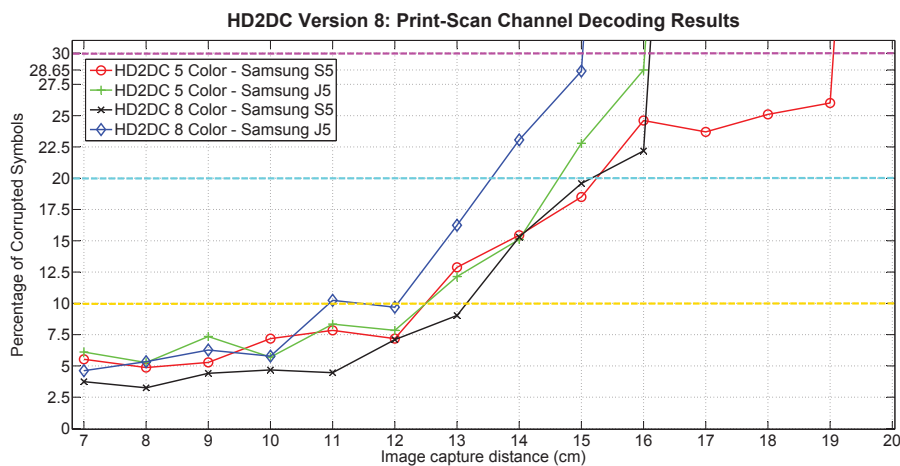


Figure 3.15: HD2DC Version 8 decoding results due to capture distance (7 cm to 20 cm) on Samsung Galaxy S5 and J5.

Our tests were performed using 5 different HD2DCs images for each color, version, and compression algorithm. HD2DC compressed images were processed until their maximum decodable compression rate. Notice that there is a big difference between the images in Figure 3.17 and in Figure 3.18, which correspond to versions of HD2DC-5 and HD2DC-8. As expected, the image compressed with JPEG has the worst quality (a higher number of visible degradations around finder patterns), while the image compressed with H.264/AVC has the best quality (fewer number of visible degradations). Figure 3.19 (a), (b) and (c) depict a zoom area of the barcode images corresponding to the maximum decodable bitrates for HD2DC-8 Version 8. In Appendix I, we present additional decoding results of HD2DC barcode images compressed with JPEG, JPEG2000, and H.264/AVC.

Figures 3.20, 3.21, 3.22, 3.23, 3.24, 3.25, 3.26 and 3.27 show the compression results for all three codecs applied to each version of HD2DC. All successful decoded images are discriminated according to the error correction level (L, M or H - see yellow lines). These results



Figure 3.16: HD2DC Version 6 and 8-color, captured and correctly decoded with 5.69% corrupted symbols at a distance of 13cm with the Samsung Galaxy S5 camera.

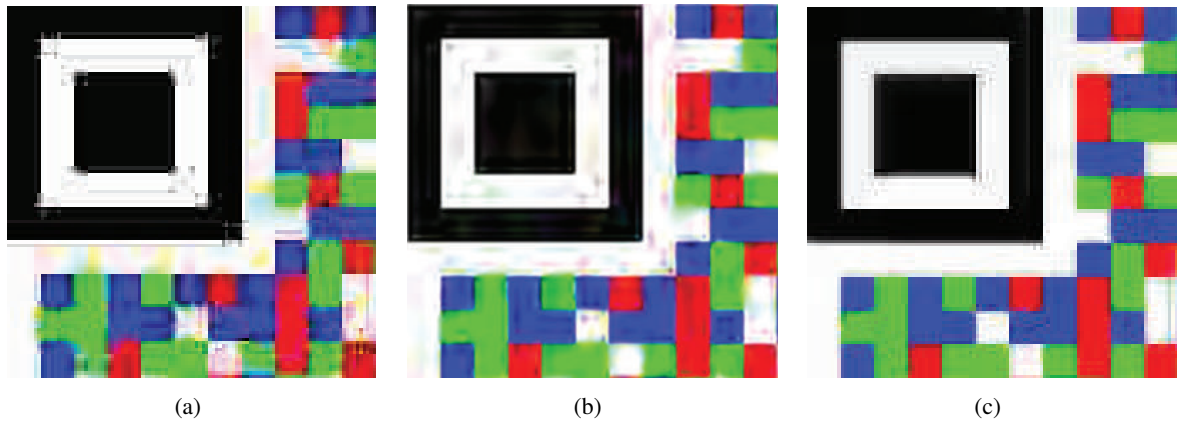


Figure 3.17: Enlarged 5-colors HD2DC of Version 4, compressed with: (a) JPEG@0.4908 bpp and 17.03% corrupted symbols, (b) JPEG2000@0.4720 bpp and 2.92% corrupted symbols, finally (c) H.264/AVC@0.4727 bpp and 0.97% corrupted symbols.

are consistent with the subjective image quality of the HD2DC barcode image presented in Figures 3.17, 3.18 and 3.19.

In the case of the JPEG, HD2DC-5 and HD2DC-8 can be decoded with rates greater than 0.4156 bpp and 0.4151 bpp, respectively, which correspond to the highest JPEG compression rates (level 100 in JPEG compression) possible for these images. At these rates, the HD2DC barcodes are decoded with an average symbol error of 27.93%. The Reed-Solomon algorithm can correct this percentage of corrupted symbols for an H error correction level, i.e. the HD2DC barcodes are perfectly decoded for JPEG bitrates greater than 0.4151 bpp.

For JPEG2000, HD2DC-5 and HD2DC-8 can be decoded with compression rates greater than 0.0816 bpp and 0.1169 bpp, respectively, which correspond to JPEG2000 compression levels 285 and 200. For this rate, we obtain an average error symbol of 26.31% and 28.67%, respectively.

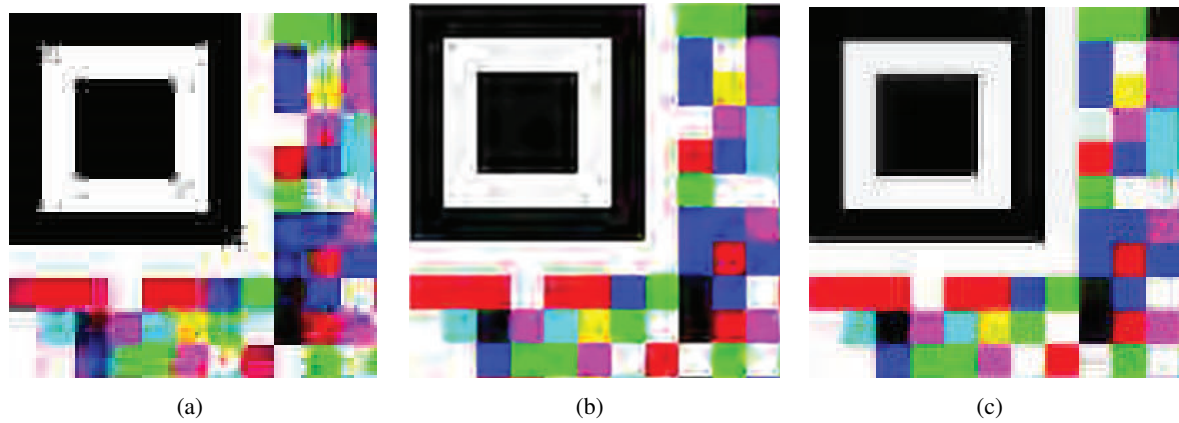


Figure 3.18: Enlarged 8-colors HD2DC of Version 1, compressed with: (a) JPEG@0.4151 bpp and 27.93% corrupted symbols, (b) JPEG2000@0.4002 bpp and 1.80% corrupted symbols, finally (c) H.264/AVC@0.3929 bpp and 0% corrupted symbols.

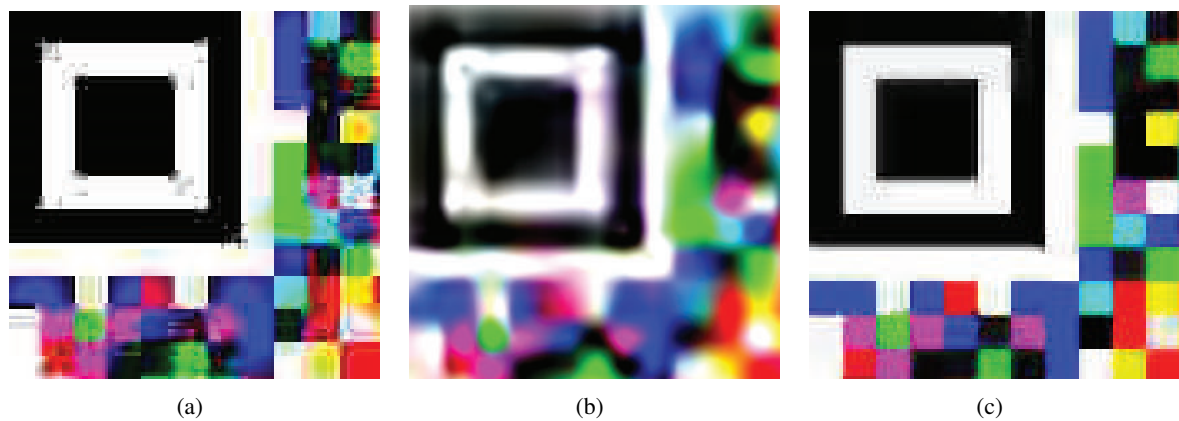


Figure 3.19: Enlarged 8-colors HD2DC of Version 8, compressed with: (a) JPEG@0.4654 bpp and 25.92% corrupted symbols, (b) JPEG2000@0.1106 bpp and 29.50% corrupted symbols, finally (c) H.264/AVC@0.5725 bpp and 1.82% corrupted symbols.

Therefore, information symbols were corrected recovered using an H error correction level. Results for JPEG2000 show how the color constellation affects the error rate. HD2DC-8 presented a higher error percentage than HD2DC-5 for the same compression parameters.

For the H.264/AVC compression algorithm, HD2DC-5 and HD2DC-8 can be decoded with rates higher than 0.3514 bpp and 0.3627, respectively. This rate is also the highest compression rate possible for this codec, which corresponds to level 51 in H.264/AVC. The maximum percentage of corrupted symbols for these rates are 1.35% for the HD2DC-5 and 2.7% for HD2DC-8.

Finally, results show that, even when compressing HD2DC images using the three compression algorithms introduced in this chapter, we obtained a good performance. More specifically, a perfect HD2DC barcode can be decoded from a JPEG2000 compressed image, for compression rates around 3.5 times lower than the compression ratios required for JPEG and H.264/AVC codecs.

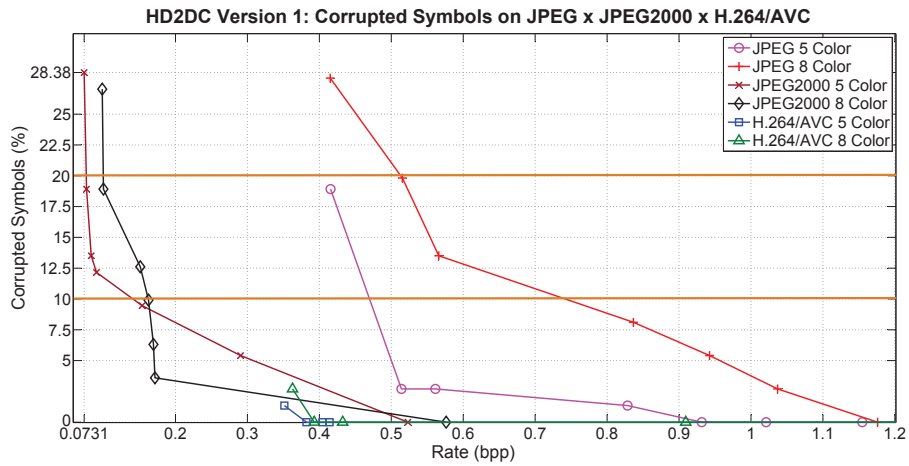


Figure 3.20: Percentage of corrupted symbols of HD2DC Version 1 versus compression bitrate (0-1.2 bpp).

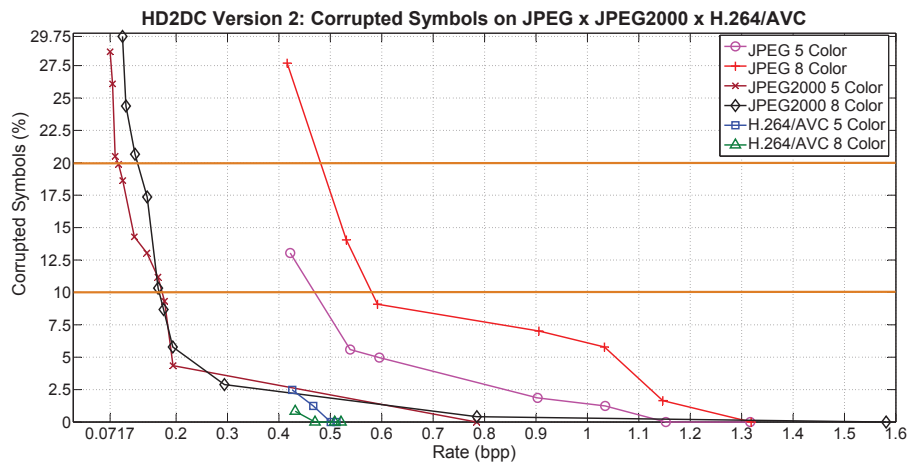


Figure 3.21: Percentage of corrupted symbols of HD2DC Version 2 versus compression bitrate (0-1.6 bpp).

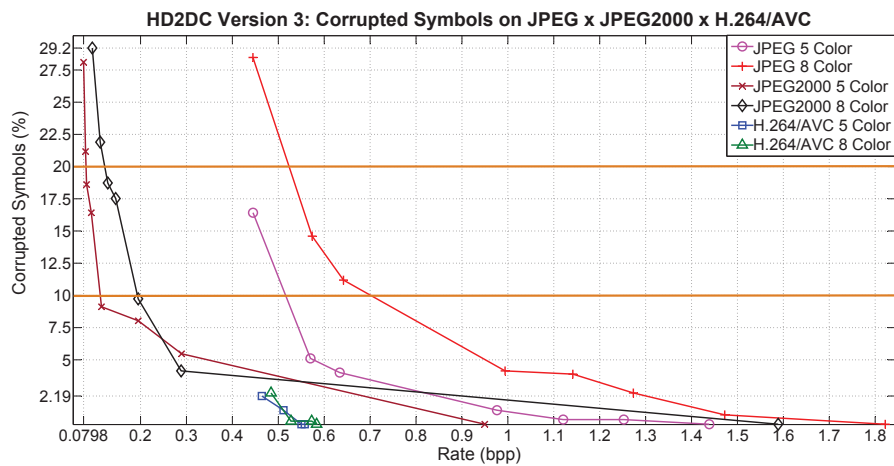


Figure 3.22: Percentage of corrupted symbols of HD2DC Version 3 versus compression bitrate (0-2 bpp).

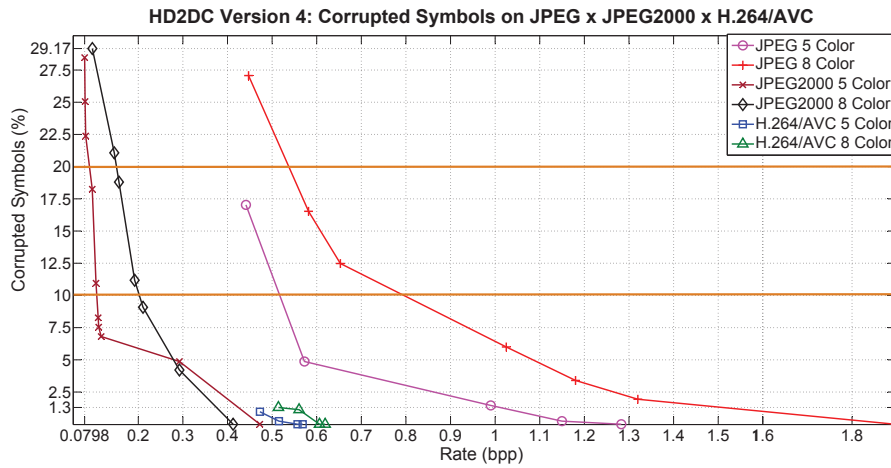


Figure 3.23: Percentage of corrupted symbols of HD2DC Version 4 versus compression bitrate (0-1.9 bpp).

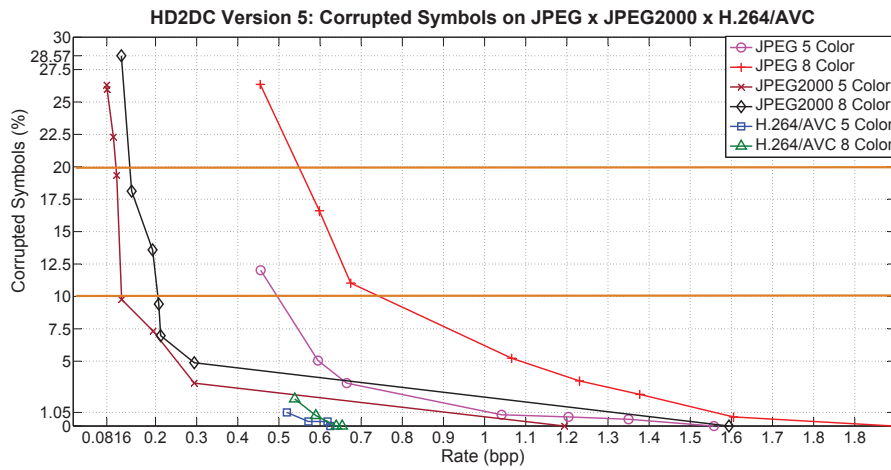


Figure 3.24: Percentage of corrupted symbols of HD2DC Version 5 versus compression bitrate (0-2 bpp).

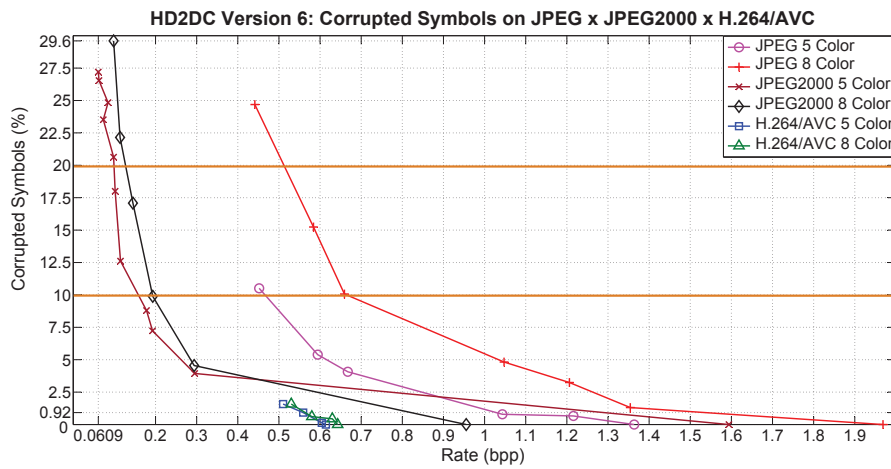


Figure 3.25: Percentage of corrupted symbols of HD2DC Version 6 versus compression bitrate (0-2 bpp).

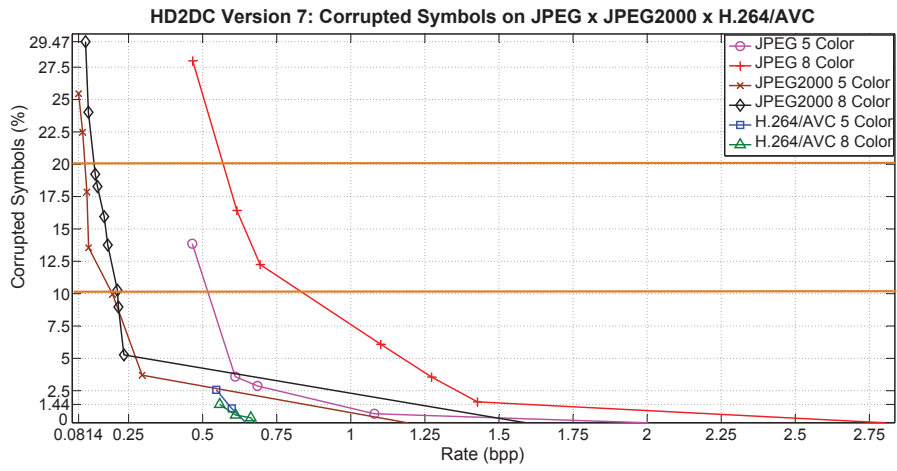


Figure 3.26: Percentage of corrupted symbols of HD2DC Version 7 versus compression bitrate (0-2.8 bpp).

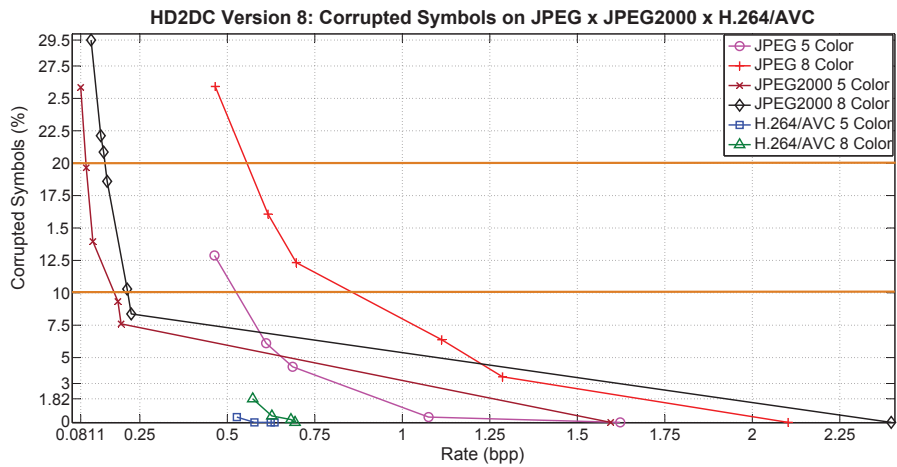


Figure 3.27: Percentage of corrupted symbols of HD2DC Version 8 versus compression bitrate (0-2.5 bpp).

4 A (2,2) XOR-BASED VISUAL CRYPTOGRAPHY SCHEME USING COLOR INTERFERENCE

This Chapter describes our proposal of a new Visual Cryptography scheme. The method uses only 2 shares and does not require a pixel expansion [53]. We implemented a VC scheme that works with a mobile phone or tablet, taking advantage of the screen available in this screen.

4.1 PROPOSED VISUAL CRYPTOGRAPHY SHARES STRUCTURE

It is quite simple to implement a VC scheme with a printed transparency and a mobile screen using the traditional method of pixel expansion creation (see Figure 2.4). To avoid pixel expansion, this work explores the use of colors as pixel components for both shares. One simple and cheap material that can easily be used to produce shares is the Polyvinyl Chloride (PVC) [54]. The proposed scheme uses a 0.3 mm thick PVC printed transparency (same material used for business card) as Share 1, which makes this VC scheme a very cheap solution for an unexpanded pixel VC scheme.

The superimposition of any printed PVC transparency on a mobile screen generates a subtractive filtered image. More specifically, when PVC transparency is backlit, you get a subtractive color mixing. Cyan, magenta and yellow are the most commonly used subtractive primary colors. If you overlap all three in effectively equal mixture, all the light is subtracted and the perceived color is black. Therefore, the resulting intensity and saturation of the perceived colors always decrease, which means that the observer will only perceive luminance changes rather than color changes. For a better understanding of this phenomenon, consider the printed PVC transparency as a film of uniform thickness and refraction index n . Notice that light wavelength λ_n passing through the PVC film is given by the following equation [55]:

$$\lambda_n = \lambda / n, \quad (4.1)$$

where λ is the light wavelength in vacuum and n is the refraction index for visible light. Figure 4.1(a) shows a graph of the refraction index of a PVC transparency for different wavelengths.

Color temperature of the light (Kelvin degrees) is determined by measuring a heated object that emits light. As the physical temperature of the object rises, the color transitions from red (long wavelengths) to blue (short wavelengths). These long and short wavelengths extremes corresponds to the warm and cool colors, respectively. Figure 4.1 (b) shows the warm and cool colors that compose the visible color spectrum.

Due the superposition principle [55], which happens when the PVC transparency (Share 1) is

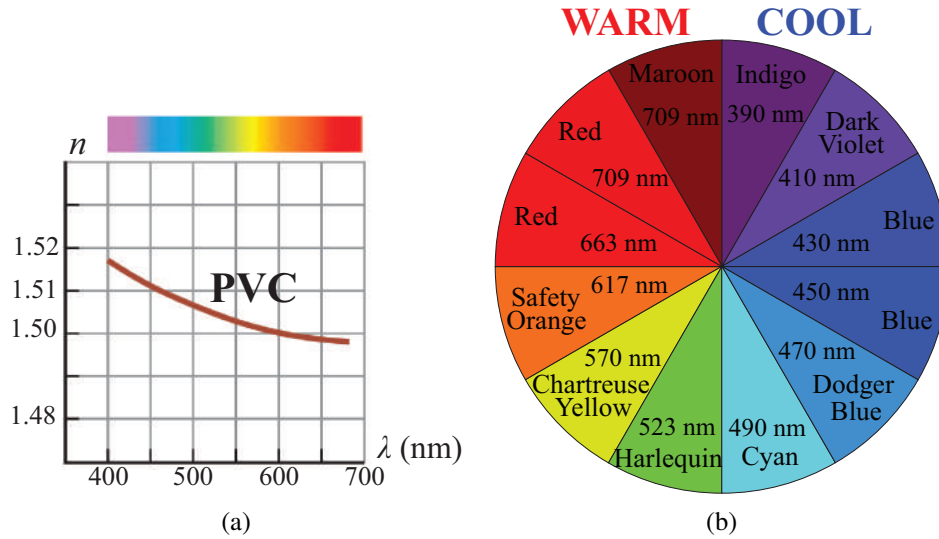


Figure 4.1: Color in PVC transparency: (a) Non-printed PVC transparency index refraction and (b) Color wavelengths of warm and cool colors.

placed on the mobile screen (Share 2), the refracted light observed at the PVC surface corresponds to the algebraic subtraction of the mobile screen light and the color on the PVC. When the source pulse refracts in the printed PVC transparency, a decreased (filtered) resulting pulse is shown to the observer. This resulting pulse is produced by a partial destructive interference [55] caused by the PVC transparency superimposition. The destructive interference degree is defined according to the colors emitted by the mobile screen and the colors printed on the PVC transparency.

A less destructive interference is presented when a color C_1 is printed on a PVC transparency and overlapped on a similar color \hat{C}_1 . This happens because the source light color and the filtering PVC printed color are practically the same, resulting in a high intensity observed color. On the other hand, a great destructive interference occurs when a color C_1 is printed on PVC transparency and is overlapped on a different screen color \hat{C}_2 . In this case, the source color light and the filtering PVC printed color are too different, resulting in a low intensity image. The more different the source light color is from the filtering PVC color (e.g. warm and cool colors), the more intense is the destructive interference. This is the reason the saturation and intensity of the perceived image decreases. Figure 4.1 (b) depicts the visible colors for different values of wavelength, which are separated into warm and cool colors.

Notice from the visible color spectrum in Figure 4.1 (b) that the more distant wavelengths correspond to Violet/Blue colors (around 435 nm) and Orange/Red colors (around 640 nm). Figure 4.2 illustrates the desired VC system behavior for each refracted and observed pixel, considering the incident wavelength and the color printed on the PVC. This illustration shows the resulting intensity perceived by an observer for two color destructive interferences levels (low and high). We consider the visible spectrum limits (superior or inferior in Figure 4.1 (b)) as the light source coming from the mobile screen and the filtering color as the color printed on the PVC transparency. The following options are possible:

- The colors displayed on the mobile screen and printed on the PVC are both of short wavelength (cool colors). This generates a low destructive interference and, therefore, a medium/high level intensity pixel is perceived.
- A long period color wavelength (warm color) is displayed on a mobile screen and a short wavelength color (cool color) is printed on a PVC transparency. This generates a high destructive interference and a low intensity level pixel is perceived.
- A short period color wavelength (cool color) is displayed on a mobile screen and a long wavelength color (warm color) is printed on a PVC transparency. This generates a high destructive interference and a low intensity level pixel is perceived.
- The colors displayed on the mobile screen and printed on the PVC are both of long wavelength (warm color). This generates a low destructive interference and, therefore, a medium/high level intensity pixel is perceived.

Table 4.1 shows the desired decoded color and luminance combinations.

4.2 PROPOSED VISUAL CRYPTOGRAPHY ANALYSIS

To create a VC scheme with no pixel expansion, the produced single pixel should follow the pixel structure shown in Figure 4.2. Here, n_1 and n_2 , respectively, are index refraction values of the color printed PVC transparencies, C_1 and C_2 are the colors chosen for the PVC transparency and the mobile screen. In this scheme, two different luminance levels for each pixel can be perceived.

The proposed VC scheme generates Shares 1 and 2 using a binary secret image, S , for which the darker pixels correspond to '0' and the lighter pixels correspond to '1'. The size (in pixels) of each share is equal to the size of the secret image, i.e. there is no pixel expansion. In other words, the algorithm takes a binary secret image (S) as the input and generates as outputs 2 shares: F_1 and F_2 , with $M \times N$ pixels.

The algorithm generates each pixel of Share 1, $F_1(x, y)$, by randomly selecting for these pixels, either a color C_1 or a color C_2 . To choose the color of each pixel of Share 2, $F_2(x, y)$, the algorithm takes into consideration the value of the corresponding pixel in the secret image $S(x, y)$ and in Share 1 $F_1(x, y)$. If the pixel in $S(x, y)$ is '1', the pixel in $F_2(x, y)$ has the same color than the pixel in $F_1(x, y)$. But, if the pixel in $S(x, y)$ is '0', the pixel in $F_2(x, y)$ should have opposite color of the

Table 4.1: Proposed VC scheme decoding architecture.

Pixel from Share 1	Pixel from Share 2	Decoded Pixel
Cool color	Cool color	High luminance
Cool color	Warm color	Low luminance
Warm color	Cool color	Low luminance
Warm color	Warm color	High luminance

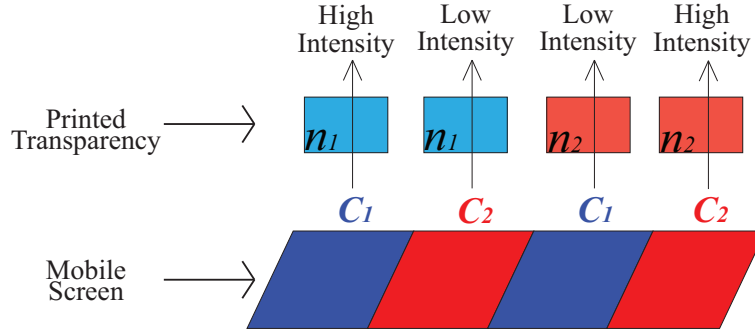


Figure 4.2: Proposed VC scheme with single pixel structure.

pixel in $F_1(x, y)$. This can be summarized by the following equation:

$$F_2(x, y) = \begin{cases} C_1, & \text{if } S(x, y) = 1 \text{ and } F_1(x, y) = C_1 \\ C_2, & \text{if } S(x, y) = 1 \text{ and } F_1(x, y) = C_2 \\ C_1, & \text{if } S(x, y) = 0 \text{ and } F_1(x, y) = C_2 \\ C_2, & \text{if } S(x, y) = 0 \text{ and } F_1(x, y) = C_1 \end{cases} \quad (4.2)$$

where $0 \leq x \leq M$ and $0 \leq y \leq N$.

This VC scheme follows the most important principle of information security for VC schemes. If a software-networking MitM attack occurs, the attacker can access only Share 2 (mobile image), as Share 1 (printed PVC transparency) is a physical object and therefore, not vulnerable to software-networking attacks. Even if the attacker obtains Share 2, he will not be able to decode the secret image because he cannot superimpose Share 1 on Share 2.

The proposed VC scheme follows the One-Time Pad algorithm operation. To prove this, consider that $F_1(x, y)$ (ciphertext), $F_2(x, y)$ (key) and $S(x, y)$ (message), are represented as arrays of n bits. For any $S(x, y)$ and $F_1(x, y)$, we have the following probabilities P :

$$P(S(x, y)|F_1(x, y)) = \frac{P(S(x, y) \cap F_1(x, y))}{P(F_1(x, y))} = \frac{P(F_1(x, y)|S(x, y)) \cdot P(S(x, y))}{P(F_1(x, y))}. \quad (4.3)$$

Conditioning $F_1(x,y)$ over all $S(x,y)$:

$$P(F_1(x,y)) = \sum_{S(x,y)} P(F_1(x,y)|S(x,y)) \cdot P(S(x,y)). \quad (4.4)$$

Also, for any $S(x,y)$ and $F_1(x,y)$, we have:

$$P(F_1(x,y)|S(x,y)) = P(k = (F_1(x,y) \oplus S(x,y))) = 2^{-n}, \quad (4.5)$$

so that $P(F_1(x,y)) = 2^{-n} \cdot \sum_{S(x,y)} P(S(x,y)) = 2^{-n}$. Which shows that $P(S(x,y)|F_1(x,y)) = P(S(x,y))$, and proves that the proposed VC scheme acts as an One-Time Pad cryptosystem, where $F_1(x,y)$, $F_2(x,y)$ and $S(x,y)$ are used as Ciphertext, Key and Secret Message, respectively.

4.3 PROPOSED VISUAL CRYPTOGRAPHY RESULTS: COLOR SELECTION AND SHARES GENERATION

As seen in the previous section, the proposed VC scheme uses color interference to generate non-expanded shares. But, for a correct system operation, we must select an appropriate set of colors. To make this selection, we chose 40 different colors, ranging from blue to red, and printed them on transparencies. Then, we tested 40 colors against the same colors displayed in a mobile device (Samsung Galaxy S7 Edge and Samsung Galaxy Tab A). This way, one color was displayed on a mobile screen and the other was printed on a PVC transparency. The experiment consisted of measuring the luminance coming out of the surface of the colored PVC transparency share, when superimposed to another color displayed on the mobile screen.

To measure the luminance, we used the Konica Minolta TS-100 luminance meter. As shown in Figure 4.3 (a), the luminance meter was positioned at a distance of 10 cm from the mobile display, in a room illuminated with artificial light at 250 lux. Again, the luminance meter was used to measure the luminance coming out of a single color printed PVC transparency superimposed on the colored mobile screen. The brightness level of the mobile screen was set at maximum level, so luminance results could have a large possible range. As illustrated in Figure 4.3 (b), the experiment was performed in a room with 2 lamps of 32 W and 2,350 lm. The mobile screen had its laterals covered to ensure that no light coming from the lamps would reflect on it, i.e. the light on the surface of the transparency came only from the mobile screen.

The measurements took approximately two months and were performed following these steps:

1. The mobile phone display was placed orthogonally to the luminance meter. Their distance was 10 cm.
2. One of the 20 *warm* colors printed on PVC transparencies was picked and superimposed on the mobile screen, which displayed all 20 *warm* colors in a sequence. The luminance was

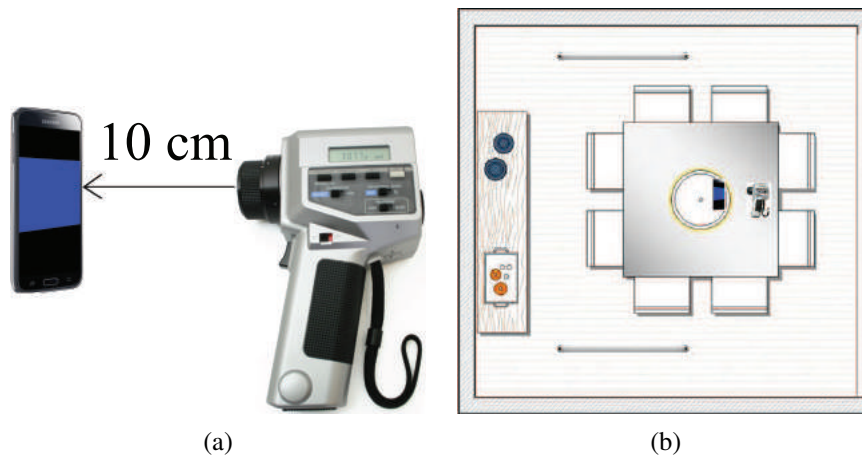


Figure 4.3: Luminance detection: (a) Lumens measurement of a blue printed PVC transparency superimposed on the Samsung Galaxy S5 screen with blue color and (b) Schematic representation.

measured for each superimposed combination pair.

3. The mobile screen displayed 20 *cool* colors in sequence, maintaining the same PVC transparency chosen in the last step. The luminance was measured for each superimposed combination pair.
4. The two last steps are repeated for all remaining 19 *warm* colors printed on PVC transparencies.
5. One of the 20 *cool* colors printed on PVC transparencies is picked and superimposed to the mobile screen displaying all 20 *cool* colors in sequence. The luminance is measured for each superimposed combination pairs.
6. The mobile screen displays the 20 warm colors in sequence, maintaining the PVC transparency chosen in the previous step. The luminance is measured for each superimposed combination pairs.
7. Finally, steps 5 and 6 were repeated for all remaining 19 *cool* colors printed on PVC transparencies.

Results corroborated the warm and cool colors destructive interference theory (see Figure 4.2) and showed that some colors cannot be used for this VC scheme, like for example colors on the boundaries of warm and cool colors (see Figure 4.1 (b)). More specifically, colors such as maroon, indigo, and dark violet are too dark, while colors like chartreuse yellow, harlequin, and cyan are too light. In other words, if we use these 2 color groups, the resulting perceived color will be either too dark or too light, even if combined with their corresponding opposite colors in the warm and cool color constellation (see Figure 4.1 (b)).

Therefore, not all color combinations can be used in the architecture shown in Table 4.1. Table 4.2 shows examples of unsuccessful color interference combinations on Shares 1 and 2. For these cases, the attacker can easily decode the estimated secret image. For example, in the

Table 4.2: Undesired color combinations of Share 1 and 2.

VC Structure	Share 1 Pixel Color (R,G,B)	Share 2 Pixel Color (R,G,B)	Luminance cd/m ²
1	Yellow (255,255,0)	Yellow (255,255,0)	310.10
1	Yellow (255,255,0)	Red (255,0,0)	144.90
1	Red (255,0,0)	Yellow (255,255,0)	103.50
1	Red (255,0,0)	Red (255,0,0)	82.90
2	Blue (0,0,255)	Blue (0,0,255)	11.70
2	Blue (0,0,255)	Green (0,0,255)	9.18
2	Green (0,0,255)	Blue (0,0,255)	80.06
2	Green (0,0,255)	Green (0,0,255)	165.80
3	Cyan (0,255,255)	Cyan (0,255,255)	187.80
3	Cyan (0,255,255)	Orange (255,165,0)	162.30
3	Orange (255,165,0)	Cyan (0,255,255)	87.44
3	Orange (255,165,0)	Orange (255,165,0)	146.9
4	Cyan (0,255,255)	Cyan (0,255,255)	187.80
4	Cyan (0,255,255)	Yellow (255,255,0)	215.50
4	Yellow (255,255,0)	Cyan (0,255,255)	206.80
4	Yellow (255,255,0)	Yellow (255,255,0)	310.10

first VC structure of Table 4.2, if a yellow pixel is encoded on Share 1, it is obvious that a high luminance pixel is on the secret image. Similarly, when a red pixel is encoded on Share 1, a low luminance pixel will be decoded on the secret image.

Luminance results for both mobile devices were very similar, with almost no difference. Table 4.2 shows examples of unsuccessful color interference combinations on Shares 1 and 2. For these cases, the attacker can easily decode the estimated secret image. For example, in the first VC structure of Table 4.2, if a yellow pixel is encoded in Share 2, it is obvious that a high luminance pixel ('1') is present in the secret image. Similarly, if a red pixel is encoded in Share 1, a low or medium luminance pixel will be decoded in the secret image ('0').

On the other hand, for both mobile devices, using blue and red scales produces the desired color interference for a Xor-Based VC scheme, allowing the implementation of the proposed scheme detailed in Table 4.1. Therefore, in this work we created an algorithm to find the best interference color scheme for red and blue scales. Table 4.3 shows the three best blue and red color combinations that are able to provide the maximum binary entropy value, while presenting the low and high destructive color interferences showed in Figure 4.2. Since a blue or red pixel can be decoded with a high or a low luminance, depending on the printed pixel of Share 1, an intercepted Share 2 does not reveal any information about the secret image.

The VC scheme proposed in this work uses the structure shown in lines 2-5 of Table 4.3, where blue (cool colors) corresponds to the color C_1 in the proposed algorithm and red (warm colors) corresponds to C_2 . Figure 4.4 shows the luminance value for C_1 and C_2 . For Share 1, these two colors correspond to RGB values $C_1 = (0,170,255)$ and $C_2 = (255,10,0)$, while for Share 2 they correspond to $C_1 = (0,180,255)$ and $C_2 = (255,40,0)$. The blue line in Figure 4.4 corresponds to the measured luminance values obtained when using cool colors in Share 1, for a set of cool and

Table 4.3: Proposed VC color blocks with color interference.

VC Structure	Share 1 Pixel Color (R,G,B)	Share 2 Pixel Color (R,G,B)	Luminance cd/m ²
1	Blue (0,170,255)	Blue (0,180,255)	83.55
1	Blue (0,170,255)	Red (255,40,0)	27.28
1	Red (255,10,0)	Blue (0,180,255)	28.14
1	Red (255,10,0)	Red (255,40,0)	78.41
2	Blue (0,170,255)	Blue (0,180,255)	83.50
2	Blue (0,170,255)	Red (255,30,0)	26.19
2	Red (255,10,0)	Blue (0,180,255)	28.14
2	Red (255,10,0)	Red (255,30,0)	78.29
3	Blue (0,170,255)	Blue (0,170,255)	73.66
3	Blue (0,170,255)	Red (255,0,0)	25.17
3	Red (255,10,0)	Blue (0,170,255)	24.61
3	Red (255,10,0)	Red (255,0,0)	77.51

warm color in Share 2. On the other hand, the red line in Figure 4.4 corresponds to the measured luminance values obtained when using warm colors in Share 1, for a set of cool and warm color in Share 2.

The two green lines in Figure 4.4 indicate the combinations with the largest and equal distances of luminance difference. Notice that for the cool colors in Share 2, the best value is (0,180,255), while for the warm colors in Share 2 the best values is (255,40,0). For this particular combination, the luminance differences between low and high destructive color interference values are 55.41 cd/m² and 51.13 cd/m², which represent the best contrast intensity for the color printed PVC film. Figure 4.5 shows an example of the shares generated from a binary secret image with 136 × 136 pixels.

4.4 PROPOSED VISUAL CRYPTOGRAPHY RESULTS: DECRYPTED IMAGE

After the desired color interference pixels are selected, the proposed VC scheme can be implemented and tested. As mentioned earlier, all our tests were performed using the first structure of Table 4.3 (lines 2-5), for which we considered a Samsung Galaxy S7 Edge, a Samsung Galaxy Tab A, and a set of color printed PVC transparencies with different pixel sizes. Color printed PVC transparencies were printed with 35 different pixel sizes. The first transparency had 60 × 60 pixels. For the remaining transparencies, pixels size increases in steps of 4 × 4, reaching 200 × 200 pixels. Figure 4.6 shows Share 1 on 60 × 60 pixels and 136 × 136, and Share 2 on 60 × 60 and 136 × 136 pixels.

Experimental results show that secret images are easily recognized by users. Notice that, in the decoded images, lighter areas are composed by blue or red pixels with medium to high luminosity, while darker areas are formed by blue or red pixels with low luminosity. This luminosity display shows uniformly light and dark pixels on the decoded image, effect that is not obtained in most

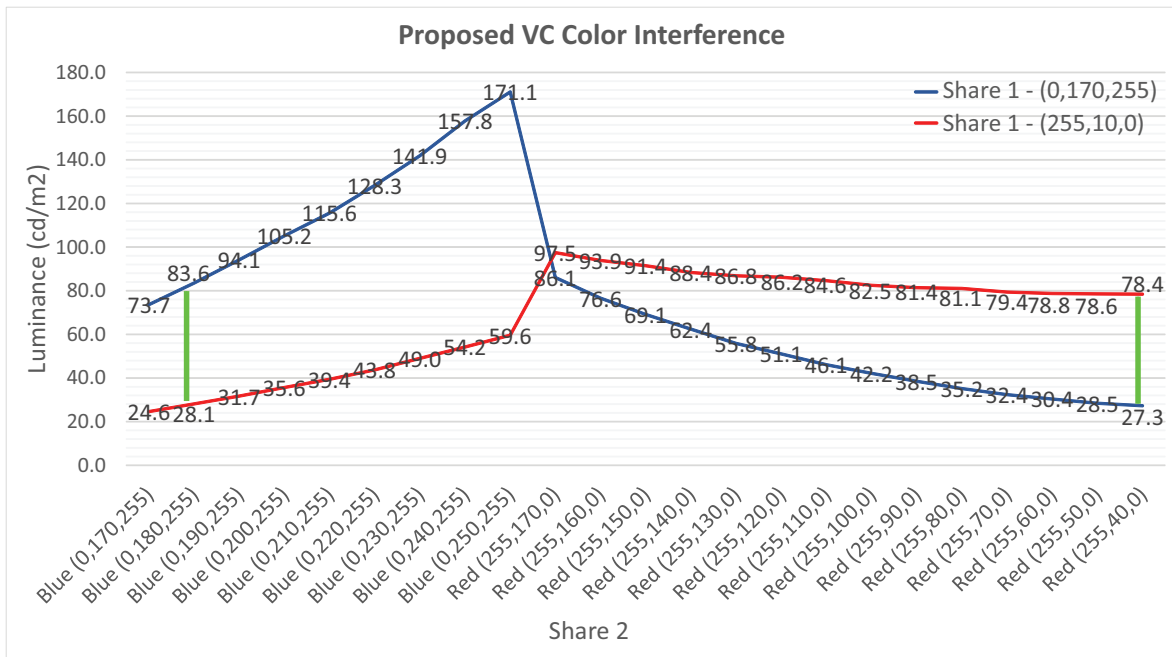


Figure 4.4: Measured luminance values for combinations of Shares 1 and 2, with cool and warm colors. Measurements were performed considering the first structure of Table 4.3 (lines 2-5) and using a Samsung Galaxy S7 Edge (Share 2) and a set of color printed PVC transparencies (Share 1).

VC schemes that convey light pixel using a set of both light and dark pixels.

Our results show that the spatial resolution of the shares is a factor that greatly affects the quality of the decoded image. For example, the semantic content of the simple binary images (60×60 pixels) in Figures 4.7 (a) and (c) are easy to recognize (soccer player and paw symbol, respectively). On the other hand, the Lena image (60×60 pixels) in Figure 4.7 (b) is not as easily recognizable because such a complex content requires a larger spatial resolution. On the other hand, Figure 4.7 (f) shows the Lena image with a better resolution (136×136 pixels). Notice that the semantic content is now easier to recognize. Results also showed that the proposed method is not as sensitive to alignment, when compared with earlier VC methods.

Another interesting characteristic of the proposed method is that the secret image can only

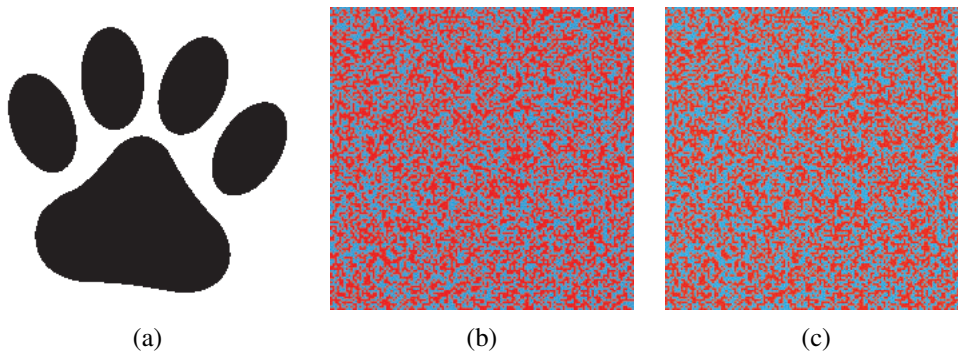


Figure 4.5: (a) Secret image (S), (b) Share 1 (F_1), and (c) Share 2 (F_2).

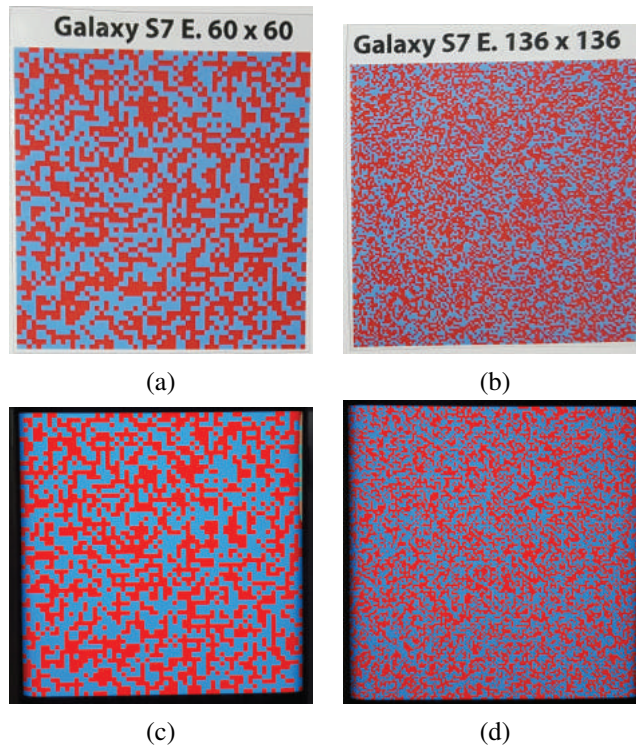


Figure 4.6: Proposed VC scheme shares: (a) Share 1 with 60×60 pixels, (b) Share 1 with 136×136 pixels, (c) Share 2 of soccer player image with 60×60 pixels, and (d) Share 2 of Lena image with 136×136 pixels.

be decoded if the observer is in an orthogonal position with respect to the mobile screen plane. Otherwise, a tilted and unaligned image will be perceived, as shown in Figures 4.7 (d) and (h). These particular examples correspond to versions of Figures 4.7 (c) and (c), which were captured with an approximate angle of 45 degrees. Notice that the secret image cannot be decoded in these images, a feature that improves user privacy and security. Our experiments also show that the environment luminosity does not affect the decoded image. Figure 4.7 (c) was captured in a completely dark room, while the remaining pictures of Figure 4.7 were captured in a completely light room.

4.5 ANIMATED VISUAL CRYPTOGRAPHY DECRYPTION

To improve the reusability of Share 1, one possibility is to use a sequence of images as Share 2 in the mobile device. More specifically, animated figures can be in a Graphics Interchange Format (GIF) file composed by $p > 1$ candidate images. The idea is that only one of the p images is the correct image that is able to reveal the secret image. The remaining $p - 1$ candidate images are simply pseudo-random images, which can be generated using the same generation process used for Share 1. In the case of a MitM (Man in the Middle) attack, the attacker does not know which of the p candidate images must be used to decode the secret image. This extension of the proposed method enhances the security and allows for Share 2 to be reused.

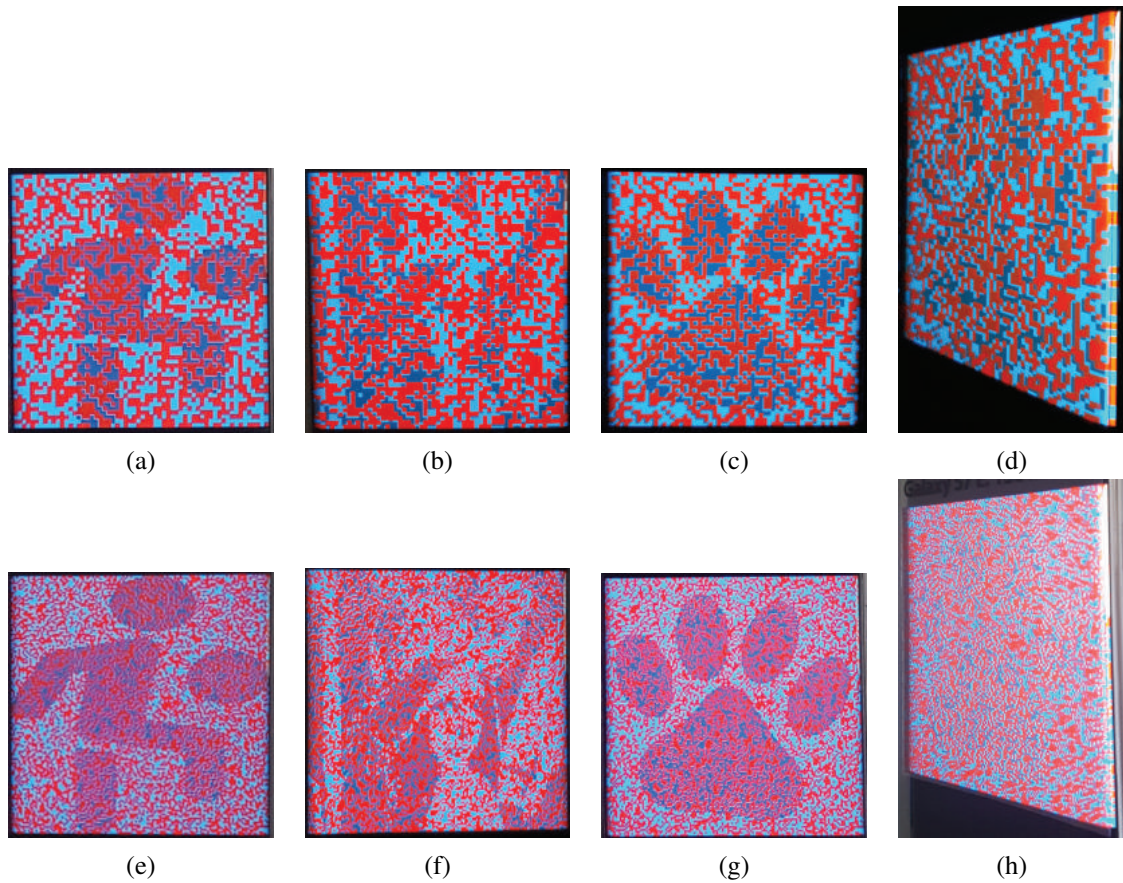


Figure 4.7: Proposed VC scheme decoded images: (a) Soccer player with 60×60 pixels, (b) Lena with 60×60 pixels, (c) Dog paw symbol captured in a dark environment with 60×60 pixels, (d) Tilted snapshot of (c), (e) Soccer player with 136×136 pixels, (f) Lena with 136×136 pixels, (g) Dog paw symbol with 136×136 pixels, and (h) Tilted snapshot of (g).

The GIF file is generated with predefined pauses of time, for our tests we used 1 second for each frame. Figures 4.8 (a) to (f) show the result of the encode and decode animated images of our proposed VC scheme on a Samsung Galaxy Tab A. The encoded image is a Lena figure with original resolution of 512×512 pixels, the VC spatial resolution is 200×200 pixels and $p = 4$, where three shares 2 are meaningless and only one share 2 can be decoded by the human vision.

4.6 DATA VALIDATION SYSTEM: PROPOSED VC SCHEME AND HD2DC

A secure data validation tool can be implemented combining the proposed VC Scheme and the HD2DC. We designed a robust cryptosystem using the HD2DC as storage and retrieval tool of Share 2. The secret image, Share 1, and Share 2 are previously generated, following the procedure described in the preceding section of this Chapter. The structure of this validation tool is generated by the following steps:

1. Each pixel is defined as a bit, with '0' representing a blue pixel and '1' a red pixel.

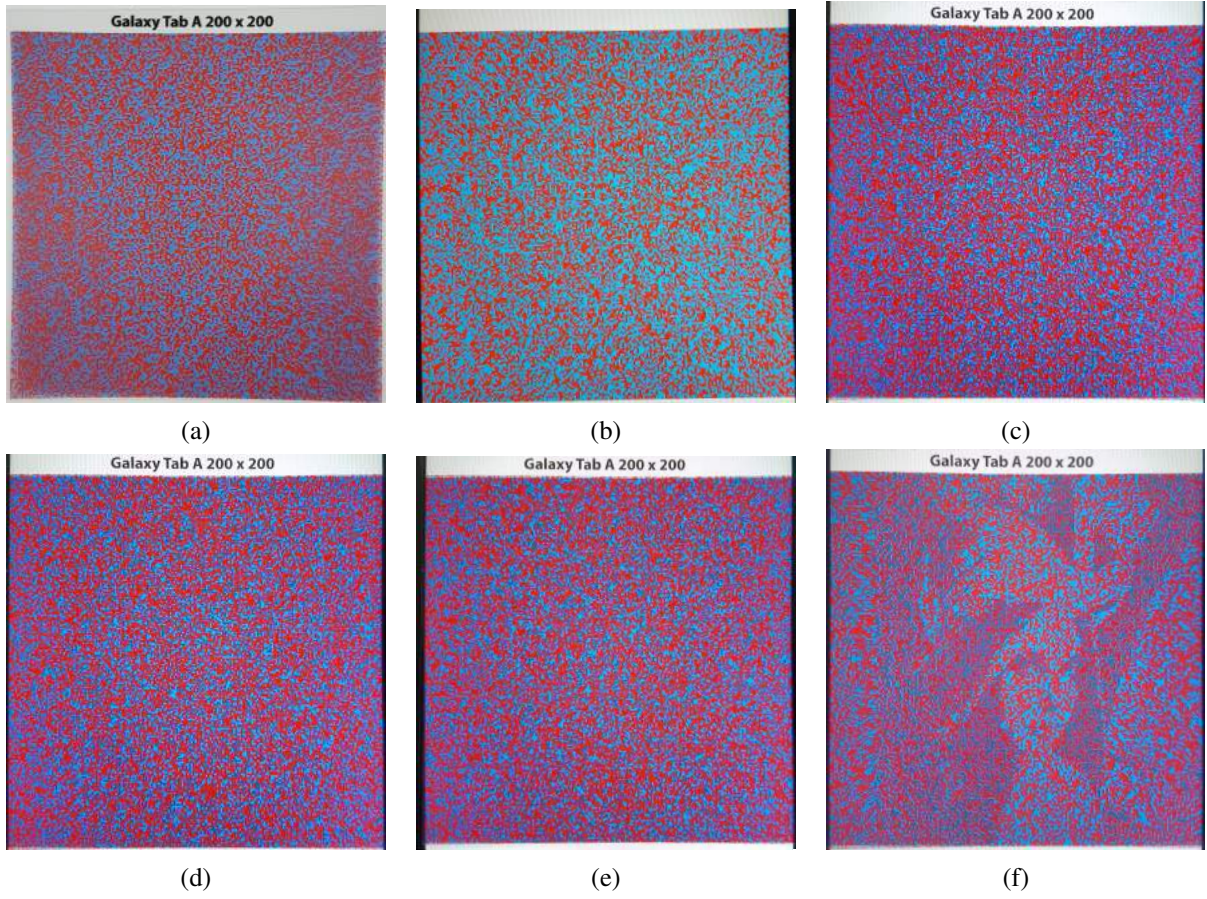


Figure 4.8: Proposed animated VC scheme images of 200×200 pixels: (a) Share 1, (b) Share 2, (c) first wrong decoded secret image, (d) second wrong decoded secret image, (e) third wrong decoded secret image, and (f) correctly decoded secret image.

2. The 1024-bit Rivest-Shamir-Adleman (RSA) asymmetric cryptography algorithm is used to encrypt Share 2. Share 2 is divided into sequences of 177 bytes and encrypted into sequences of 128 bytes. The amount of encrypted bytes is given by the following equation:

$$B = 128 \cdot \left\lceil \frac{M^2 \cdot 0.125}{117} \right\rceil, \quad (4.6)$$

where M is the number of pixels per side of $F_2(x,y)$ and B is the amount of bytes that the HD2DC has to store.

Due to the maximum storage capacity B of 2,906 bytes in a HD2DC, the maximum spatial resolution of $F_1(x,y)$ and $F_2(x,y)$ is $M = 140 \times 140$.

3. The HD2DC code is generated by coding B bytes of $F_2(x,y)$.

The following steps are necessary to correctly decode and display $F_2(x,y)$:

1. The HD2DC image is captured and decoded. The B encrypted bytes are decrypted using the Private Key of the 1024-RSA algorithm.

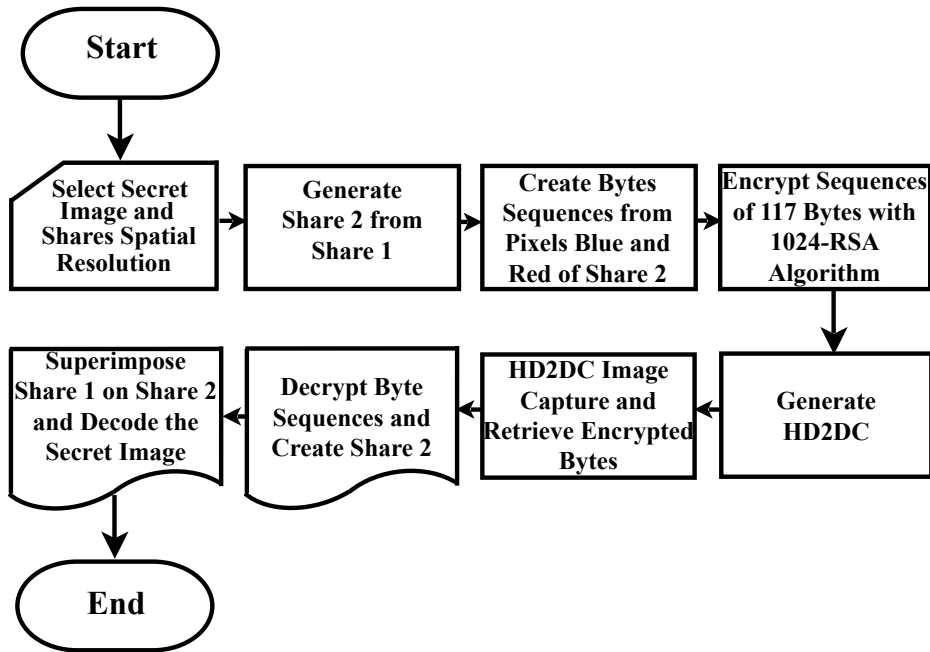


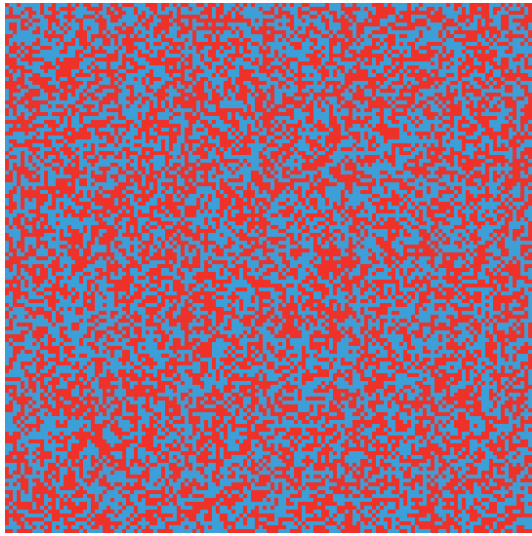
Figure 4.9: HD2DC and proposed VC Scheme Cryptosystem.

2. The Share 2 image is generated from the decoded bits contained on the 1024-bit RSA decryption.
3. $F_1(x,y)$ is superimposed on the generated $F_2(x,y)$ image and $S(x,y)$ is revealed.

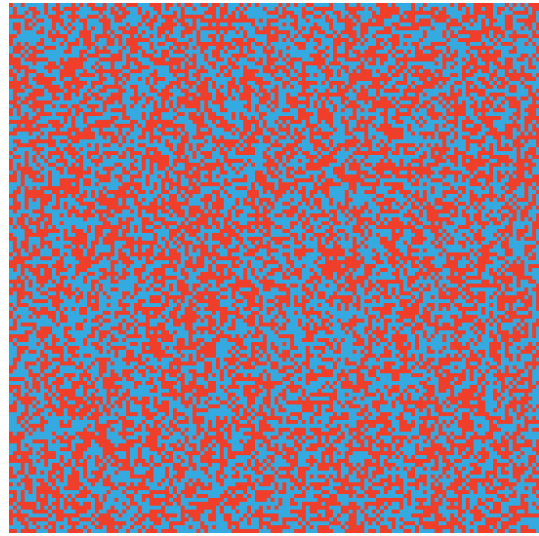
Figure 4.9 shows the encoding and decoding steps of the proposed VC scheme using the HD2DC as a transmission medium for Share 2. An example of the encoding and decoding process of a secret image with the Whatsapp application symbol is shown in Figure 4.10. These figures show a 136×136 Share 2 encoded on a single HD2DC with version 8, 8-color and Low (10%) error-correction level. In this case, the HD2DC is generated with $B = 2,560$ bytes. The HD2DC is correctly decoded by correcting 13 wrong symbols.

The correct coding and decoding of HD2DC also shows that the HD2DC image can be captured from a display, not only from a printed HD2DC. Since 1024-RSA encryption algorithm is used, no meaningful data is retrieved if a standard HD2DC reader is used to decode the HD2DC showed in Figure 4.10 (c). The smartphone used for decoding is a Samsung Galaxy S7 Edge.

The main objective of using a 2D-barcode to store encrypted Share 2 is to allow reuse of Share 1. As the proposed VC scheme is a One-Time Pad (Xor-based) cryptosystem, the reuse of the Ciphertext $F_1(x,y)$ and the key $F_2(x,y)$ is not recommended. Using a RSA encrypted Share 1 ($F_1(x,y)$) increases the security level on the proposed VC scheme.



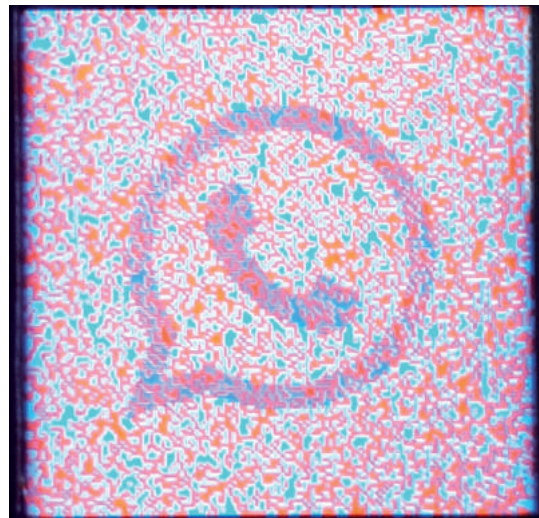
(a)



(b)



(c)



(d)

Figure 4.10: Proposed VC scheme and HD2DC Cryptosystem: (a) Share 1 with 136×136 pixels, (b) Share 2 with 136×136 pixels, (c) HD2DC carrying the 1024-RSA encrypted Share 2, and (d) Decoded secret image.

5 CONCLUSIONS

In this work, our goal was to propose novel alternatives for image-based data validation systems. We approached this subject by analyzing two study cases: an alternative 2D colored barcode, called High Density Two Dimensional Code (HD2DC), and a Visual Cryptography with Color Interference scheme.

Studying 2D barcodes and Visual Cryptography schemes (Chapter 2), we observed that no current 2D barcode presents a high density information capacity, which is a requirement for transmitting high amounts of information in small printed areas. Also, most Visual Cryptography schemes require a pixel expansion and at least two superimposed transparencies, which limit their usability in real applications. Therefore, in this work we propose new solutions to increase information density in 2D barcodes and make Visual Cryptography schemes more feasible.

First, we proposed the HD2DC barcode as a new alternative standard for 2D barcodes (Chapter 3). HD2DC can be generated with 5 or 8 module colors, 8 different versions, and 3 error correction levels, resulting in 48 different 2D barcode formats. In our tests we used all versions of HD2DC, considering a $0.2 \text{ mm} \times 0.2 \text{ mm}$ module area. HD2DC images were printed on regular office A4 paper with 120 g/m^2 , using a Xerox Color 560 printer. We tested them with the Samsung Galaxy S5 and J5 cameras, which allowed us to evaluate the percentage of corrupted symbols versus capturing distance. All printed HD2DC, encoded with Low error correction level, taken from distances varying from 7cm to 12cm, were correctly decoded. This means that a very high amount of information can be stored in a HD2DC image.

The robustness of HD2DC to JPEG, JPEG2000, and H.264/AVC compression algorithms were also analyzed. We used resized HD2DC barcode images before applying the compression algorithms. HD2DC-5 images compressed with JPEG, JPEG2000, and H.264/AVC were decoded for bitrates greater than 0.4156 bpp, 0.0816 bpp, and 0.3514 bpp, respectively. HD2DC-8 images compressed with JPEG, JPEG2000 and H.264/AVC were decoded for rates greater than 0.4151 bpp, 0.1169 bpp, and 0.3627 bpp, respectively. The lowest possible bitrate achieved with JPEG and H.264/AVC algorithms were correctly decoded for HD2DC-5 and HD2DC-8. Among these compression algorithms, JPEG2000 obtained the smallest bitrate for HD2DC barcodes. HD2DC is capable of storing 2,906 Bytes in an area of $2 \times 2 \text{ cm}$, allowing a storage capacity of 4,687 Bytes per in^2 . Up to our knowledge, HD2DC is currently the highest density 2D-barcode.

Second, we proposed a new Visual Cryptography scheme (Chapter 4). The proposed method does not require pixel expansion and only needs 2 shares. One share is a 0.3 mm thick color printed PVC transparency, while the other is an image displayed on a mobile device. Several combinations of warm and cool colors printed on transparencies and mobile displayed images had their luminance measured by a luminance meter. This experiment was performed to find adequate colors to be used in our scheme, considering the color interference between the two shares. The

scheme reaches the maximum entropy required value for a binary Visual Cryptography scheme. The selected colors have the following R, G and B values: Blue (0, 170, 255) and Red (255, 10, 0) for Share 1 and Blue (0, 180, 255) and Red (255, 40, 0) for Share 2. Practical results illustrated that a cheap and practical application of Visual Cryptography can be designed with the proposed system.

An animated GIF Share 2, composed of $p > 1$ images, is proposed in order to improve the reusability of Share 1. Also, a validation system composed by the two proposed technologies is presented in Chapter 4, showing that both technologies can be used together to compose a data validation cryptosystem. In this approach, the HD2DC carries a 1024-RSA encrypted data of Share 2, creating a robust communication channel for data validation.

Future works in 2D-barcodes include the possibility of studying the maximum amount of colors per module in function of: (1) camera sensor quality, (2) printed material, and (3) printer quality. A 2D-barcode system that is able to decode higher quantity of different colors per module increases the number of stored bits per module, and its storage density. Another topic for future works is to use modern error-correction codes, such as Turbo Codes or Low-Density Parity-Check (LDPC) codes, instead of the traditional Reed-Solomon error-correction algorithm.

On VC schemes, future works include the possibility of using different materials than the PVC printed transparency. Also, evaluate the viability of develop a real-time Xor-Based Embedded Extended Visual Cryptography (EVC) schemes using digital Halftoning algorithm. Finally, research the implementation of a ternary or quaternary real-time VC scheme for non-expanded pixels and only 2 shares.

5.1 COMPUTER-IMPLEMENTED INVENTIONS AND PATENTS

The works presented on this Thesis are under intellectual property of the Fundação Universidade de Brasília:

- Max Eduardo Vizcarra Melgar and Mylène Christine Queiroz de Farias, HD2DC BAR-CODE, Computer-Implemented Invention (CII), Registration Number BR 51 2017 000523-0, June, 2017. Certificate in Appendix.
- Max Eduardo Vizcarra Melgar and Mylène Christine Queiroz de Farias, COLOR VC SYSTEM, Computer-Implemented Invention (CII), Registration Number BR 51 2017 000524-9, June, 2017. Certificate in Appendix.
- Max Eduardo Vizcarra Melgar and Mylène Christine Queiroz de Farias, Código de Barras de Alta Densidade, Submitted patent request, CDT - UnB. Supporting document in Appendix.
- Max Eduardo Vizcarra Melgar and Mylène Christine Queiroz de Farias, Lâmina de Criptografia Visual, Submitted patent request, CDT - UnB. Supporting document in Appendix.

5.2 PUBLICATIONS

P1: Max E. Vizcarra Melgar; Alexandre Zaghetto; Bruno Macchiavello and Anderson C.A. Nascimento. CQR CODES: COLORED QUICK-RESPONSE CODES. In: IEEE Second International Conference on Consumer Electronics, Berlin. ICCE 2012.

P2: Max E. Vizcarra Melgar; Alexandre Zaghetto; Bruno Macchiavello; Anderson C.A. Nascimento; Mylène C Q Farias. Avaliação do Efeito do JPEG e JPEG2000 na Decodificação de CQR Codes. In: XXXI Simpósio Brasileiro de Telecomunicações, Fortaleza. SBrT 2013.

P3: Max E. Vizcarra Melgar; Farias, Mylène Christine Queiroz; Alexandre Zaghetto. An evaluation of the effect of JPEG, JPEG2000, and H.264/AVC on CQR codes decoding process. In: Digital Photography and Mobile Imaging XI, 2015, San Francisco. Proc. SPIE, Digital Photography and Mobile Imaging XI, 2015. v. 9404.p. 94040Q.

P4: Max E. Vizcarra Melgar; Mylène C. Q. Farias; Flávio de Barros Vidal; and Alexandre Zaghetto, A High Density Colored 2D-Barcode: CQR Code-9, XXIX Conference on Graphics, Patterns and Images (SIBGRAPI 2016), São José dos Campos, SP, Brazil, p.329-334.

P5+: Max E. Vizcarra Melgar; Mylène C. Q. Farias. High Density Two-Dimensional Code. *Inpress.*

P6+: Max E. Vizcarra Melgar; Mylène C. Q. Farias. A (2,2) XOR-Based Visual Cryptography Scheme Without Pixel Expansion. *Inpress.*

BIBLIOGRAPHY

- 1 Max E. Vizcarra Melgar; Zaghetto A.; Macchiavello B. and Nascimento A. C. A. Cqr codes: Colored quick-response codes. *Proceedings of the 2ND IEEE International Conference on Consumer Electronics - Berlin (IEEE 2012 ICCE-Berlin)*, September 2012.
- 2 H. Bagherinia and R. Manduchi. A theory of color barcodes. *Proceedings of the IEEE Color and Photometry in Computer Vision Workshop*, June 2011.
- 3 Marco Querini, Antonio Grillo, Alessandro Lentini and Giuseppe F. Italiano. 2d color barcodes for mobile phones. *International Journal of Computer Science and Applications*, v. 8, p. 136–155, 2011.
- 4 Marco Querini and Giuseppe F. Italiano. Reliability and data density in high capacity color barcodes. *Computer Science and Information Systems*, v. 11, p. 1595–1615, October 2014.
- 5 Max E. Vizcarra Melgar, Mylène C. Q. Farias, Flávio de Barros Vidal and Alexandre Zaghetto. A high density colored 2d-barcode: Cqr code-9. *XXIX Conference on Graphics, Patterns and Images - SIBGRAPI2016*, p. 329 – 334, October 2016.
- 6 Feng Liu and Chuankun Wu. Embedded extended visual cryptography schemes. *IEEE Transactions on Information Forensics and Security*, v. 6, p. 307–322, 2011.
- 7 Young-Chang Hou. Visual cryptography for color images. *Pattern Recognition*, n. 36, p. 1619–1629, 2003.
- 8 Pim Tuyls, Tom Kevenaar, Geert-Jan Schrijen, Toine Staring, and Marten van Dijk. Visual crypto displays enabling secure communications. *Security in Pervasive Computing*, p. 271–284, 2004.
- 9 Shiori Sugawara, Kenji Harada and Daisuke Sakai. High-chroma visual cryptography using interference color of high-order retarder films. *Optical Review*, v. 22, p. 544–552, 2015.
- 10 GARTNER, I. *Market Share: Devices, All Countries, 4Q14 Update*. [S.l.], 2015.
- 11 GARTNER, I. *Gartner IT Glossary - Mobile Payment*. <<http://www.gartner.com/it-glossary/mobile-payment/>>. Accessed February 02, 2018 [Online]). [S.l.].
- 12 Gartner, Inc. *Newsroom*. <<http://www.gartner.com/newsroom/id/2939217>>. Accessed February 02, 2018 [Online]).
- 13 G1. *Bancos perdem R\$ 685 milhões com fraudes eletrônicas*. <<http://g1.globo.com>>. Accessed February 02, 2018 [Online]).
- 14 Xing Fang and Justin Zhan. Online banking authentication using mobile phones. *2010 5th International Conference on Future Information Technology*, p. 1–5, 2010.
- 15 Franco Callegati; Walter Cerroni; Marco Ramilli. Man-in-the-middle attack to the https protocol. *IEEE Security & Privacy*, v. 7, p. 78–81, 2009.
- 16 Petr Hanaek; Kamil Malinka; Jiri Schafer. E-banking security - comparative study. *Security Technology, 2008. ICCST 2008*, October 2008.
- 17 Hien Thi Thu Truong, Eemil Lagerspetz, Petteri Nurmi, Adam J. Oliner, Sasu Tarkoma, N. Asokan, and Sourav Bhattacharya. The company you keep: Mobile malware infection rates and inexpensive risk indicators. *Computing Research Repository (CoRR)*, 2013.

- 18 C. Castelfranchi. The role of trust and deception in virtual societies. *Proceedings of the 34th Annual Hawaii International Conference on System Sciences*, p. 8, 2011.
- 19 Fabio Piva and Ricardo Dahab. *Proceedings of the International Conference on Security and Cryptography*, p. 317–324, 2011.
- 20 ISO/IEC 18004:2005. Information technology - automatic identification and data capture techniques - qr code 2005 bar code symbology specification. *Information technology*, August 2005.
- 21 Young Sil Lee, Nack Hyun Kim, Hyotaek Lim, HeungKuk Jo and Hoon Jae Lee. Online banking authentication system using mobile-otp with qr-code. *Computer Sciences and Convergence Information Technology (ICCIT)*, p. 644–648, November 2010.
- 22 Max E. Vizcarra Melgar; Santander, L.A. An alternative proposal of tracking products using digital signatures and qr codes. *Proc. of the 2014 IEEE Colombian Conference on Communications and Computing*, June 2014.
- 23 Guenther Starnberger, Lorenz Frohofer and Karl M. Goechka. Qr-tan secure mobile transaction authentication. *International Conference on Availability, Reliability and Security*, p. 578 – 583, March 2009.
- 24 David Conde-Lagoa, Enrique Costa-Montenegro, Francisco J. González-Castaño and Felipe Gil-Castañeira. Secure tickets based on qr-codes with user-encrypted content. *2010 IEEE International Conference on Consumer Electronics (ICCE)*, p. 257 – 258, 257 - 258 2010.
- 25 Iuliia Tkachenko, William Puech, Olivier Strauss, Jean-Marc Gaudin, Christophe Destruel and Christian Guichard. Improving the module recognition rate of high density qr codes (version 40) by using centrality bias. *4th International Conference on Image Processing Theory, Tools and Applications (IPTA)*, October 2014.
- 26 Hiroko Kato and Keng T Tan. Pervasive 2d barcodes for camera phone applications. *IEEE Pervasive Computing*, v. 6, p. 76 – 85, 2007.
- 27 ISO/IEC 10918-1:1994. Digital compression and coding of continuous-tone still images: Requirements and guidelines. *Information technology*, 1994.
- 28 Keng T Tan, Douglas Chai, Hiroko Kato and Siong Khai Ong. Designing a color barcode for mobile applications. *IEEE Pervasive Computing*, p. 50 – 55, June 2012.
- 29 Jae-Youn Shim, Seong-Whan Kim. Design of circular dot pattern code (cdpc) for maximum information capacity and robustness on geometric distortion/noise. *Multimedia Tools and Applications*, p. 1941–1955, 2014.
- 30 Joceli Mayer, J.C.M. Bermudez, A. P. Legg, B. F. Uchôa-Filho, D. Mukherjee, A. Said, R. Samadani, S. Simske. Design of high capacity 3d print codes with visual cues aiming for robustness to the ps channel and external distortions. In: *Proceedings of the IEEE 11th International Workshop on Multimedia Signal Processing*, p. 50 – 55, October 2009.
- 31 Orhan Bulan and Gaurav Sharma. High Capacity Color Barcodes: Per Channel Data Encoding via Orientation Modulation in Elliptical Dot Arrays. In: *IEEE Transactions on Image Processing*. [S.l.: s.n.], 2011. v. 20, p. 1337–1350.
- 32 Henryk Blasinski, Orhan Bulan and Gaurav Sharma. Per-Colorant-Channel Color Barcodes for Mobile Applications: An Interference Cancellation Framework. In: *IEEE Transactions on Image Processing*. [S.l.: s.n.], 2013. v. 22, p. 1498 – 1511.

- 33 Berlekamp E. R. Nonbinary bch decoding. *Proc. of the Int. Symp. Inf. Theory (ISIT)*, v. 14 n.2, 1967.
- 34 Max E. Vizcarra Melgar; Farias C. Q. M.; Zaghetto A. An evaluation of the effect of jpeg, jpeg2000 and h.264/avc on cqr codes decoding process. *Proceedings of SPIE-IS&T Electronic Imaging*, v. 9404, February 2015.
- 35 Moni Naor and Adi Shamir. Visual cryptography. *Annual International Conference on the Theory and Applications of Cryptographic Techniques - EUROCRYPT*, v. 950, p. 1–12, 1994.
- 36 Z. Zhou, G. R Arce, and G. Di Crescenzo. Halftone visual cryptography. *IEEE International Conference on Image Processing*, v. 1, 2003.
- 37 Feng Liu and Wei Qi Yan. Visual cryptography for image processing and security theory, methods, and applications. *Springer*, 2014.
- 38 Xin Liu, Shen Wang, Jianzhi Sang, and Weizhe Zhang. A novel mapping-based lossless recovery algorithm for vss. *Journal of Real-Time Image Processing*, p. 1–10, 2016.
- 39 F. Liu, C.K. Wu, and X.J. Lin. Colour visual cryptography schemes. *IET Information Security*, p. 151–165, 2008.
- 40 Berlekamp E. R. Algebraic coding theory. *McGraw-Hill*, 1968.
- 41 R. C. Gonzalez and R. E. Woods. Digital image processing. *Prentice Hall*, 2002.
- 42 Nobutuki Otsu. A threshold selection method from gray-level histograms. *IEEE Transactions on Systems, Man and Cybernetics*, v. 9, n. 1, January 1979.
- 43 Canny J. A computational approach to edge detection. *IEEE Transactions on Pattern Analysis and Machine Intelligence*, v. 8, n. 6, p. 679–698, June 1986.
- 44 Richard Hartley and Andrew Zisserman. Multiple view geometry in computer vision. *Cambridge University Press*, n. 2nd Edition, 2004.
- 45 Zhibo Yang, Huanle Xu, Jianyuan Deng, Chen Change Loy, and Wing Cheong Lau. Robust and fast decoding of high-capacity color qr codes for mobile applications. *ArXiv e-prints. Computer Science - Computer Vision and Pattern Recognition*, January 2018.
- 46 ISO/IEC 15444-1:2004. Jpeg 2000 image coding system: Core coding system. *Information technology*, 2004.
- 47 D. S. Taubman and M. W. Marcellin. Jpeg 2000: Image compression fundamentals, standards and practice. *Kluwer Academic*, 2002.
- 48 Queiroz R. L. Fringe benefits of the h.264/avc. *Proc. of International Telecommunications Symposium*, p. 208–212, September 2006.
- 49 Marpe D; George V; Wiegand T. Performance comparison of intra-only h.264/avc and jpeg2000 for a set of monochrome iso/iec test images. *Contribution JVT ISO/IEC MPEG and ITU-T VCEG*, Doc JVT M-014, October 2004.
- 50 Marpe D. Performance evaluation of motion-jpeg2000 in comparison with h.264/avc operated in pure intra coding mode. *Wavelet Applications in Industrial Processing*, v. 5266, p. 129–137, October 2004.
- 51 Alexandre Zaghetto and Ricardo L. de Queiroz. Segmentation-driven compound document coding based on h.264/avc-intra. *Image Processing, IEEE Transactions*, v. 16, p. 1755–1760, July 2007.

- 52 Alexandre Zaghetto and Ricardo L. de Queiroz. Scanned document compression using block-based hybrid video codec. *Image Processing, IEEE Transactions*, v. 22, p. 2420–2428, June 2013.
- 53 Feng Liu and Wei Qi Yan. Visual cryptography for image processing and security: Theory, methods, and applications. *Springer*, 2014.
- 54 M. W. Allsopp and G. Vianello. Poly (vinyl chloride). *Ullmann's Encyclopedia of Industrial Chemistry*, 2012.
- 55 Raymond A. Serway and John W. Jewett. Physics for scientists and engineers with modern physics. *Brooks/Cole*, 2014.

6 APPENDIX

6.1 COMPUTER-IMPLEMENTED INVENTIONS

HD2DC Barcode

(2,2) Xor-Based VC Using Color Interference

6.2 ONGOING PATENTS REQUEST

HD2DC Barcode

(2,2) Xor-Based VC Using Color Interference

6.3 HD2DC COMPRESSION RESULTS



INPI INSTITUTO
NACIONAL
DA PROPRIEDADE
INDUSTRIAL

REPÚBLICA FEDERATIVA DO BRASIL
Ministério Da Indústria, Comércio Exterior e Serviços
Instituto Nacional da Propriedade Industrial

Diretoria de Patentes, Programas de Computador e Topografias de Circuitos Integrados

Certificado de Registro de Programas de Computador

Processo nº: BR 51 2017 000523-0

O Instituto Nacional da Propriedade Industrial expede o presente certificado de Registro de Programas de Computador, válido por 50 anos a partir de 1º de janeiro subsequente à data de Criação: 03 de outubro de 2016, em conformidade com o parágrafo 2º, artigo 2º da Lei Nº 9.609, de 19 de Fevereiro de 1998.

Título: **HD2DC BARCODE**

Data de Criação: 03 de outubro de 2016

Titular(es): FUNDAÇÃO UNIVERSIDADE DE BRASÍLIA (00.038.174/0001-43), Endereço: UNIVERSIDADE DE BRASÍLIA, ED. CDT CAMPUS UNIVERSITÁRIO DARCY RIBEIRO ASA NORTE, BRASÍLIA, DF, 70904970

Autor(es): MAX EDUARDO VIZCARRA MELGAR (744.093.361-34)
/ MYLENE CHRISTINE QUEIROZ DE FARIAS (832.343.654-15)

Linguagem: MATLAB

Campo de Aplicação: IF-02

Tipo Programa: TC-03

Expedido em: 13 de junho de 2017

Aprovado por Julio Cesar Castelo Branco Reis Moreira

Julio Cesar Castelo Branco Reis Moreira

Diretor de Patentes, Programas de Computador e Topografias de Circuitos Integrados



Figure 6.1: HD2DC Computer-Implemented Invention certificate.



INPI INSTITUTO
NACIONAL
DA PROPRIEDADE
INDUSTRIAL

REPÚBLICA FEDERATIVA DO BRASIL
Ministério Da Indústria, Comércio Exterior e Serviços
Instituto Nacional da Propriedade Industrial

Diretoria de Patentes, Programas de Computador e Topografias de Circuitos Integrados

Certificado de Registro de Programas de Computador

Processo nº: BR 51 2017 000524-9

O Instituto Nacional da Propriedade Industrial expede o presente certificado de Registro de Programas de Computador, válido por 50 anos a partir de 1º de janeiro subsequente à data de Criação: 09 de setembro de 2016, em conformidade com o parágrafo 2º, artigo 2º da Lei Nº 9.609, de 19 de Fevereiro de 1998.

Título: COLOR VC SYSTEM

Data de Criação: 09 de setembro de 2016

Titular(es): FUNDAÇÃO UNIVERSIDADE DE BRASÍLIA (00.038.174/0001-43), Endereço: UNIVERSIDADE DE BRASÍLIA, ED. CDT CAMPUS UNIVERSITÁRIO DARCY RIBEIRO ASA NORTE, BRASÍLIA, DF, 70904970

Autor(es): MAX EDUARDO VIZCARRA MELGAR (744.093.361-34)
/ MYLENE CHRISTINE QUEIROZ DE FARIAS (832.343.654-15)

Linguagem: MATLAB

Campo de Aplicação: FN-03

Tipo Programa: PD-03

Expedido em: 13 de junho de 2017

Aprovado por Julio Cesar Castelo Branco Reis Moreira

Julio Cesar Castelo Branco Reis Moreira
Diretor de Patentes, Programas de Computador e Topografias de Circuitos Integrados



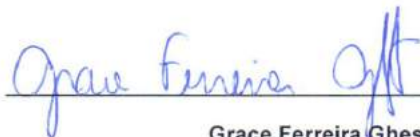
Figure 6.2: COLOR VC SYSTEM Computer-Implemented Invention certificate.

Brasília, 06 de fevereiro de 2018.

DECLARAÇÃO

Declaramos que o Centro de Apoio ao Desenvolvimento Tecnológico – CDT, unidade gestora de propriedade intelectual da UnB/FUB, recebeu os documentos descritivos do processo tecnológico “**Código de Barras de Alta Densidade**”, por parte do aluno **Max Eduardo Vizcarra Melgar**, CPF nº **744.093.361-34**, vinculado ao Departamento de Engenharia Elétrica da Faculdade de Tecnologia da Universidade de Brasília, e que o referido é inventor do **pedido de patente** que será depositado junto ao Instituto Nacional da Propriedade Industrial – INPI, em nome da **Fundação Universidade de Brasília – FUB**.

Ressalta-se que o referido pedido de patente atende aos requisitos de patenteabilidade e que a fase de busca de anterioridade não originou documentos com conteúdo similar ou impeditivo a proteção. Por assim sendo, a presente invenção encontra-se em vias de depósito.



Grace Ferreira Ghesti

Gerência de Inovação e Transferência de Tecnologia - GITT

CDT/ UnB

Figure 6.3: Código de Barras de Alta Densidade patent request support document.

Brasília, 06 de fevereiro de 2018.

DECLARAÇÃO

Declaramos que o Centro de Apoio ao Desenvolvimento Tecnológico – CDT, unidade gestora de propriedade intelectual da UnB/FUB, recebeu os documentos descritivos do processo tecnológico “Lâmina de Criptografia Visual”, por parte do aluno **Max Eduardo Vizcarra Melgar**, CPF nº **744.093.361-34**, vinculado ao Departamento de Engenharia Elétrica da Faculdade de Tecnologia da Universidade de Brasília, e que o referido é inventor do **pedido de patente** que será depositado junto ao Instituto Nacional da Propriedade Industrial – INPI, em nome da **Fundação Universidade de Brasília – FUB**.

Ressalta-se que o referido pedido de patente atende aos requisitos de patenteabilidade e que a fase de busca de anterioridade não originou documentos com conteúdo similar ou impeditivo a proteção. Por assim sendo, a presente invenção encontra-se em vias de depósito.



Grace Ferreira Ghesti

Gerência de Inovação e Transferência de Tecnologia - GITT

CDT/ UnB

Figure 6.4: Lâmina de Criptografia Visual patent request support document.

Table 6.1: HD2DC-5 color JPEG Results: Corrupted Symbols (%) versus Compression Bitrate (bpp).

Version	Error Correction Level L-M-H (%)	Corrupted Symbols (%)	Compression Bitrate	Status
1	9.46% - 18.92% - 29.73%	0%	0.9316 bpm	Successful
1	9.46% - 18.92% - 29.73%	1.35%	0.8284 bpm	Successful
1	9.46% - 18.92% - 29.73%	2.70%	0.5613 bpm	Successful
1	9.46% - 18.92% - 29.73%	2.70%	0.5141 bpm	Successful
1	9.46% - 18.92% - 29.73%	18.92%	0.4156 bpm	Successful
2	9.94% - 19.88% - 29.81%	0%	1.1526 bpm	Successful
2	9.94% - 19.88% - 29.81%	1.24%	1.0345 bpm	Successful
2	9.94% - 19.88% - 29.81%	4.97%	0.5953 bpm	Successful
2	9.94% - 19.88% - 29.81%	5.59%	0.5386 bpm	Successful
2	9.94% - 19.88% - 29.81%	13.04%	0.4220 bpm	Successful
3	9.85% - 19.71% - 29.93%	0%	1.4386 bpm	Successful
3	9.85% - 19.71% - 29.93%	1.09%	0.9763 bpm	Successful
3	9.85% - 19.71% - 29.93%	4.01%	0.6337 bpm	Successful
3	9.85% - 19.71% - 29.93%	5.11%	0.5701 bpm	Successful
3	9.85% - 19.71% - 29.93%	16.42%	0.4449 bpm	Successful
4	9.98% - 19.95% - 29.93%	0%	1.2828 bpm	Successful
4	9.98% - 19.95% - 29.93%	1.46%	0.9901 bpm	Successful
4	9.98% - 19.95% - 29.93%	4.38%	0.6399 bpm	Successful
4	9.98% - 19.95% - 29.93%	4.87%	0.5725 bpm	Successful
4	9.98% - 19.95% - 29.93%	17.03%	0.4414 bpm	Successful
5	9.93% - 19.86% - 29.97%	0%	1.5577 bpm	Successful
5	9.93% - 19.86% - 29.97%	0.87%	1.0413 bpm	Successful
5	9.93% - 19.86% - 29.97%	3.31%	0.6648 bpm	Successful
5	9.93% - 19.86% - 29.97%	5.05%	0.5951 bpm	Successful
5	9.93% - 19.86% - 29.97%	12.02%	0.4556 bpm	Successful
6	10.12% - 20.11% - 30.09%	0 %	1.3637 bpm	Successful
6	10.12% - 20.11% - 30.09%	0.79%	1.0433 bpm	Successful
6	10.12% - 20.11% - 30.09%	4.07%	0.6675 bpm	Successful
6	10.12% - 20.11% - 30.09%	5.39%	0.5944 bpm	Successful
6	10.12% - 20.11% - 30.09%	10.51%	0.4520 bpm	Successful
7	10.06% - 20.02% - 30.08%	0%	2.0311 bpm	Successful
7	10.06% - 20.02% - 30.08%	0.72%	1.0795 bpm	Successful
7	10.06% - 20.02% - 30.08%	2.87%	0.6849 bpm	Successful
7	10.06% - 20.02% - 30.08%	3.59%	0.6098 bpm	Successful
7	10.06% - 20.02% - 30.08%	13.86%	0.4650 bpm	Successful
8	10.07% - 20.07% - 30.06%	0%	2.1024 bpm	Successful
8	10.07% - 20.07% - 30.06%	6.38%	1.1124 bpm	Successful
8	10.07% - 20.07% - 30.06%	12.33%	0.6969 bpm	Successful
8	10.07% - 20.07% - 30.06%	16.07%	0.6161 bpm	Successful
8	10.07% - 20.07% - 30.06%	25.92%	0.4654 bpm	Successful

Table 6.2: HD2DC-8 color JPEG Results: Corrupted Symbols (%) versus Compression Bitrate (bpp).

Version	Error Correction Level L-M-H (%)	Corrupted Symbols (%)	Compression Bitrate	Status
1	9.91% - 19.82% - 29.73%	0%	1.1761 bpm	Successful
1	9.91% - 19.82% - 29.73%	8.11%	0.8365 bpm	Successful
1	9.91% - 19.82% - 29.73%	13.51%	0.5660 bpm	Successful
1	9.91% - 19.82% - 29.73%	19.82%	0.5154 bpm	Successful
1	9.91% - 19.82% - 29.73%	27.93%	0.4151 bpm	Successful
2	9.94% - 19.88% - 29.81%	0%	1.3185 bpm	Successful
2	9.94% - 19.88% - 29.81%	5.79%	1.0332 bpm	Successful
2	9.94% - 19.88% - 29.81%	9.09%	0.5917 bpm	Successful
2	9.94% - 19.88% - 29.81%	14.05%	0.5311 bpm	Successful
2	9.94% - 19.88% - 29.81%	27.69%	0.4160 bpm	Successful
3	9.98% - 19.95% - 29.93%	0%	1.8219 bpm	Successful
3	9.98% - 19.95% - 29.93%	4.14%	0.9939 bpm	Successful
3	9.98% - 19.95% - 29.93%	11.19%	0.6419 bpm	Successful
3	9.98% - 19.95% - 29.93%	14.60%	0.5737 bpm	Successful
3	9.98% - 19.95% - 29.93%	28.47%	0.4448 bpm	Successful
4	9.89% - 19.94% - 29.98%	0%	1.8965 bpm	Successful
4	9.89% - 19.94% - 29.98%	6%	1.0249 bpm	Successful
4	9.89% - 19.94% - 29.98%	12.48%	0.6530 bpm	Successful
4	9.89% - 19.94% - 29.98%	16.53%	0.5816 bpm	Successful
4	9.89% - 19.94% - 29.98%	27.07%	0.4472 bpm	Successful
5	9.99% - 19.98% - 29.97%	0%	1.9956 bpm	Successful
5	9.99% - 19.98% - 29.97%	5.23%	1.0658 bpm	Successful
5	9.99% - 19.98% - 29.97%	11.03%	0.6746 bpm	Successful
5	9.99% - 19.98% - 29.97%	16.61%	0.5982 bpm	Successful
5	9.99% - 19.98% - 29.97%	26.36%	0.4546 bpm	Successful
6	10.07% - 20.05% - 30.04%	0%	1.9687 bpm	Successful
6	10.07% - 20.05% - 30.04%	4.82%	1.0474 bpm	Successful
6	10.07% - 20.05% - 30.04%	10.07%	0.6593 bpm	Successful
6	10.07% - 20.05% - 30.04%	15.24%	0.5840 bpm	Successful
6	10.07% - 20.05% - 30.04%	24.69%	0.4414 bpm	Successful
7	10.06% - 20.05% - 30.05%	0%	2.8220 bpm	Successful
7	10.06% - 20.05% - 30.05%	6.09%	1.1009 bpm	Successful
7	10.06% - 20.05% - 30.05%	12.25%	0.6938 bpm	Successful
7	10.06% - 20.05% - 30.05%	16.43%	0.6154 bpm	Successful
7	10.06% - 20.05% - 30.05%	27.99%	0.4664 bpm	Successful
8	10.02% - 20.03% - 30.05%	0%	2.1024 bpm	Successful
8	10.02% - 20.03% - 30.05%	6.38%	1.1124 bpm	Successful
8	10.02% - 20.03% - 30.05%	12.33%	0.6969 bpm	Successful
8	10.02% - 20.03% - 30.05%	16.07%	0.6161 bpm	Successful
8	10.02% - 20.03% - 30.05%	25.92%	0.4654 bpm	Successful

Table 6.3: HD2DC-5 color JPEG2K Results: Corrupted Symbols (%) versus Compression Bitrate (bpp).

Version	Error Correction Level L-M-H (%)	Corrupted Symbols (%)	Compression Bitrate	Status
1	9.46% - 18.92% - 29.73%	0%	0.5231 bpm	Successful
1	9.46% - 18.92% - 29.73%	9.46%	0.1536 bpm	Successful
1	9.46% - 18.92% - 29.73%	18.92%	0.0764 bpm	Successful
1	9.46% - 18.92% - 29.73%	28.38%	0.0731 bpm	Successful
1	9.46% - 18.92% - 29.73%	>29.73%	0.0712 bpm	Unsuccessful
2	9.94% - 19.88% - 29.81%	0%	0.7846 bpm	Successful
2	9.94% - 19.88% - 29.81%	9.32%	0.1776 bpm	Successful
2	9.94% - 19.88% - 29.81%	19.88%	0.0882 bpm	Successful
2	9.94% - 19.88% - 29.81%	28.57%	0.0717 bpm	Successful
2	9.94% - 19.88% - 29.81%	>29.81%	0.0675 bpm	Unsuccessful
3	9.85% - 19.71% - 29.93%	0%	0.9497 bpm	Successful
3	9.85% - 19.71% - 29.93%	9.12%	0.1149 bpm	Successful
3	9.85% - 19.71% - 29.93%	18.61%	0.0825 bpm	Successful
3	9.85% - 19.71% - 29.93%	28.10%	0.0759 bpm	Successful
3	9.85% - 19.71% - 29.93%	>29.93%	0.0699 bpm	Unsuccessful
4	9.98% - 19.95% - 29.93%	0%	0.7925 bpm	Successful
4	9.98% - 19.95% - 29.93%	8.27%	0.1101 bpm	Successful
4	9.98% - 19.95% - 29.93%	18.25%	0.0968 bpm	Successful
4	9.98% - 19.95% - 29.93%	28.47%	0.0798 bpm	Successful
4	9.98% - 19.95% - 29.93%	>29.93%	0.0769 bpm	Unsuccessful
5	9.93% - 19.86% - 29.97%	0%	1.1943 bpm	Successful
5	9.93% - 19.86% - 29.97%	9.76%	0.1177 bpm	Successful
5	9.93% - 19.86% - 29.97%	19.34%	0.1056 bpm	Successful
5	9.93% - 19.86% - 29.97%	26.31%	0.0816 bpm	Successful
5	9.93% - 19.86% - 29.97%	>29.97%	0.0776 bpm	Unsuccessful
6	10.12% - 20.11% - 30.09%	0%	1.5940 bpm	Successful
6	10.12% - 20.11% - 30.09%	8.80%	0.1781 bpm	Successful
6	10.12% - 20.11% - 30.09%	18.00%	0.1019 bpm	Successful
6	10.12% - 20.11% - 30.09%	27.20%	0.0609 bpm	Successful
6	10.12% - 20.11% - 30.09%	>30.09%	0.0588 bpm	Unsuccessful
7	10.06% - 20.02% - 30.08%	0%	1.1964 bpm	Successful
7	10.06% - 20.02% - 30.08%	9.96%	0.1960 bpm	Successful
7	10.06% - 20.02% - 30.08%	17.86%	0.1092 bpm	Successful
7	10.06% - 20.02% - 30.08%	25.46%	0.0814 bpm	Successful
7	10.06% - 20.02% - 30.08%	>30.08%	0.0772 bpm	Unsuccessful
8	10.07% - 20.07% - 30.06%	0%	1.5954 bpm	Successful
8	10.07% - 20.07% - 30.06%	9.33%	0.1874 bpm	Successful
8	10.07% - 20.07% - 30.06%	19.65%	0.0969 bpm	Successful
8	10.07% - 20.07% - 30.06%	27.85%	0.0811 bpm	Successful
8	10.07% - 20.07% - 30.06%	>30.06%	0.0770 bpm	Unsuccessful

Table 6.4: HD2DC-8 color JPEG2K Results: Corrupted Symbols (%) versus Compression Bitrate (bpp).

Version	Error Correction Level L-M-H (%)	Corrupted Symbols (%)	Compression Bitrate	Status
1	9.91% - 19.82% - 29.73%	0%	0.5763 bpm	Successful
1	9.91% - 19.82% - 29.73%	9.91%	0.1625 bpm	Successful
1	9.91% - 19.82% - 29.73%	18.92%	0.0999 bpm	Successful
1	9.91% - 19.82% - 29.73%	27.03%	0.0982 bpm	Successful
1	9.91% - 19.82% - 29.73%	>29.73%	0.0955 bpm	Unsuccessful
2	9.91% - 19.82% - 29.73%	0%	1.581 bpm	Successful
2	9.91% - 19.82% - 29.73%	8.68%	0.1757 bpm	Successful
2	9.91% - 19.82% - 29.73%	17.36%	0.1438 bpm	Successful
2	9.91% - 19.82% - 29.73%	29.75%	0.0958 bpm	Successful
2	9.91% - 19.82% - 29.73%	>29.73%	0.0876 bpm	Unsuccessful
3	9.98% - 19.95% - 29.93%	0%	1.5887 bpm	Successful
3	9.98% - 19.95% - 29.93%	9.73%	0.1949 bpm	Successful
3	9.98% - 19.95% - 29.93%	18.73%	0.1286 bpm	Successful
3	9.98% - 19.95% - 29.93%	29.20%	0.0949 bpm	Successful
3	9.98% - 19.95% - 29.93%	>29.93%	0.0876 bpm	Unsuccessful
4	9.89% - 19.94% - 29.98%	0%	1.5920 bpm	Successful
4	9.89% - 19.94% - 29.98%	9.08%	0.2106 bpm	Successful
4	9.89% - 19.94% - 29.98%	18.80%	0.1567 bpm	Successful
4	9.89% - 19.94% - 29.98%	29.17%	0.0970 bpm	Successful
4	9.89% - 19.94% - 29.98%	>29.98%	0.0822 bpm	Unsuccessful
5	9.99% - 19.98% - 29.97%	0%	1.5941 bpm	Successful
5	9.99% - 19.98% - 29.97%	9.41%	0.2079 bpm	Successful
5	9.99% - 19.98% - 29.97%	18.12%	0.1420 bpm	Successful
5	9.99% - 19.98% - 29.97%	28.57%	0.1169 bpm	Successful
5	9.99% - 19.98% - 29.97%	>29.97%	0.0447 bpm	Unsuccessful
6	10.07% - 20.05% - 30.04%	0%	0.9553 bpm	Successful
6	10.07% - 20.05% - 30.04%	9.89%	0.1933 bpm	Successful
6	10.07% - 20.05% - 30.04%	17.08%	0.1451 bpm	Successful
6	10.07% - 20.05% - 30.04%	29.60%	0.0981 bpm	Successful
6	10.07% - 20.05% - 30.04%	>30.04%	0.0826 bpm	Unsuccessful
7	10.06% - 20.05% - 30.05%	0%	1.5960 bpm	Successful
7	10.06% - 20.05% - 30.05%	8.97%	0.2157 bpm	Successful
7	10.06% - 20.05% - 30.05%	19.23%	0.1375 bpm	Successful
7	10.06% - 20.05% - 30.05%	28.47%	0.1048 bpm	Successful
7	10.06% - 20.05% - 30.05%	>30.05%	0.0996 bpm	Unsuccessful
8	10.02% - 20.03% - 30.05%	0%	2.3968 bpm	Successful
8	10.02% - 20.03% - 30.05%	8.37%	0.2254 bpm	Successful
8	10.02% - 20.03% - 30.05%	18.60%	0.1566 bpm	Successful
8	10.02% - 20.03% - 30.05%	29.50%	0.1106 bpm	Successful
8	10.02% - 20.03% - 30.05%	>30.05%	0.1061 bpm	Unsuccessful

Table 6.5: HD2DC-5 color H.264/AVC Results: Corrupted Symbols (%) versus Compression Bitrate (bpp).

Version	Error Correction Level L-M-H (%)	Corrupted Symbols (%)	Compression Bitrate	Status
1	9.46% - 18.92% - 29.73%	0%	1.4330 bpm	Successful
1	9.46% - 18.92% - 29.73%	0%	0.4142 bpm	Successful
1	9.46% - 18.92% - 29.73%	0%	0.4044 bpm	Successful
1	9.46% - 18.92% - 29.73%	0%	0.3821 bpm	Successful
1	9.46% - 18.92% - 29.73%	1.35%	0.3514 bpm	Successful
2	9.94% - 19.88% - 29.81%	0%	1.8491 bpm	Successful
2	9.94% - 19.88% - 29.81%	0%	0.5120 bpm	Successful
2	9.94% - 19.88% - 29.81%	0%	0.5008 bpm	Successful
2	9.94% - 19.88% - 29.81%	1.24%	0.4668 bpm	Successful
2	9.94% - 19.88% - 29.81%	2.48%	0.4259 bpm	Successful
3	9.85% - 19.71% - 29.93%	0%	2.0713 bpm	Successful
3	9.85% - 19.71% - 29.93%	0%	0.5576 bpm	Successful
3	9.85% - 19.71% - 29.93%	0%	0.5504 bpm	Successful
3	9.85% - 19.71% - 29.93%	1.09%	0.5113 bpm	Successful
3	9.85% - 19.71% - 29.93%	2.19%	0.4641 bpm	Successful
4	9.98% - 19.95% - 29.93%	0%	2.1151 bpm	Successful
4	9.98% - 19.95% - 29.93%	0%	0.5686 bpm	Successful
4	9.98% - 19.95% - 29.93%	0%	0.5570 bpm	Successful
4	9.98% - 19.95% - 29.93%	0.24%	0.5153 bpm	Successful
4	9.98% - 19.95% - 29.93%	0.97%	0.4727 bpm	Successful
5	9.93% - 19.86% - 29.97%	0%	2.3548 bpm	Successful
5	9.93% - 19.86% - 29.97%	0%	0.6250 bpm	Successful
5	9.93% - 19.86% - 29.97%	0.35%	0.6182 bpm	Successful
5	9.93% - 19.86% - 29.97%	0.35%	0.5718 bpm	Successful
5	9.93% - 19.86% - 29.97%	1.05%	0.5194 bpm	Successful
6	10.12% - 20.11% - 30.09%	0%	2.3423 bpm	Successful
6	10.12% - 20.11% - 30.09%	0%	0.6142 bpm	Successful
6	10.12% - 20.11% - 30.09%	0.13%	0.6042 bpm	Successful
6	10.12% - 20.11% - 30.09%	0.92%	0.5590 bpm	Successful
6	10.12% - 20.11% - 30.09%	1.58%	0.5102 bpm	Successful
7	10.06% - 20.02% - 30.08%	0%	2.4998 bpm	Successful
7	10.06% - 20.02% - 30.08%	0%	0.6578 bpm	Successful
7	10.06% - 20.02% - 30.08%	0%	0.6473 bpm	Successful
7	10.06% - 20.02% - 30.08%	1.13%	0.5981 bpm	Successful
7	10.06% - 20.02% - 30.08%	2.57%	0.5460 bpm	Successful
8	10.07% - 20.07% - 30.06%	0%	2.4267 bpm	Successful
8	10.07% - 20.07% - 30.06%	0%	0.6350 bpm	Successful
8	10.07% - 20.07% - 30.06%	0%	0.6240 bpm	Successful
8	10.07% - 20.07% - 30.06%	0%	0.5774 bpm	Successful
8	10.07% - 20.07% - 30.06%	0.41%	0.5272 bpm	Successful

Table 6.6: HD2DC-8 color H.264/AVC Results: Corrupted Symbols (%) versus Compression Bitrate (bpp).

Version	Error Correction Level L-M-H (%)	Corrupted Symbols (%)	Compression Bitrate	Status
1	9.91% - 19.82% - 29.73%	0%	1.5023 bpm	Successful
1	9.91% - 19.82% - 29.73%	0%	0.9093 bpm	Successful
1	9.91% - 19.82% - 29.73%	0%	0.4325 bpm	Successful
1	9.91% - 19.82% - 29.73%	0%	0.3929 bpm	Successful
1	9.91% - 19.82% - 29.73%	2.70%	0.3627 bpm	Successful
2	9.94% - 19.88% - 29.81%	0%	1.8884 bpm	Successful
2	9.94% - 19.88% - 29.81%	0%	0.5207 bpm	Successful
2	9.94% - 19.88% - 29.81%	0%	0.5085 bpm	Successful
2	9.94% - 19.88% - 29.81%	0%	0.4702 bpm	Successful
2	9.94% - 19.88% - 29.81%	0.83%	0.4317 bpm	Successful
3	9.98% - 19.95% - 29.93%	0%	2.1800 bpm	Successful
3	9.98% - 19.95% - 29.93%	0%	0.5835 bpm	Successful
3	9.98% - 19.95% - 29.93%	0.24%	0.5727 bpm	Successful
3	9.98% - 19.95% - 29.93%	0.24%	0.5277 bpm	Successful
3	9.98% - 19.95% - 29.93%	2.43%	0.4842 bpm	Successful
4	9.89% - 19.94% - 29.98%	0%	2.3203 bpm	Successful
4	9.89% - 19.94% - 29.98%	0%	0.6189 bpm	Successful
4	9.89% - 19.94% - 29.98%	0%	0.6062 bpm	Successful
4	9.89% - 19.94% - 29.98%	1.13%	0.5604 bpm	Successful
4	9.89% - 19.94% - 29.98%	1.30%	0.5141 bpm	Successful
5	9.99% - 19.98% - 29.97%	0%	2.4866 bpm	Successful
5	9.99% - 19.98% - 29.97%	0%	0.6538 bpm	Successful
5	9.99% - 19.98% - 29.97%	0%	0.6394 bpm	Successful
5	9.99% - 19.98% - 29.97%	0.81%	0.5897 bpm	Successful
5	9.99% - 19.98% - 29.97%	2.09%	0.5384 bpm	Successful
6	10.07% - 20.05% - 30.04%	0%	2.4698 bpm	Successful
6	10.07% - 20.05% - 30.04%	0.26%	0.6428 bpm	Successful
6	10.07% - 20.05% - 30.04%	0.44%	0.6298 bpm	Successful
6	10.07% - 20.05% - 30.04%	0.61%	0.5800 bpm	Successful
6	10.07% - 20.05% - 30.04%	1.58%	0.5301 bpm	Successful
7	10.06% - 20.05% - 30.05%	0%	2.5883 bpm	Successful
7	10.06% - 20.05% - 30.05%	0.21%	0.6775 bpm	Successful
7	10.06% - 20.05% - 30.05%	0.41%	0.6626 bpm	Successful
7	10.06% - 20.05% - 30.05%	0.62%	0.6112 bpm	Successful
7	10.06% - 20.05% - 30.05%	1.44%	0.5577 bpm	Successful
8	10.02% - 20.03% - 30.05%	0%	2.6542 bpm	Successful
8	10.02% - 20.03% - 30.05%	0.17%	0.6935 bpm	Successful
8	10.02% - 20.03% - 30.05%	0.22%	0.6817 bpm	Successful
8	10.02% - 20.03% - 30.05%	0.50%	0.6272 bpm	Successful
8	10.02% - 20.03% - 30.05%	1.82%	0.5725 bpm	Successful